Ronja Erika Björklund

Utilization of Recycled Concrete Fines for Carbon Capture and Subsequent Use as Supplementary Cementitious Material

Master's thesis in Materials Science and Engineering
Supervisor: Harald Justnes
Co-supervisor: Iveta Nováková, Annika Steien, and Knut Kjellsen
June 2022

Master's thesis

NTNU
Norwegian University of
Science and Technology

NORCEM
HEIDELBERGCEMENT Group

Ronja Erika Björklund

Utilization of Recycled Concrete Fines for Carbon Capture and Subsequent Use as Supplementary Cementitious Material

NTNU
Norwegian University of
Science and Technology

Abstract

Concrete is the most common construction material in the world, but the cement production stands for 5-7 % of the total global CO_2 emissions. [26] To decrease the amount CO_2 generated from the production, supplementary materials as Fly Ash (FA) are frequently used in composite cements. However, the availability of FA in the future is uncertain as coal power plants are replaced by renewable energy. [27][31] At the same time, concrete waste is generated in several steps within the construction industry. At ready mix plants, precast element plants, demolition of constructions etc. In this study, the potential of reusing concrete waste as supplementary material in composite cements is investigated. The potential for carbonating the concrete fines and capturing CO_2 is also examined. Composite cement containing 20 wt% recycled concrete fines and 80 wt% Industrisement, was strength tested according to NS-EN 196-1. The composite cements exceeded the requirements for strength class 32,5 R and 42,5 R after 28 days. Both composite cements containing 20 wt% carbonated or non-carbonated were tested. However, the strength test did not show any clear difference between cements containing carbonated or non-carbonated material. Thermogravimetric Analysis (TGA) of the carbonated material showed potential for capturing 0.1 g CO_2/g recycled concrete fines. Which means that 10 % of the originally emitted CO_2 due to the clinker production potentially can be captured and stored in the material. The compressive strength divided by the reference, showed several composite cements exceeding 80 %. Which indicates that the concrete fines contribute with strength, not only the clinker phases. Isothermal calorimetry showed less cumulative heat J/g powder for the composite cements compared with the reference. However, the composite cements showed higher heat than the reference when adjusted to J/g cement, which indicate that the concrete fines contribute to the heat development. The results showed that higher CaO/SiO_2 - ratio, higher content Calcium Carbonate ($C\hat{C}$), and smaller particle size gave higher compressive strength. The study shows potential for using carbonated recycled concrete fines in composite cement. Future studies should further investigate the strength and durability of the composite cements, effective carbonation method at scale, and the availability of qualified concrete waste.

Abstrakt

Betong är det vanligaste byggmaterialet i världen, men cementproduktionen står för 5-7 % av det totala CO_2-utsläppet. [26] För att minska mängden CO_2 från tillverkningen blandas ofta cement med mineraliskt tillsatsmaterial som flygaska. Tillgängligheten på flygaska i framtiden är dock osäker eftersom kolkraftverk ersätts med förnybar energi. [27][31] Samtidigt genereras betongavfall från flera olika branscher inom byggindustrin, som fabriker för betongblandning och prefabelement, och vid rivning av konstruktioner mm. I den här studien undersöks potentialen av att återanvända betongavfall som tillsatsmaterial i cement. Potentialen för att karbonatisera betongavfallet och binda upp CO_2 blir också undersökt. Cementblandningar med 80 vt% Industrisement och 20 vt% återvunnet betongpulver styrketestades enligt NS-EN 196-1. Cementblandningarna uppnådde högre styrka än kraven för hållfasthetsklasserna 32,5 R och 42,5 R efter 28 dagar. Både cement inblandad med 20 vt% karbonateiserat eller ej karbonatiserat betongpulver testades. Resultaten visade dock ingen tydlig skillnad i styrka mellan cementblandningarna inehållande karbonateiserat och ej karbonatiserat betongpulver. Termogravimetrisk analys av de karbonatiserade betongmaterialen visade en förmåga att binda upp 0.1 g CO_2/g betongpulver. Vilket betyder att 10 % av den ursprungliga CO_2 från cementtillverkningen potentiellt kan fångas in och lagras i materialet. Flera av de blandade cementen översteg 80 % i relativ tryckhållfasthet till referensprovet. Vilket indikerar på att det inblandade betongpulvret också bidrar till styrkan, inte bara klinkern. Isotermisk kalorimetri visade lägre kumulativ värme J/g pulver, för cementen innehållande betongpulver jämfört med referensen. Cementblandningarna visade dock högre värme än referensen när värmeutvecklingen justerades till J/g cement, vilket pekar på att betongpulvret bidrar i värmeutvecklingen. Resultaten visade på att ökat CaO/SiO_2 - förhållande, ökat CaO_3 innehåll, och minskad partikelstorlek gav ökad styrka. Studien visar att det finns potential för att använda karbonatiserat betongpulver inblandat i cement. Framtida studier borde vidare undersöka styrka och beständighet av cement med inblandat betongpulver, effektiv karbonatiseringsmetod i stor skala, och tillgängligheten av dugligt betongavfall.

Preface

This master thesis is associated with the course TMT4905 at NTNU in Trondheim. The master thesis is a mandatory final work within the master´s program of materials science and engineering. The desired learning outcome is to work systematic and gain specialised knowledge, through both practical work and literature study. To achieve one´s own results and compare with similar research to give a deeper scientific explanation. The project is an independent work with guidance from supervisors. [21]

This master thesis is a continuation on the specialisation project "Use of Fines from Recycled Concrete into New Cement". Section "Short Notations Cement Chemistry" is taken from the specialisation project.

Table of Contents

List of Figures

List of Tables

Short Notations Cement Chemistry

Cement chemistry consist of big compounds and thus long names. To facilitate communication short notations are often used. The short notation for the major oxides and minerals are shown in Table 1 and Table 2. These tables are reused from the project "Use of Fines from Recycled Concrete into New Cementreport" by Ronja Björklund.

Table 1: Common oxides in cement chemistry. [13][12]

Oxide name	Formula	Short
Calcium Carbonate	$CaCO_3$	$C\hat{C}$
Calcium Hydroxide	$Ca(OH)_2$	CH
Calcium Oxide	CaO	C
Carbon Dioxide	CO_2	$\hat{C}$
Silicone Dioxide	SiO_2	S
Aluminium Oxide	Al_2O_3	A
Ferric Oxide	Fe_2O_3	F
Sulfur Trioxide	SO_3	$\hat{S}$
Magnesium Oxide	MgO	M
Sodium Oxide	Na_2O	N
Potassium Oxide	K_2O	K

Table 2: Common minerals in cement chemistry. [13][12]

Mineral name	Formula	Short
Alite	$3\,CaO \cdot SiO_2$	C_3S
Belite	$2\,CaO \cdot SiO_2$	C_2S
Aluminate	$3\,CaO \cdot Al_2O_3$	C_3A
Ferrite	$4\,CaO \cdot Al_2O_3 \cdot Fe_2O_3$	C_4AF
Gypsum	$CaSO_4 \cdot 2\,H_2O$	$C\hat{S}H_2$
Hemihydrate	$CaSO_4 \cdot 0.5\,H_2O$	$C\hat{S}H_{1/2}$
Anhydrite	$CaSO_4$	$C\hat{S}$
Aphthithalite	$K_3Na(SO_4)_2$	$K_3N\hat{S}_4$
Ettringite (E, AF_t)		$C_3A \cdot 3\,C\hat{S} \cdot H_{32}$
Monosulphate (MS, AF_m)		$C_3A \cdot C\hat{S} \cdot H_{12}$

Abbreviations

CĈ Calcium Carbonate. i, ix, xi, 21, 32, 33, 55, 59, 60, 63, 65, 66

CH Calcium Hydroxide. vii, 7, 8, 10, 11, 58

CSH Calcium Silica Hydrate. 7, 9–11, 13, 14, 58

DSF Densified Silica Fume. vii, 8, 13, 14

DTG Differential Thermogravimetric Analysis. vii–x, 4, 10, 30, 31, 58, 60, 61, 79–87

FA Fly Ash. i, viii, xi, 1, 6, 7, 10, 11, 13, 17, 34

LOI Loss On Ignition. 38, 60

pp percentage point. 33

PSD Particle Size Distribution. 19

RB Composite cement samples. xi, 19, 20, 28, 35, 36, 38, 46, 49, 52, 55, 56, 62, 63

RH Relative Humidity. 9

RPM Revolutions Per Minute. 23

SF Silica Fume. xi, 6–8, 10, 11

TGA Thermogravimetric Analysis. i, iii, vii, viii, x, 4, 9, 10, 16, 19, 21, 30, 66, 79–86

TM Test Material. viii, xi, 16, 17, 19, 30, 34, 35, 38, 60, 63

XRD X-ray Diffraction. vii–ix, xi, xii, 4, 11, 12, 16, 19, 22, 23, 41–45, 60

XRF X-ray Fluorescence. viii, xi, xii, 4, 11, 16, 19, 22, 23, 38, 39, 60

1 Introduction

1.1 Background and Motivation

Cement production has challenges with CO_2 emissions and supply of FA. Additionally, the European Union has put up recycling goals for construction and demolition waste. It is therefore of great interest to investigate whether concrete waste can capture CO_2 and be reused in new cement.

1.1.1 Challenges within Cement Production

The most common material for construction in the world is concrete. [26] Cement is the main ingredient in concrete, together with water and aggregates. [12] [26] During the cement production limestone is heated at 1450 °C to form clinker. The chemical reactions also produce CO_2, approximately 1 tonne CO_2 per tonne clinker. 60 % of the CO_2 comes from the chemical process, and 40 % of the CO_2 emissions is due to combustion of fuels, transportation, etc. The cement industry alone stands for about 5-7 % of the total CO_2 emissions in the world, when all sectors and industries are included. [26]

One measure to reduce the amount CO_2 from cement production is to lower the clinker content in the cement and replace it with other materials. [26] In Norway, Fly Ash (FA) is frequently used. [12] FA is a byproduct from coal power plants and is imported to Norway from Poland and Turkey. However, many coal power plants are shutting down in Europe, and FA is becoming less available. [27] [31] The availability also varies throughout the year along with the need for electricity, which means high production during the winter and lower during the summer. Cement has the opposite season variation. [31] The interest for new materials to use in cement is therefore high.

1.1.2 Waste Construction and Demolition

One third of all waste generated in the EU originates from construction and demolition. The waste includes concrete, bricks, glass, plastics, metals, and wood. The EU has therefore introduced rules to ensure that the waste is managed in an environmentally responsible way. To facilitate the creation of circular economy, and to promote reuse of valuable waste. In 2008 the EU set the following goals:

- By 2020 recycling of construction and demolition shall be increased by minimum 70 wt%.

- Encourage and facilitate selective demolition. To ensure safe handling of dangerous material, and recycling of high-quality materials.

- Waste generation should be reduced. [39]

In 2018, a protocol and guidelines for construction and demolition waste were introduced. These were aligned with the waste framework directive from 2008. [39] [8]

In 2020, 1.5 million tonnes concrete and brick waste was sorted and delivered in Norway. Figure 1 shows the concrete and brick waste in Norway for the last 8 years. In 2020, 52 % of the concrete and brick waste was delivered to landfill, 36 % was recycled, and 2 % was used as filler or covering

material. In the next ten years one expects to see an increase in concrete and brick waste, as several constructions, offshore installations, and facilities are forecast to be demolished. [22]
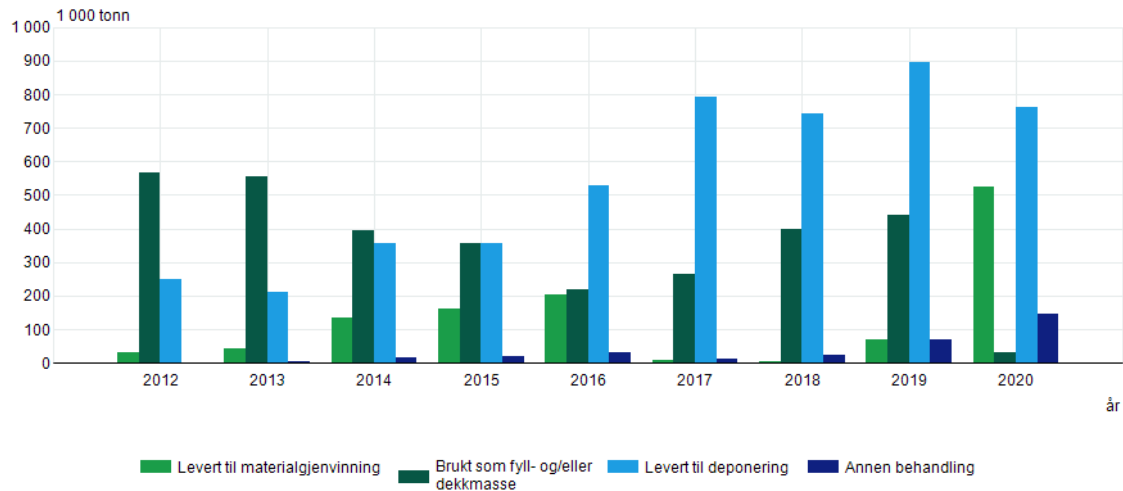
Figure 1: Concrete and brick waste generated in Norway per year. Light green: material delivered to recycling. Dark green: material used as filling material. Light blue: landfill. Dark blue: other treatment. [37]

1.1.3 Ongoing CO_2 Reducing Projects in Norway and Sweden

Norcem AS in Norway has worked over 30 years to replace non-renewable fossil fuels with alternative fuels. Figure 2 the fuels used in the cement production at Norcem´s Kjøpsvik cement plant the last years. Coal has been reduced over the years and replaced by FAB, car tires, waste oil, and bone meal. FAB is short form for "refined waste fuel" in Norwegian, and is typically made of paper, plastic, and textiles. [3] In Kjøpsvik 1/3 of the waste originates from local households, and 2/3 is imported waste from industries in the Netherlands and Great Britain, (per Norcem´s own data numbers received from Norcem Kjøpsvik). Bone meal is a waste product from the slaughter industry. Any dangerous substances in the waste are destroyed by the high temperature in the cement production. The metal wires in the car tires also work as a supply of minerals. [3]

Norcem has a vision of "zero emission" concrete production by 2030. This is planned to be achieved through CO_2 capture and storage. This is a part of the project Langskip which has been approved financial support by Stortinget. [2][9] Norway´s government will cover two thirds of the costs, which is estimated to be 16.8 billions Norwegian kroner. [9] A CO_2 capture facility on the cement plant will have a planned capacity of 400 000 tonnes per year, which equals about half the annual CO_2 emissions. [2]

Cementa in Sweden also has an ongoing CO_2 capture and storage project. The project has received support by Energimyndigheten (the Swedish Energy Agency) to the tune of 51 million swedish kroner. The project is planned to be ready 2030 and will capture up to 1.8 million tons of CO_2 annually. [1]

Brennstoff Ovn 5, Kjøpsvik
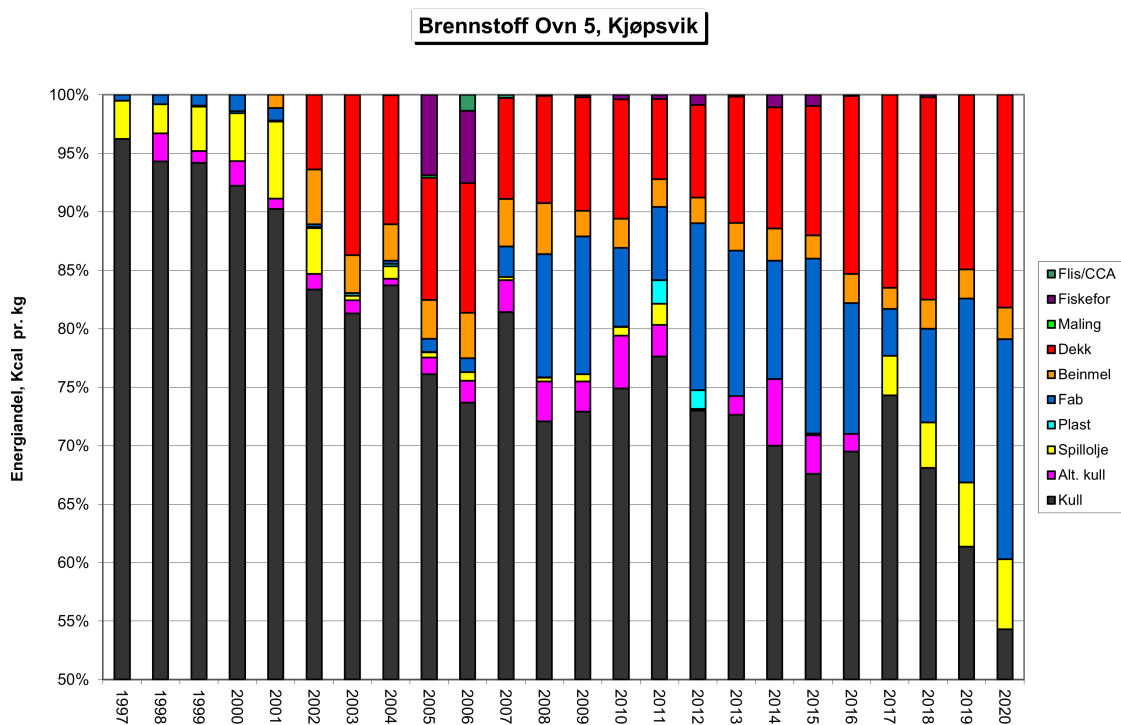
Figure 2: The development of fuel used at Norcem´s cement plant in Kjøpsvik. Dark green: wood chips. Purple: fish feed. Light green: paint. Red: car tires. Orange: bone meal. Dark blue: FAB (refined waste fuel). Light blue: plastic. Yellow: waste oil. Pink: alternative coal. Black: coal. The figure is provided from Norcem in Kjøpsvik.

1.2   Aim and Scope of the Work

The goal of this master project is to investigate the potential use of recycled cementitious waste from the concrete industry in new blended cement. Additionally, it will be explored whether cementitious waste can capture CO_2, and how this affects the properties of the material. Figure 3 shows the desired circularity of CO_2. Cement production emit CO_2, some of which is captured and stored in concrete waste. Recycled concrete waste is used in production of new cement. The composite cement is then used as building material for new constructions.

Material from different waste streams will be analysed to get a broad understanding of the available materials. The chemical properties will be investigated by TGA/Differential Thermogravimetric Analysis (DTG)-, X-ray Diffraction (XRD)-, X-ray Fluorescence (XRF)-analysis, and isothermal calorimetry. Chemical and physical properties will be tested by laser-granulometry, water demand, setting time, and compressive strength.
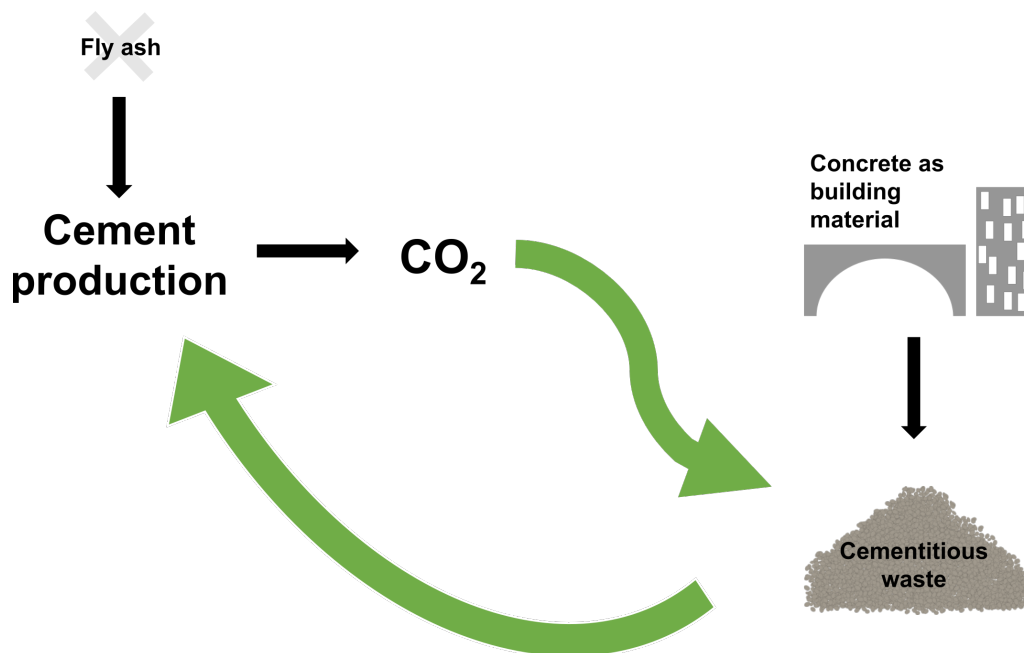
Figure 3: The desired circularity of CO_2 within the cement production and construction industry.

2 Theory

2.1 Cement Production and Cement Types

Limestone is a rock mainly consisting of calcium carbonate ($CaCO_3$), and is the main ingredient in cement. [38] [12] The rock is mined next to the cement plant and is finely ground together with bauxite, quartz, and gypsum into a raw meal. The raw meal is preheated in cyclones before it is fed into a rotary oven called kiln. The maximum temperature in the kiln is 1450 °C. Below 1300 °C, calcite is decomposed to lime (CaO) and carbon dioxide (CO_2) according to Reaction 1, called calcination. [12] About one tonne CO_2 is produced per tonne produced clinker. [26]

$$CaCO_3 \rightarrow CaO + CO_2 \tag{1}$$

At a temperature between 1300-1450 °C the mass is partially melted. Nodules called clinker with a diameter between 3-20 mm are formed at this temperature when the mass is semi-solid. After the process in a kiln the clinker is quenched with air. The clinker is finely ground to cement together with a few percent of gypsum. Gypsum is added to avoid flash set. Some cement types contain other material such as fly ash or limestone, these are added during the grinding. [12] Around 4 % limestone is added in the cement mill during production of both Industrisement and Standard FA cement at Norcem in Kjøpsvik and Brevik. [17][33][32][16]

The major phases in Portland clinker are tricalcium silicate (C_3S), dicalsium silicate (C_2S), tricalcium aluminate (C_3A) and tetracalcium aluminateferrite (C_4AF). They typically make up 50-70 %, 15-30 %, 5-10 % and 5-15 % of the clinker´s mass. [12]

The process steps at Cementa´s cement plant can be seen in Figure 4.
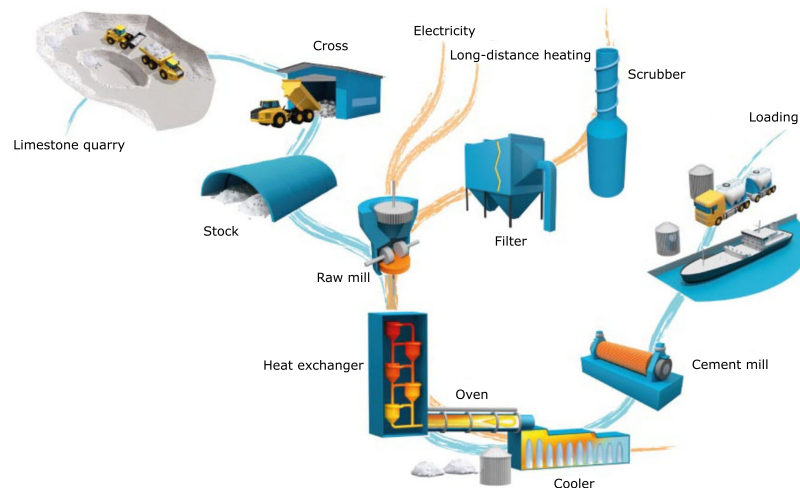
Figure 4: The process steps at a cement plant. [7] (The figure has been translated from Swedish to English.)

There are different cement types for different applications. CEM I is often called Portland cement, and consist of 95 - 100 % clinker. In Norway, Portland cement goes under the name Industrisement. Industrisement have high reactivity and heat development, short setting time and high early strength. Industrisement is commonly used in the precast-concrete industry, and for casting dur-

ing winter time when high heat and strength development is desirable. CEM II and CEM III are refereed to as Portland-composite cements, since they consist of both clinker and other material as FA or Silica Fume (SF). In Norway Standardsement FA and Anleggsement FA are two produced CEM II types. Standardsement FA is typically used for building structures, while Anleggsement FA is common in bridges and harbours. Anleggsement FA has low heat development which makes thick sections and large foundations less prone to cracking. Cement types can also be designed to be usable with alkali reactivate aggregates. [12]

Table 3 contains the cement notation, specific weight, initial setting time, and compressive strength are shown for different cement types produced in Norway. The number in the product name refers to which strength class the cement type belongs to. N stands for ordinary early strength, and R for high early strength. Cement standards according to NS-EN 197-01 for three strength classes 32.5 N, 42.5 N and 52.5 N are shown in Table 4. [36]

Table 3: Physical and mechanical properties of cement types produced in Norway. Specific weight, initial setting time, and compressive strengt.

Product Name	Spec.weight	Init. sett. time	Compressive strength (MPa)			
	(kg/dm^3)	(min)	1 day	2 day	7 day	28 day
INDUSTRISEMENT CEM I 52,5 R [29]	3.13	110	33	41	50	59
STANDARDSEMENT FA CEM II/B-M 42.5 R [30]	3.00	140	20	31	42	55
ANLEGGSEMENT FA CEM II/A-V 42.5 N [28]	3.02	165	12	21	37	53

Table 4: Mechanical and physical requirements for strength class 32.5 N, 42.5 N and 52.5 N according to NS-EN 197-01. [36]

Strength Class	Compressive Strength [MPa]			Initial Setting Time	Expansion
	2 Days	7 Days	28 Days	[min]	[mm]
32.5 N	-	≥ 16.0	≥ 32.5 ≤ 52.5	≥ 75	≤ 10
42.5 N	≥ 10.0	-	≥ 42.5 ≤ 62.5	≥ 60	≤ 10
52.5 N	≥ 20.0	-	≥ 52.5 -	≥ 45	≤ 10

Initial setting time gives an indication on when the cement paste cease to be plastic and fluid, and is measured according to standard NS-EN 196-3. Expansion, also called soundness, is a test on how hardened cement paste maintain its volume. It is measured according to standard NS-EN 196-3. [12]

2.2 Hydration

The chemical reaction called hydration between cement and water is the reason why concrete sets and harden. [12][4] Water is chemically bound and binder is produced. The reaction is exothermic, producing heat. [12] During hydration, a suspension with particles turns into a solid material that can support stress.[4] The hydration continues for as long there are reactants, cement components and water, or space for deposits. Since cement contains several clinker phases the total reaction is complex. Different clinker phases react simultaneously and influence each other. [4] The existing knowledge of the hydration process assumes that the clinker phases react independently and are pure. These are simplifications of the real case. [12]

Tricalcium silicate C_3S is the major clinker phase in Portland cement and constitutes 55-60 wt.%. C_3S has fairly high heat development, rapid strength development, and high strength at 28 days. C_3S hydrate according to Equation 2. [12]

$$2\,C_3S + 6\,H \rightarrow C_3S_2H_3 + 3\,CH \tag{2}$$
$$1g + 0.24g \rightarrow 0.75g + 0.49g$$

Dicalcium silicate C_2S, constitutes 14-20 wt.% in Portland cement. C_2S has low heat development, reacts slow, and contributes substantially to the long term strength. Equation 3 shows the hydration of C_2S. [12]

$$2\,C_2S + 4\,H \rightarrow C_3S_2H_3 + CH \tag{3}$$
$$1g + 0.21g \rightarrow 0.99g + 0.22g$$

Tricalcium aluminate C_3A and tetracalcium aluminateferitte C_4AF contribute little to the final strength. They constitute about 5-10 wt.% and 6-10 wt.% of Portland cement respectively. A third reaction that contributes with Calcium Silica Hydrate (CSH) binder and strength is the reaction between pozzolanic material and Calcium Hydroxide (CH). Pozzolana contain silica and alumina and react accoring to Equation 4. Examples of pozzolanic material are FA and SF. [12]

$$2\,S + 3\,CH \rightarrow C_3S_2H_3 \tag{4}$$
$$1g + 1.87g \rightarrow 2.87g$$

C_2S produces more CSH gel and less CH per gram clinker phase, than C_3S as shown in Equations 2 and 3. CH is a weak hydration product. The pozzlanic hydration reaction which consumes CH and produce more CSH thus leads to better strength and durability properties. Fully hydrated cement paste contains about 70 wt.% CSH and 20 wt.% CH. CSH gel is formed as a very fine "needle-shaped" plate. The particle size is down on 1 nm. CH is crystalline. [12]

In Figure 5, 20 wt. % fine limestone(20 FL) with median particle diameter 2 μm increased the hydration compared to only Portland cement (PC). 20 wt.% coarse limestone (20 CL) with median diameter 130 μm only helped the hydration to a small extent. The hydration to FL has a bigger effect compared with the sample containing 20 wt.% quartz with equal particle size. [6]
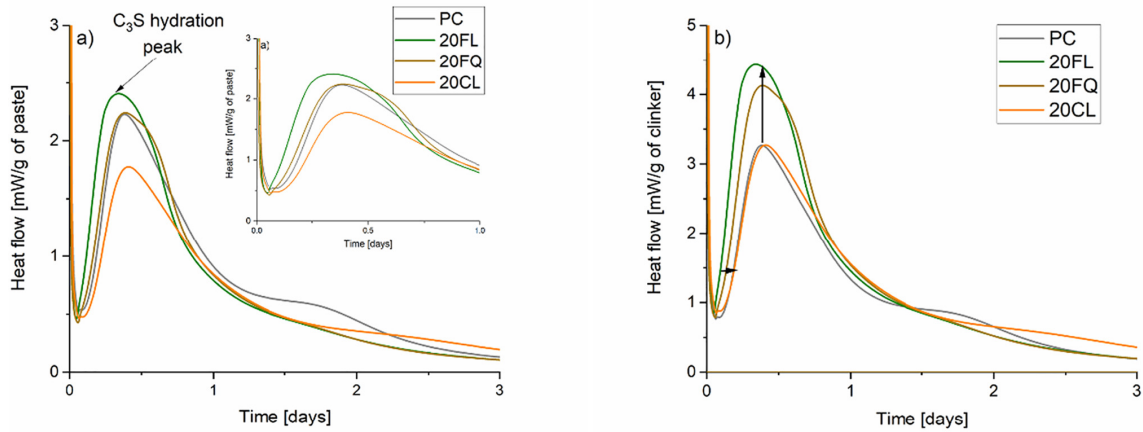
Figure 5: Impact of limestone on hydration behaviour for samples containing only Portland cement (PC), blended cement with 20 wt.% fine limestone (FL), coarse limestone (CL) and fine quartz (FQ). The graph to the left is normalized per g of paste, the one to the right is normalized per g of clinker. [6]

Figure 6 shows the CH development for samples containing Densified Silica Fume (DSF) with 4 different particle size intervals in addition to a blank reference sample. The sample with the smallest particle size DSF-IV ($<35\mu$m) show an increased CH content during the early cure. After 14 days all samples containing DSF had a decrease in CH content. This was explained by a faster consumption of CH by SF than the production of CH by cement hydration. From the result it was concluded that larger SF surface area make the reaction between SF and CH less effective and that only the surface reacts while the inner part does not react. [25]
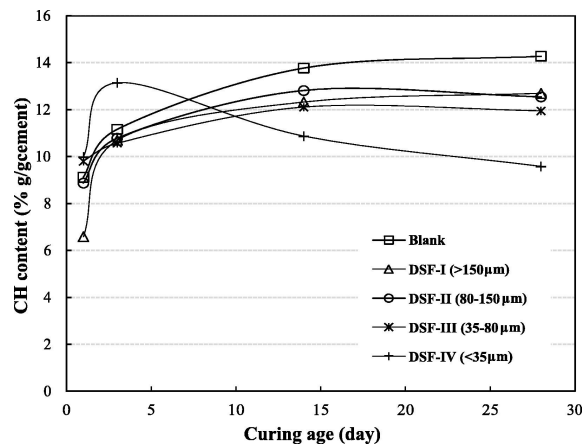
Figure 6: Calcium Hydroxide (CH) development with curing time for cements containing Densified Silica Fume (DSF) with different particle size and a reference sample. [25]

2.3   Carbonation

Concrete naturally carbonates when hydrates in the concrete react with CO_2 in the air and form carbonates, according to Reaction 5, 6 and 7. [23][14] CO_2 is thus bound up in the material permanently. Natural carbonation is a slow process. It starts at the surface and moves inwards. As the process progresses the pH slowly changes from 13 to 8 - 9. This can be a problem for reinforced concrete, since the steel can turn active and possibly corrode, and the material can lose mechanical strength. [23]

$$2\,NaOH + H_2CO_3 \rightarrow Na_2CO_3 + 2\,H_2O \tag{5}$$

$$Ca(OH)_2 + H_2CO_3 \rightarrow CaCO_3 + 2\,H_2O \tag{6}$$

$$Ca_3Si_2O_7 \cdot {}_4H_2O(s) + H_2CO_3 \rightarrow CaCO_3(s) + Ca_2Si_2O_6 \cdot xH_2O + (5-x)H_2O \tag{7}$$
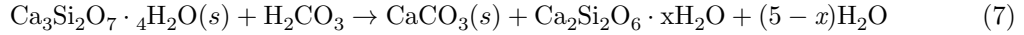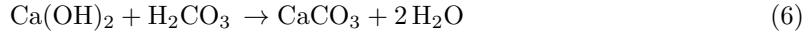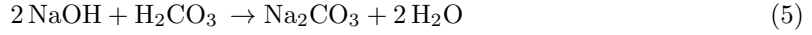
Enforced carbonation on recycled concrete or cement paste has been investigated in several studies. [43][42][19][10][15][11][41] Zajac et al. showed in their study that enforced carbonation of ground cement paste can be a fast process compared to the natural carbonation. The cement paste was almost completely carbonated after 6 h in an aqueous solution. The main products from the carbonation was calcite and alumina-silica gel rich in alkalis. No other calcium carbonate phases than calcite was formed.[43] Zajac et al. also discovered in another study that that the speed of the carbonation was independent from the CO_2 concentration in the solution and cement type as starting material. With wet carbonation the reaction was first limited by CO_2 dissolution when portlandite was the reactant. When it ran out of portlandite, the reaction was limited by diffusion of calcium, and dissolution of other hydrates. The produced alumina-silica gel based on composite cement paste was richer in alumina. [42] Ho et al. also carbonated concrete fines using in a aqueous solution with low-purity CO_2. The CO_2 uptake of the concrete fines was 0.13 g-CO_2/g-concrete fines. [11]

Lu et al. carbonated cement paste powder in a chamber with 99 % CO_2, at 20 ± 1 °C, and 60 ± 5 % RH. Analysis showed that the main products was calcite and silica gel, and that the calcite content was around 55.2 %. [19] By a two-step carbonation of recycled cement paste powder, a Ca-rich residue with 71 wt% calcite, and an alumina-silica gel rich residue was produced by Fang et al. [10]

By using TGA it is possible to identify the produced carbonates, and amount of carbonates in a concrete or cement paste. $CaCO_3$ as calcite decomposes at 760 - 950 °C or 650 - 950 °C. Calcite probably originate from carbonation of portlandite $Ca(OH)_2$. Aragonite and vaterite, two less stable phases of $CaCO_3$, decompose at 530 - 760 or 530 - 650 °C. Aragonite and vaterite are most likely products from carbonation of CSH. The temperature range is not precise. [40] $Ca(OH)_2$ decomposes at 420 °C, or 420-460 °C. [24][35] CSH and AFt (Ettringite) decompose at around 120 °C, for example 105-420 °C. [34]
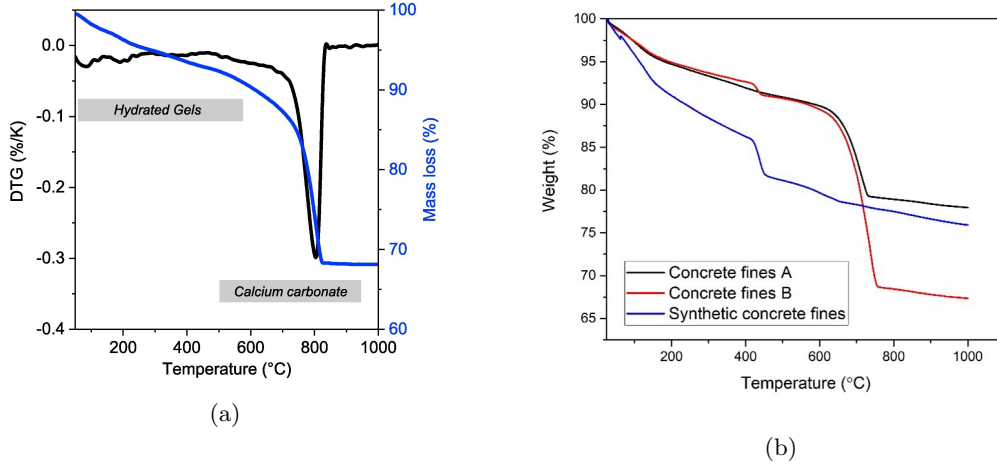
Figure 7: (a) TGA and DTG data of the carbonated cement paste from a study Zajac et al. [41] (b) TGA data of carbonated recycled concrete fines A and B, and simulated carbonated concrete fines from a study by Ho et al. [11]

2.4 Fillers and Pozzolana

Blended cement with fillers or pozzolana is frequently used to reduce the total CO_2 from the cement production and to reduce the costs. The material can be chemically active or non active. Non active materials are refereed to as fillers. Chemically active material reacts with Portland cement clinker or with its own hydration products. The most commonly used materials in Norway are FA and SF. [12]

As presented in Equation 4, the silica in pozzolanic materials reacts with CH from the cement hydration reaction, and form CSH gel. Table 5 shows the mean particle size, and SiO_2 content for Portland cement, FA and SF.

Table 5: Characteristics of FA and SF in comparison with Portland cement. [12]

Material	Mean particle size [μm]	SiO_2 [%]
Portland cement	10-20	20
FA	10-20	45-55
SF	0.1	85-98

SF is a by-product from the silicon and ferrosilicon production. SF has an amorphous structure, high silica content, and very fine spherical particles. The surface area is also very high. These properties make SF very reactive with CH, forming CSH. The small particles also contribute with a filler effect, possibly distributing the CSH phase, as well as making the pores finer. SF hydration is slow in the start since it is dependent on CH from the Portland cement hydration. When the reaction has started it is fast and almost fully reacted after 28 days.

FA originates from coal burning plants. The properties of FA depend on the coal burning plant, and the variation of properties varies more than for SF. FA particles are hollow and contain small spheres. FA is therefore ground together with the cement clinker to crush and access the smaller particles. If FA is ground too much, the particles will turn irregular and the good spherical

properties will be lost. In addition to silica, FA contains 20-30 % glassy aluminate phase that will also hydrate. These hydration products will also give an pozzolanic effect, but not to the level of CSH. FA reacts slower than SF due to its larger particles. The formation of CSH gel contributes to a finer pore structure in the same way as SF. [12]

Other kinds of used additives are blast furnace slag, volcanic rocks and minerals, diatomaceous earth, and rich husk ash. Blast furnace slag contains both SiO_2 and CaO, and are thus self reactive. But the reaction is very slow and needs an activator in the form of CH or sulphate to react. [12] Xiaodong et al. added 0 - 3 % SF to a blended cement with about 40 % FA. Analyzes showed that 2.0 % SF reduced water consumption with 4.5 %. The fluidity of cement paste can be increased by a small addition of SF. [20]

XRF data by Zajac et al. showed that carbonated concrete powder mainly contained CaO and SiO_2. The XRF data on cement clinker (C), fly ash (FA), carbonated cement paste (cCP), limestone (L), and anhydrite (A) are also seen in Table 6. [41]

Table 6: XRF data to cement clinker (C), fly ash (FA), carbonated cement paste (cCP), limestone (L), and anhydrite (A). [41]

Component	C	FA	cCP	L	A
LOI	0.35	4.31	30.33	43.12	4.20
SiO2	20.13	52.25	18.67	1.76	2.48
Al2O3	5.66	24.85	5.39	0.47	0.69
TiO2	0.29	1.25	0.41	0.02	0.02
MnO	0.04	0.05	0.09	0.02	0.00
Fe2O3	3.69	6.57	1.07	0.09	0.18
CaO	64.89	5.36	38.36	53.45	38.59
MgO	1.64	1.72	2.40	0.54	1.61
K2O	1.18	1.58	0.37	0.08	0.19
Na2O	0.10	0.63	1.12	0.00	0.02
SO3	0.92	0.26	1.27	0.15	50.90
P2O5	0.20	0.89	0.05	0.03	0.01
Sum	99.09	99.72	99.53	99.73	98.89

In a study by Lu et al., carbonated cement paste containing mainly $CaCO_3$ and silica gel. Non-carbonated cement paste contained CSH and CH. [19] The fresh concrete slurry waste in the study by Kumar Kaliyavaradhan et al. contained about 52.8 % CaO and about 27.3 % SiO_2. XRD result from the same study showed that the concrete slurry before carbonation contained portlandite, CSH, dolmite, quartz, and calcite. After the carbonation calcite was dominating in the material. [15] Calcite and amorphous alumina-silica phase were the main components in the carbonated concrete powder in the study to Zajac et al. [41] XRD data of carbonated cement paste powder in the study by Lu et al. showed that the main phases were calcite and aragonite. While the non-carbonated cement paste powder mainly contained portlandite (CH) and ettringite (AFt). The XRD pattern is seen in Figure 8. [19]
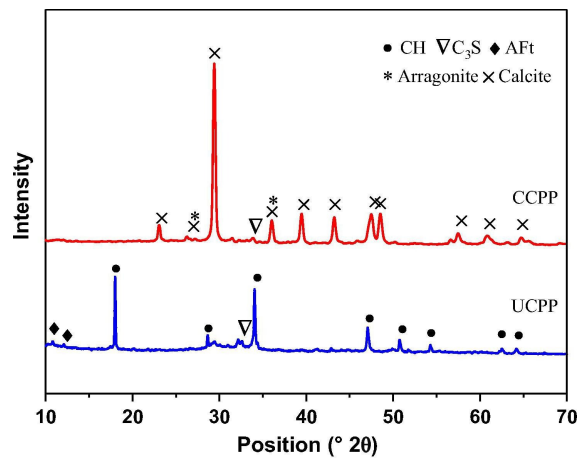
Figure 8: XRD result of carbonated cement paste powder (CCPP) and non-carbonated cement paste powder (UCPP) from the study by Lu et al. [19]

2.5 Compressive strength

In a study by Zajac et al. 38.64 wt% carbonated recycled concrete paste was used in composite cement together with 57.96 wt% clinker and 3.40 wt% anhydrite. Two blended cements, one only containing limestone and the other containing both limestone an FA were tested as reference samples. The sample containing carbonated concrete paste had the highest compressive strength up to 90 days. After 90 days, the sample with both limestone and FA was the sample with the highest strength. After 28 days the sample containing carbonated concrete paste achieved about 43 MPa in compressive strength. High surface area and the chemical composition were considered responsible for the pozzolanic properties and high rate. Carbonated concrete paste formed CSH and hemi- and monocarbonate, which resulted in a fine microstructure and increased compressive strength at early age. [41]

Lu et al. got increased compressive strength of cement paste samples with 10 to 20 wt% cement replaced with carbonated cement paste powder (CCPP) up to 90 days. 30 wt% carbonated cement paste gave a decrease in compressive strength. 10 to 30 wt% non-carbonated cement paste powder (UCPP) decreased the strength. Maximum achieved compressive strength after 28 days was 58.4 MPa for the sample containing 20 wt% carbonated cement paste. Which equaled 12 % higher compressive strength compared with the reference sample. The sample with 20 wt% non-carbonated cement paste achieved 44.2 MPa, which equals 85 % strength of the reference sample. The compressive strength development can be seen in Figure 9. [19]
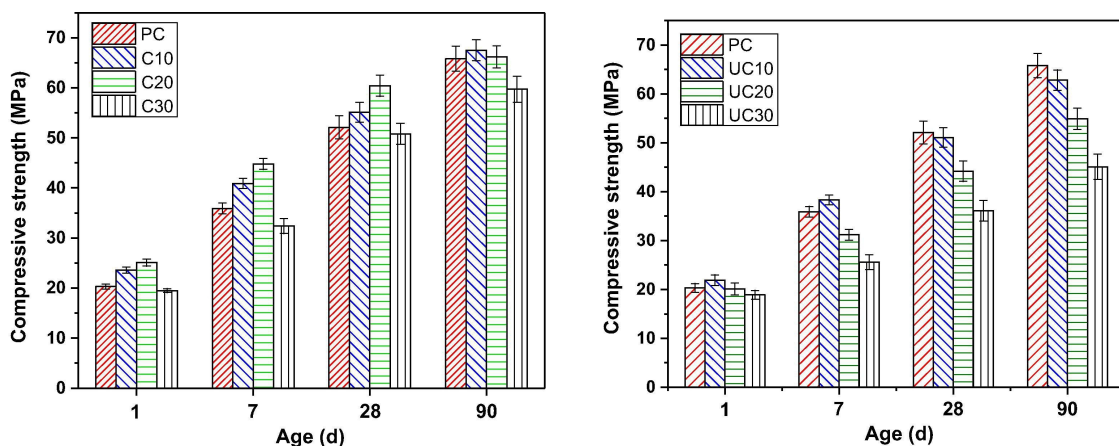
(a) Compressive strength of cement pastes with CCPP   (b) Compressive strength of cement pastes with UCPP

Figure 9: Compressive strength of composite cements containing 10 - 30 wt% carbonated respective non-carbonated cement paste [19]

Kumar Kaliyavaradhan et al. substituted 20 wt% cement with carbonated concrete slurry waste (CSW) and achieved 88.5 % strength after 7 days compared with the reference test, and 84.9 % strength after 28 days. The samples containing 20 % non-carbonated CSW obtained lower strength than the carbonated sample, reaching 76.8 % strength and 78.9 % strength after 7 and 28 days respectively. The higher strength for the sample containing carbonated material compared with the sample containing non-carbonated material was suggested to be due to the interaction between C_3A and $CaCO_3$ forming calcium carboaluminate hydrate. [15]

In a study by Chenxin et al. mortar compressive strength was tested with cement containing 10 % respective 20 % DSF. The test was done with 4 different DSF particles size intervals, and one

reference sample. The results in Figure 10a and 10b show that particle size below 80 μm increased compressive strength after 28 days. The improved strength is suggested to be due to the increased pozzolanic activity with finer particles, which results in more hydration products. [25]

(a) 10 %   (b) 20 %
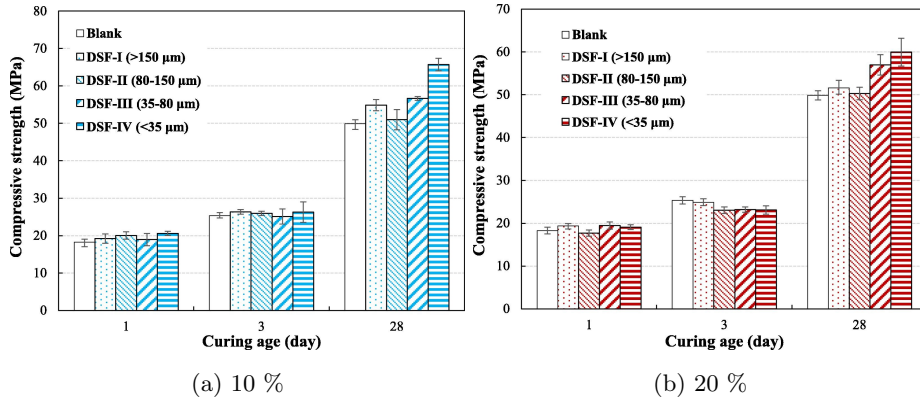
Figure 10: Compressive strength on mortar with cement containing (a) 10 % respective (b) 20 % DSF. Four samples with different DSF particle size and one reference sample. [25]

Decreasing Ca/Si - ratio increase compressive strength of CSH pastes according to Kunther et al.. This is partly explained by lower molar CSH volume and higher surface area. The compressive strength development for different Ca/Si - ratios are seen in Figure 11. [18]
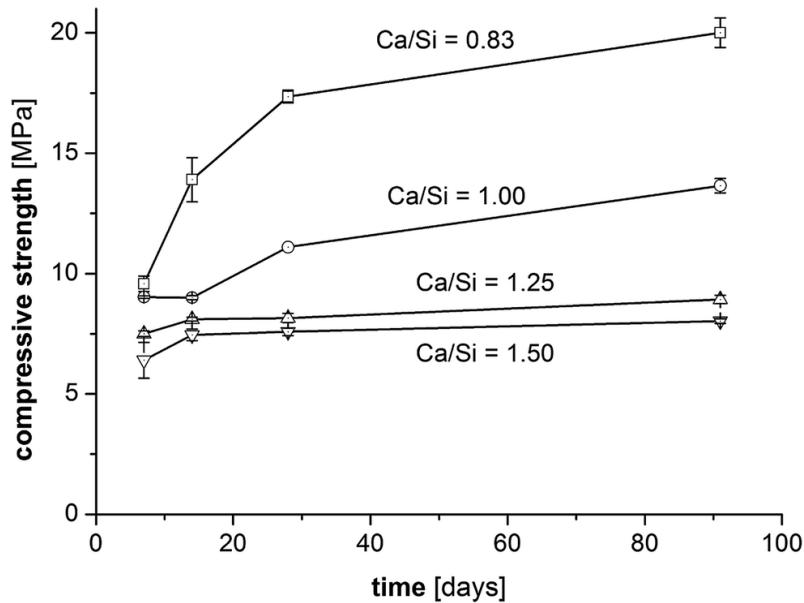
Figure 11: Compressive strength development with different Ca/Si - ratios. [18]

2.6 Particle size distribution

In addition to the composition, the hydration behaviour is also affected by the fineness of the particles as already mentioned. [12]

The particle size of cement is in the range 0.001 to 0.1 mm, with the average size 20 μm, (0.02 mm). Laser diffraction can be used to obtain the particle size distribution. By the Blaine-air permeability test, the specific surface area can be measured. The Blaine specific surface area of

Norwegian cement is normally in the range 360 to 550 m^2/kg. High surface area gives higher reactivity toward water. This implies promoted hydration, heat development and early-strength development. [12]

Figure 12 shows the hydration development for two samples, sample (a) with Blaine = 310 m^2/kg and sample (b) with Blaine = 484 m^2/kg. The curves show the increased hydration and temperature behaviour for sample (b) with higher Blaine surface area. [12]
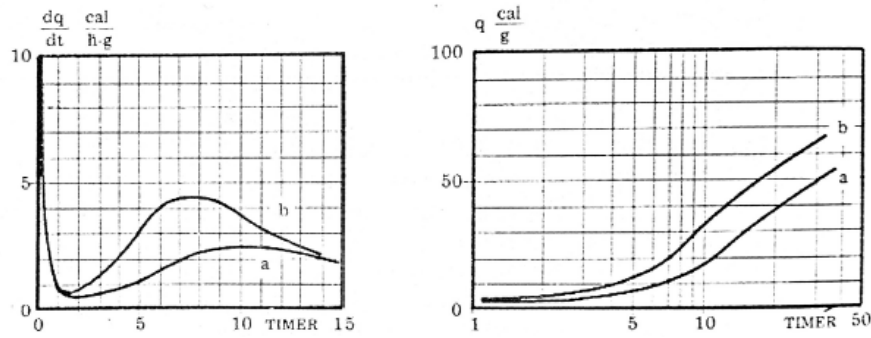
Figure 12: Heat development for two cements with different fineness. [12]

A study by Kumar Kaliyavaradhan et al. showed an increase in mean particle size of concrete slurry waste after carbonation. This was attributed to agglomeration, and the crystallisation into calcite. [15] Lu et al. experienced a decrease in particle size of there recycled concrete and cement paste powder after carbonation. [19]

2.7   Plasticizers and Superplastizisers

Plastizisers and superplastizisers are admixtures that disperse cement particles. The admixtures can disperse the particles in different ways. Electrostatic repulsion is when the negative polymers covers the particles, and work to repulse other particles. The steric hinderence effect is when the dispersion is caused by the presence of polymer chains covering the particles. Plastizisers and superplastizisers can be used to improve workability while water content is kept constant. [12]

3 Experimental

The experimental work was performed at SINTEF´s concrete laboratory in Trondheim, at the department of material science and engineering at NTNU in Trondheim, and at Norcem´s cement laboratory in Kjøpsvik. Preparation of the test materials, TGA, isothermal calorimetry, standard consistency, setting time, and compressive strength tests at 1 and 2 days were done by the author. Laser-granulometry and XRF were performed by employees at the chemical laboratory at Norcem in Kjøpsvik. Compressive strength tests at 7 and 28 days were also performed by personnel at physical laboratory at Norcem. XRD analysis was performed in Trondheim by an employee at the department of material science and engineering.

3.1 Collection of Test Material

8 different test materials with varying origin was collected for the investigation. Table 7 shows the materials and their origins. TM stands for Test Material and refers to the different concrete or cement paste powders.

Table 7: Overview of test materials and where they originates.

Test Material Carbonated	Test Material Non-carbonated	Origin
TM01	TM02	Concrete sludge with aggregates from the washing process at a concrete industry. Collected from sedimentation basin A.
TM03	TM04	Concrete sludge with aggregates from the washing process at a concrete industry. Collected from sedimentation basin B.
TM05	TM06	Concrete sludge with aggregates from the washing process at a concrete industry. Collected from sedimentation basin C.
TM07	TM08	Washing sludge from washing process at a concrete industry. Collected from a sedimentation basin.
TM09	TM10	Sludge generated from washing process of concrete trucks at ready-mix plant.
TM11	TM12	Sludge from drilling process of precast element.
TM13	TM14	Sludge generated from sawing of hollow core slabs at a precast element plant.
TM15	-	Demolished and carbonated concrete.

TM01-TM07 were received as sludge. They come from from washing water from a concrete industry. They are collected from different chambers in a sedimentation basin. TM01 and TM02 come from the same chamber, TM04 and TM05 another, TM06 and TM07 a third.

TM07 and TM08 also originates from washing water at a concrete industry, and is collected from

a sedimentation basin.

TM09 and TM10 originates from a ready mix concrete plant. The ready mix plant produces waste from its different processing steps. Washing water containing concrete and cement is produced at the premix station when the used equipment (container and mixer) are cleaned. Leftover concrete, or incorrectly produced or delivered concrete are other waste products that can be generated. Wash water from washing of the concrete truck drums are also generated. This ready mix plant reuse the washing water from the washing of the premixing station to wash the concrete mixer drums on the trucks. The waste water and waste material is collected and stored in a pile. A sample for this study was collected from the pile. The sample was collected from the top of the pile where the material was soft and possible to shovel.

TM11 and TM12 was collected as leftover sludge from the drilling of concrete products at a concrete plant. The sludge was scooped up from the industry floor with a shovel. The cement used in their production was FA cement. TM13-TM14 is leftover material from the sawing of concrete at a precast concrete element plant. The material was dried and TM13 was carbonated by Iveta Nováková. TM15 was received milled and carbonated.

3.2   Preparation of Test Material

All TM materials were dried in an oven on roasting tins at 105 ℃ for 4 days, except TM13, TM14 and TM15 which was received dried. The sludge with a lot of separated water on top was decanted before the sludge was scooped on the roasting tin. This to shorten the drying time. One fresh sludge sample with some separated water at the top can be seen in Figure 13a. The drying process of the sludge in the oven can be seen in Figure 13b. After drying, large lumps were crushed by a pestle and then each material was divided into two batches. One batch was carbonated in a chamber with 1 % concentration CO_2 gas, 20.0 ℃, and 60 % relative humidity for 7 days. The carbonated powder was then dried for 1 day at 105 ℃ to dry off any absorbed water. The other half was not carbonated. The external and internal of the carbonation chamber can be seen in Figure 14a and 14b.

| (a) | (b) |

Figure 13: (a) washing sludge as it was received wet from the industry. (b) material to dry in the oven.

All materials were milled in a Retsch RM 200 mortar for 2 minutes. The mortar´s external and
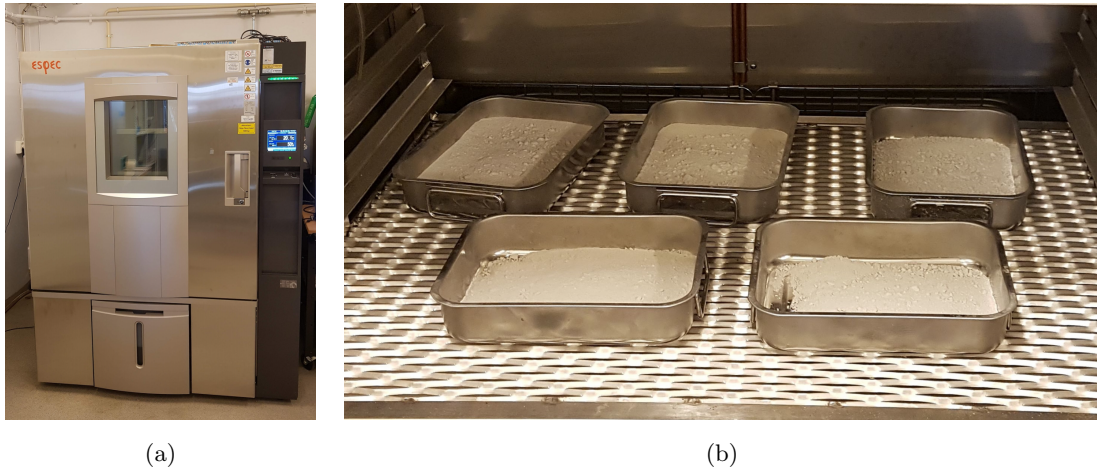
Figure 14: (a) carbonation chamber, and (b) samples inside the carbonation chamber.

internal are showed in 15a and 15b. Unmilled and milled powder can be seen in Figure 15c. Stones, metal fibers and wooden fibres were found in the test material, they were removed before the powder was milled. The stones and fibers can be seen in Figure 16.
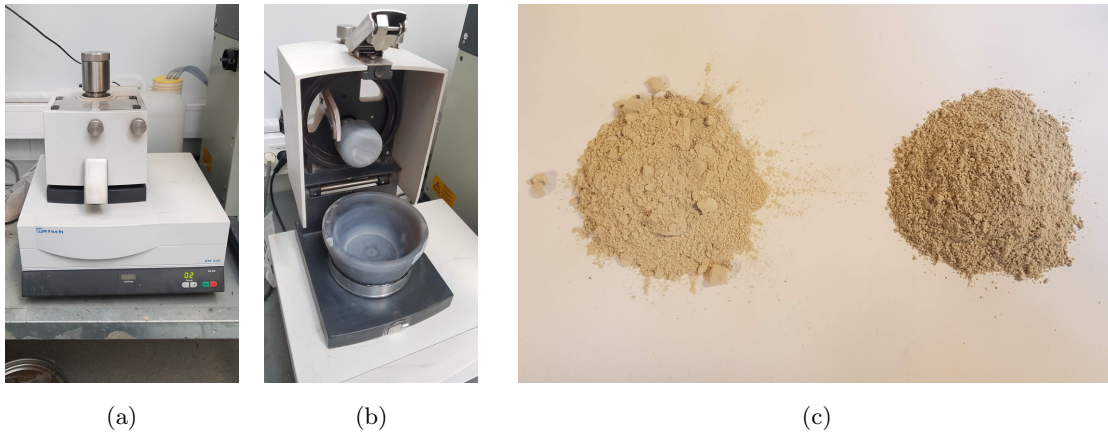
Figure 15: (a) and (b) shows the mortar, (c) shows the not crushed and finished crushed powder.
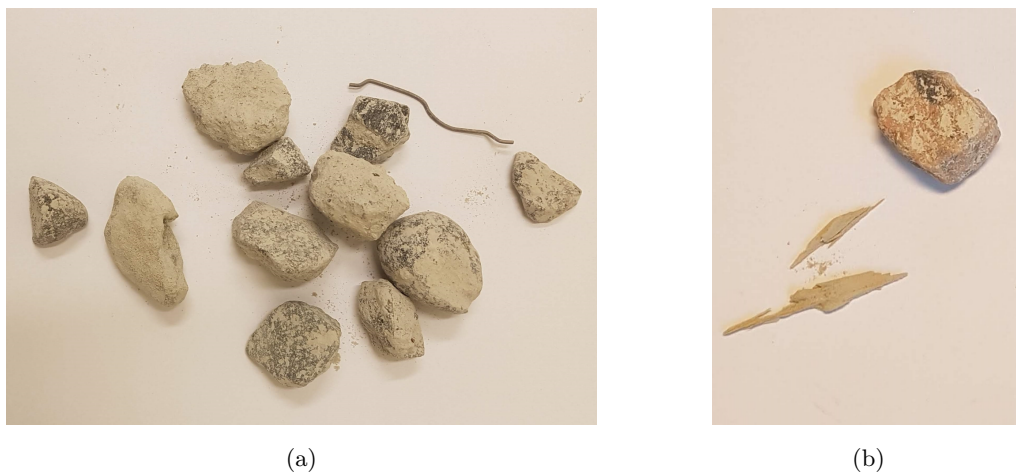
Figure 16: (a) Stones and metal fibre picked out from the sludge, and (b) stones and wooden fibre.

3.3 Characterisation Methods

Table 8 and 9 are overviews of all samples and analyses performed. RB is the ID for the composite cement samples, with 80 wt% Industrisement and 20 wt% test material. For the Isothermal calorimetry test, Industrisement from one batch was used. For the rest of the analyses on composite cements Industrisement from another batch was used, collected at Norcem cement plant in Kjøpsvik. Not all materials were tested for standard consistency, expansion, setting time, flexural and compressive strength. This was due to limited amount of material and time. Only TM09 - TM15 were analysed by XRD, this was due to time limitations.

Table 8: Overview of the TM samples and performed analyses.

Test Material (Concrete Powder)	TGA	PSD	XRF	XRD
TM01	✓	✓	✓	
TM02	✓	✓	✓	
TM03	✓	✓	✓	
TM04	✓	✓	✓	
TM05	✓	✓	✓	
TM06	✓	✓	✓	
TM07	✓	✓	✓	
TM08	✓	✓	✓	
TM09	✓	✓	✓	✓
TM10	✓	✓	✓	✓
TM11	✓	✓	✓	✓
TM12	✓	✓	✓	✓
TM13	✓	✓	✓	✓
TM14	✓	✓	✓	✓
TM15	✓	✓	✓	✓

Table 9: Overview of the RB samples and performed analyses.

Comp. Cement	Isothermal Calorimetry	Std. Consistency	Expansion Test	Setting Time	Flex. and comp. Strength
RB01	✓	✓	✓	✓	✓
RB02	✓				
RB03	✓				
RB04	✓				
RB05	✓				
RB06	✓				
RB07	✓				
RB08	✓				
RB09	✓	✓	✓	✓	✓
RB10	✓	✓	✓	✓	✓
RB11	✓	✓	✓	✓	✓
RB12	✓	✓	✓	✓	✓
RB13	✓	✓	✓	✓	✓
RB14	✓	✓	✓	✓	✓
RB15	✓	✓	✓	✓	✓

3.3.1 TGA

Crucibles made of alumina oxide were filled with test material until about two-thirds filled. Several crucibles were then placed on the sample carousel to the Mettler Toledo SDT for TGA analysis. The machine heated one sample at the time from 40-900 °C, and recorded weight loss with temperature. Nitrogen atmosphere with N_2 gas flow 50 ml/min was used for the test, and heating rate 10 °C/min. The Mettler Toledo SDT is showed in Figure 17a, pincette and crucible in Figure 17b, the scale inside the apparatus is shown in Figure 17c.
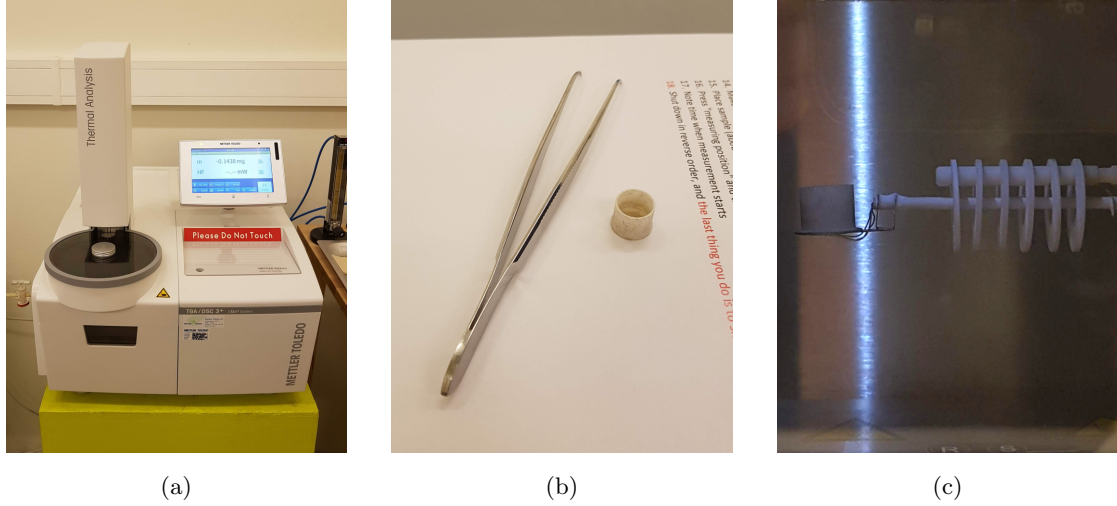
Figure 17: (a) TGA machine, (b) pincette and crucible, and (c) weight.

The amount of $C\hat{C}$ was calculated from the TGA data and Equation 8 and 9. W_1 and W_2 are the weight loss from the TGA result between the selected temperature range, 500 - 800 °C. W_0 is the start percent. M_{CaCO_3} and M_{CO_2} are the molar mass of $CaCO_3$ and CO_2, and are equal to 100 g/mol and 44 g/mol respectively. [5]

$$m_{CO_2} = \frac{W_1 - W_2}{W_0} \tag{8}$$

$$m_{CaCO_3} = m_{CO_2} \cdot \frac{M_{CaCO_3}}{M_{CO_2}} \tag{9}$$

The CO_2 uptake by the carbonated materials due to the carbonation was calculated by taking the difference in m_{CO_2} between to the carbonated and non-carbonated material, as presented in Equation 10.

$$m_{CO_2}(\text{uptake}) = m_{CO_2}(\text{Carbonated material}) - m_{CO_2}(\text{Non-carbonated material}) \tag{10}$$

3.3.2 Particle Size Distribution

Test material was sieved through a 250 μm sieve to ensure that no particles could damage the apparatus. The material that was stopped by the sieve was logged. The test material was loaded into the Cilas Particle Size 920, see Figure 18. The amount on each size interval was written down.

Figure 18: Cilas Particle Size 920 used for the particle size distribution analysis.

3.3.3 XRF and XRD

Chemical composition of both carbonated and non-carbonated test materials were investigated using XRF and XRD. XRF analysis was performed in Kjøpsvik with their with their machine configured with the settings they normally use for operation of the cement plant. XRD was performed in Trondheim, with the following settings.

- CuKα radiation ($\lambda = 1.54059$ Å)

- 40 kV and 40 mA

- range 5-70° 2θ

- step-size 0.02 ° 2θ

- Continuous rotation

XRF and XRD machines used can be seen in Figure 19. The raw data from the XRD test was analysed by the author. DIFFRAC.EVA was used to identify the present phases. PDF numbers used for identification of each phase are seen in Table 10.

Table 10: The PDF number used as reference to identify the phases present in TM09 - TM15 in the XRD result.

Phase	PDF - number
Albite	PDF 00-009-0466
Calcite	PDF 01-086-5302
Portlandite	PDF 00-044-1481
Quartz	PDF 01-075-8322
Vaterite	PDF 04-017-8634

<center>(a)   (b)</center>

Figure 19: (a) used XRD machine, and (b) used XRF machine.

3.3.4   Isothermal Calorimetry

15 samples of the different test materials were prepared in addition to one reference test only containing cement. 1 g test material and 4 g Norcem Industrisement was weight directly into the sample containers the day before the test. This to ensure the right temperature of the materials. The accuracy of the weight was 0,001 g. 2.5 g water was added into the containers using a pipette. A Vortex mixer was used to mix the cement paste for 1 minute with 4300 RPM. The samples were then placed into the isothermal calorimeter TAM AIR. A sample container is shown in Figure 20a, the mixer and pipette in Figure 20b and 20c. The calorimeter is shown in Figure 20d. The initial temperature inside the calorimeter and the temperature in the room was 20 °C. The calorimeter apparatus measured the temperature development over 7 days.

<center>(a)   (b)   (c)   (d)</center>

Figure 20: (a) Sample container, (b) Vortex mixer, (c) pipette and (d) isothermal calorimeter.

3.3.5   Standard Consistency

Standard NS-EN 196-3:2016 was followed for the standard consistence test. Deionized water, test material and cement had a temperature of 20 ± 2 °C before the test. The relative humidity was

<center>23</center>

over 50 %, and the temperature in the laboratory was 20 ± 2 °C. 400 g cement and 100 g test material was used. The right amount of water was found by trial and error. The water and composite cement was added into the mixing bowl and the mixing program on the ToniMIX was started, this was referred to as the "zero time". After 90 s at low speed the mixing stopped and the cement paste was scrapped into the middle from the sides and bottom of the bowl. After 30 s stop, mixing at low speed continued for 90 s. The cement paste was put into the vicat mould. Excess paste was removed with a metal spatula through gentle sawing motions. The top was then scrapped 2-3 times until a smooth surface was obtained. The mould was then placed in the Vicat apparatus, and the plunger was positioned at the surface of the cement paste and released 4 min ± 10 s after "zero time". After 30 s from the release or 5 s after the penetration had stopped the scale was read. The test was then repeated with different amount of water until the distance from the base-plate and the plunger was 6 ± 2 mm. The required amount of water for each test was noted. The ToniMIX and the vicat apparatus are shown in Figure 21a and 21b.

(a)   (b)
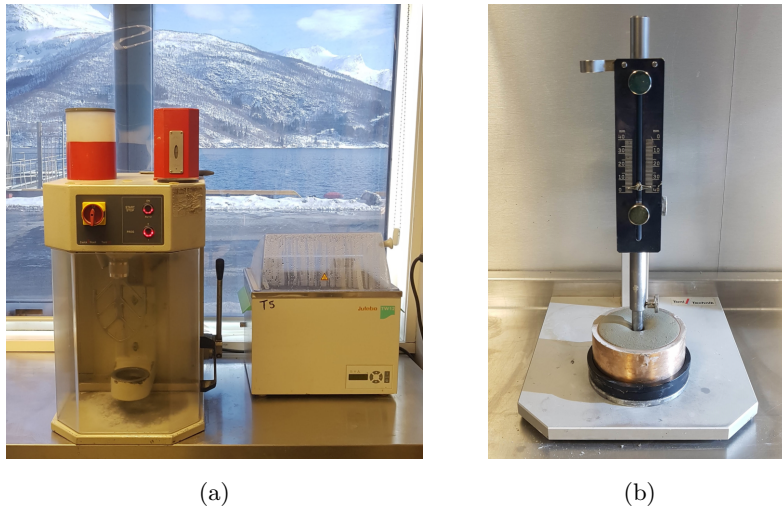
Figure 21: (a) ToniMIX, and (b) vicat apparatus.

3.3.6 Expansion Test

Expension tests were performed according to the standard NS-EN 196-3:2016. The remaining of the succeeded cement paste mix from the consistence test were used for the expansion test. Two oiled Le chatelier forms on top of a glass plate was filled with cement paste using a spatula. Cement paste was gently pressed down on one side, the form was then flipped and the last was filled from the other side. A second glass plate was gently pressed on top of the form, allowing excess cement paste to squeeze out. Weights were then placed on top of the glass plate to ensure enough pressure, see Figure 22a. The Le chatelier forms were then left on the bench for a few hours before they were submerged into the water tank for storage over the night. This step diverges slightly from the instructions in the standard. The next day, the forms were identity marked, and the distances between the indicator points were measured to the nearest 0.5 mm. They were then placed into the stand, see Figure 22b. The stand was submerged into the boiler ToniCHAT. The boiler program heats up the water from 20 °C to boiling point during 30 ± 5 min. It then maintained boiling for 3 h and ± 5 min. The distances between the indicator points were measured once more and logged.
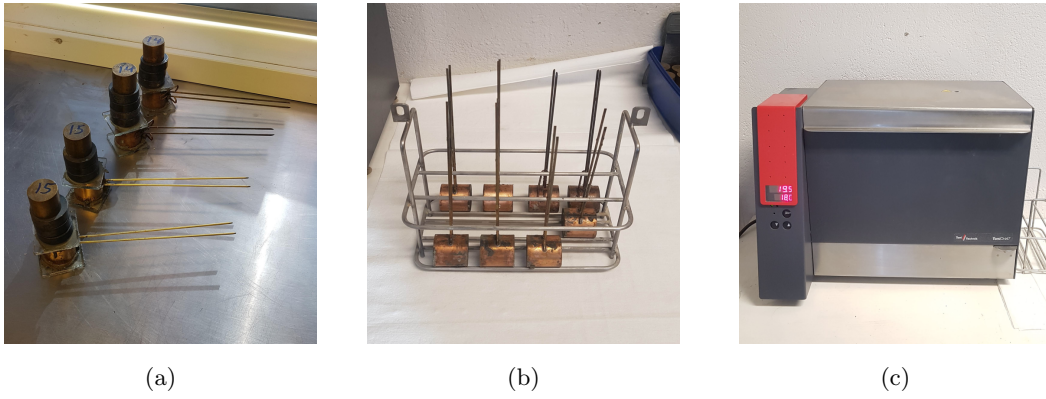
Figure 22: (a) Filled Le chatelier forms with additional mass, (b) Le chatelier forms in the stand, and (c) the boiler ToniCHAT.

3.3.7 Setting Time

The same vicat mould containing the cement paste from the succeeded standard consistence test was used for the setting time test. Standard NS-EN 196-3:2016 was also followed for this test. A metal spatula was used to smoothen the surface after the plunger. The mould was then submerged into the water bath belonging to the automatic setting time apparatus ToniSET Classic. Water percent, Vicat distance, and "zero time" was typed into the testing machine before it was started. The water bath was kept to 20 ± 1 °C during the test. After 60 minutes rest, a needle was automatically released and penetrated the cement paste at testing locations separated by more than 10 mm. The penetration distances were recorded. The initial setting time was determined by measuring elapsed time from "zero time" to the moment when the distance between base-plate and needle was 6 ± 3 mm. The initial time was rounded to the nearest 5 min. The final setting time was also determined from the measurements. The ToniSET Classic setup is shown in Figure 23a, and the needle penetrating the cement paste is shown in Figure 23b.
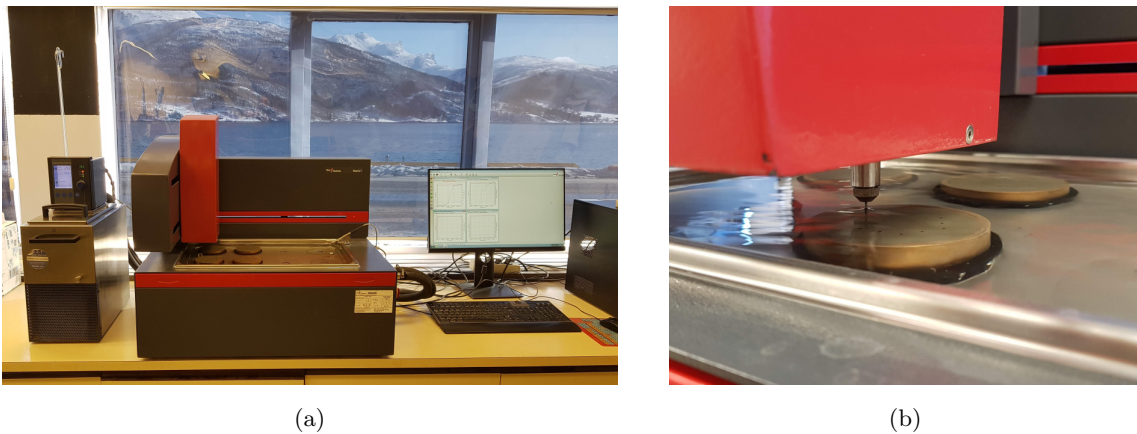
Figure 23: (a) Setup of the ToniSET classic, and (b) needle penetrating the cement paste.

3.3.8 Flexural and Compressive Strength

The compressive strength was tested according to NS-EN 196-1:2016. The cement, test material, water, and sand had a temperature of 20.0 ± 1.0 °C before the test. The temperature in the

laboratory was 20 ± 2 °C and the relative humidity was over 50 %. 450 ± 2 g blended cement was prepared by homogenizing 90 g test material and 360 g Industrisement. This gives 20 wt% supplementary material in the cement mix. The blended cement was then added into the mixing bowl. A ToniMIX mixer was used. The automatic mixer program added 225 ± 1 g deionized water and mixed at low speed for 30 s. This results in a water/cement ratio equal to 0.5. One 1350 ± 5 g bag sand was added automatically during the next 30 s. The next 30 s was mixed at high speed. When the mixer stopped the adhering mortar on the walls and bottom was scrapped in to the middle. The next 60 s was mixed at high speed. Mortar was then scooped into the feeding hopper on top of the mould in two layers while the mould was standing on a vibration table for 120 ± 1 s. The Vibrating Table Toni VIB are shown in Figure 24a. The surface of the mould was then finished using a metal straightedge. First sawing motions back and forth without any angle between the metal straightedge and the mould to spread the mortar out. Then with a small angle and straight motion to strike off left-over mortar. The latter can be seen in Figure 24b, it was however performed using two hands. The mould contained 3 prisms with dimensions 40 mm x 40 mm x 160 mm. This was repeated with 4 moulds, giving a total of 12 prisms for 6 different composite cements. Additionally, only three moulds with RB01 were made and one mould with RB15, due to limited amount of test material. The moulds were stored for 24 hours in a moist cabinet. They were then demoulded, the prisms were marked, weighed and placed in a 20.0 ± 1.0 °C water tank for storage until testing time. The water tank is shown in Figure 25.

<center>(a)   (b)   (c)</center>
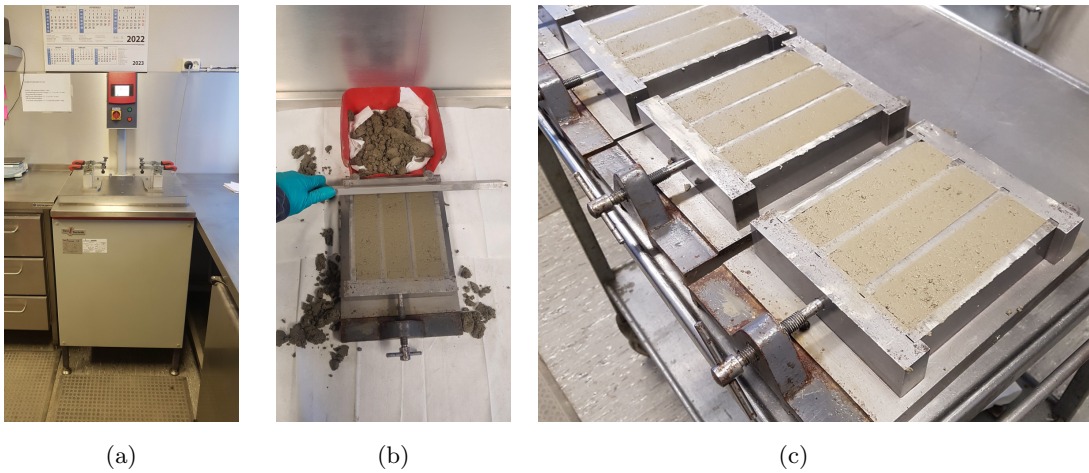
Figure 24: (a) Vibrating Table Toni VIB, (b) finishing of the moulds and (c) a set with mortar prisms.

The prisms were strength tested after 1, 2, 7 and 28 days. First they were broken using three point bending apparatus for flexural strength measurement, see Figure 26a. Then strength tested using a compressive strength apparatus, see Figure 26b. The strengths were reported in MPa by the testing machine. The average compressive strength for each age is calculated by summing up the three results S_1, S_2 and S_3 and dividing by 3, see Equation 11. The relative compressive strength is calculated by dividing the mean compressive strength, B with the reference compressive strength, A, see Equation 12.

$$\frac{S_1 + S_2 + S_3}{3} = B, \text{mean compressive strength} \tag{11}$$

Figure 25: Mortar prisms stored in a water tank until strength tested.

$$\frac{B}{A} \cdot 100\% = \%, \text{compressive strength compared to reference} \qquad (12)$$
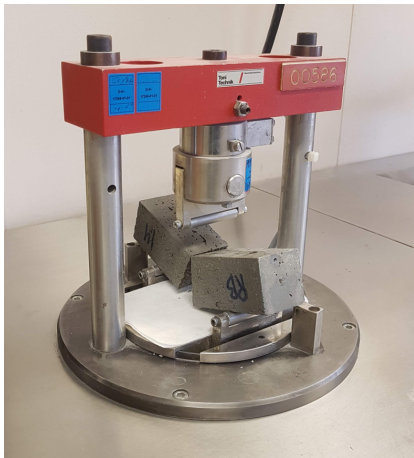
| (a) | (b) |

Figure 26: (a) Flexural strength, and (b) compression strength.

4 Results

The results from all experimental work is presented in this section.

4.1 Compressive strength

The compressive strength development for the RB samples and the reference sample is shown in Figure 27. C and NC in the label stands for carbonated respectively non-carbonated. It is observed that the strength at all ages is greater for the reference sample compared with the strength to all the RB composite cements. There is not any clear unambiguous difference between the samples containing carbonated test material (solid lines), or non-carbonated material (dashed lines). RB09 containing carbonated material show less compressive strength at 1 day compared with RB10 containing non-carbonated material, but greater strength compared to RB10 between 2 and 28 days, see Figure 66 in the Appendix. There is no distinct difference between RB11 and RB12, they alternates on showing highest strength at different times, see Figure 67 in the Appendix. RB13 containing carbonated material show less strength development compared with RB14 containing non-carbonated material at all times as can be see Figure 68 in the Appendix. The strength development to RB01 is also shown alone with the reference in Figure 65 in the Appendix. The flexural and compressive strength values are also presented in Table 20 in the Appendix.
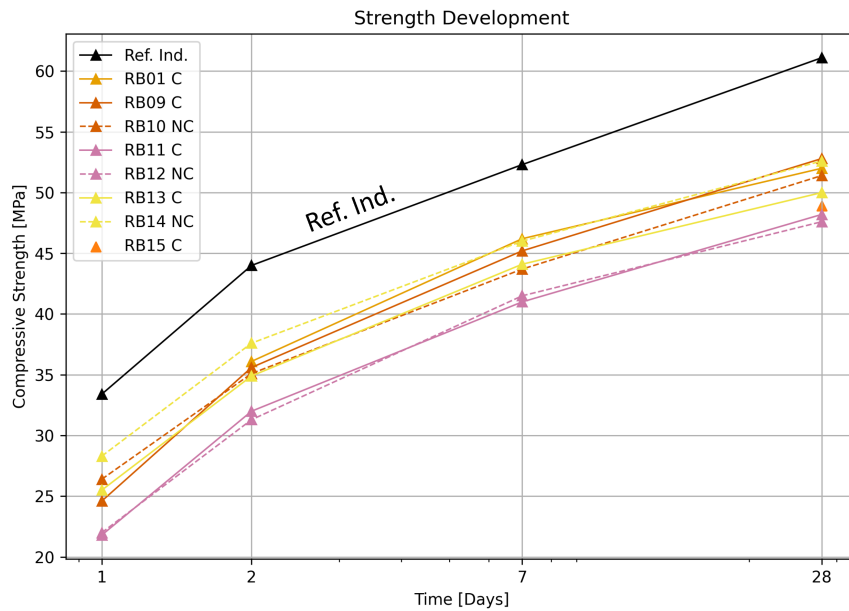
Figure 27: Compressive strength of RB01, RB09 - RB15, and the reference sample.

In Figure 28 the relative compressive strength calculated according to Equation 12 are shown. Sample RB01, RB09, RB10, RB13 and RB14 are above 80 % after 28 days. RB15 has exactly 80 % compared with the reference sample after 28 days. RB11 and RB12 have lower than 80 % after 28 days. RB10 and RB11 show a positive development in relative compressive strength at 28 days. RB09 show equal relative compressive strength at 7 days and 28 days. The rest of the samples show a decreasing development in realtive compressive strength at 28 days. The data are

also presented in Table 21 in the Appendix.
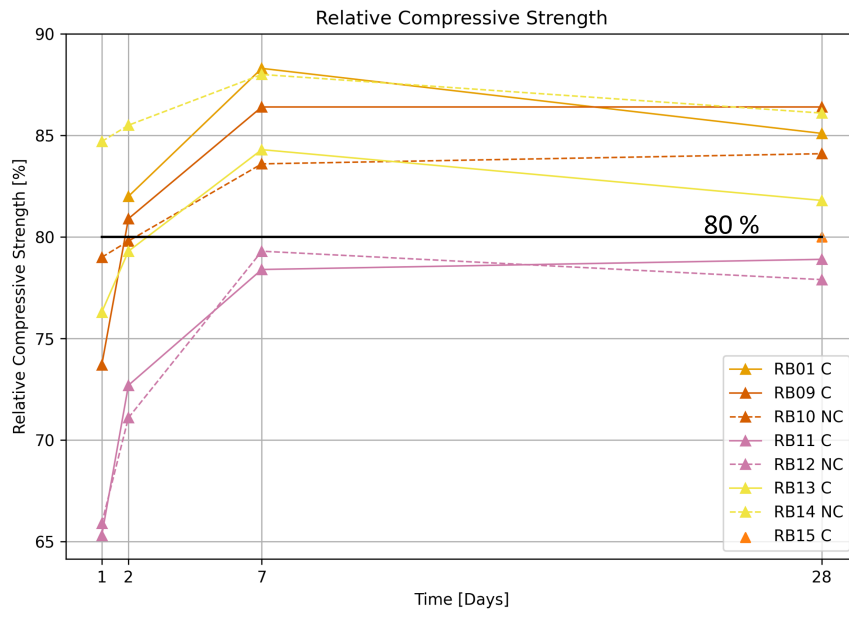
Figure 28: Relative compressive strength of of RB01 and RB09-RB15.

4.2 TGA and DTG

The TGA data are presented in Figure 29. In the figure the weight loss with temperature is shown for all the TM materials. As are shown in the figure does the total weight loss vary from about 5 to 30 % for the different samples. In Figure 30 the DTG results are presented for all the TM samples. In the figure it can be seen that the number of depressions due to weight loss varies between the different test materials. The temperature intervals at which the weight loss occur also varies. Weight loss are observed at 0 - 300 °C, 300 - 400 °C, 450 - 500 °C and 500 - 800 or 900 °C. TGA and DTG results for each carbonated and non-carbonated pair are presented in Subsection 8.2 in the Appendix. The calculated CO_2 uptake between 500 - 900 °C for all the carbonated materials are presented in Table 11. The value are given in g CO_2/ g recycled fines. In the table it can be seen that 0.10 g CO_2/ g recycled fines, is the highest value belonging to TM01, followed by 0.07 g CO_2/ g recycled fines, by both TM05 and TM09.
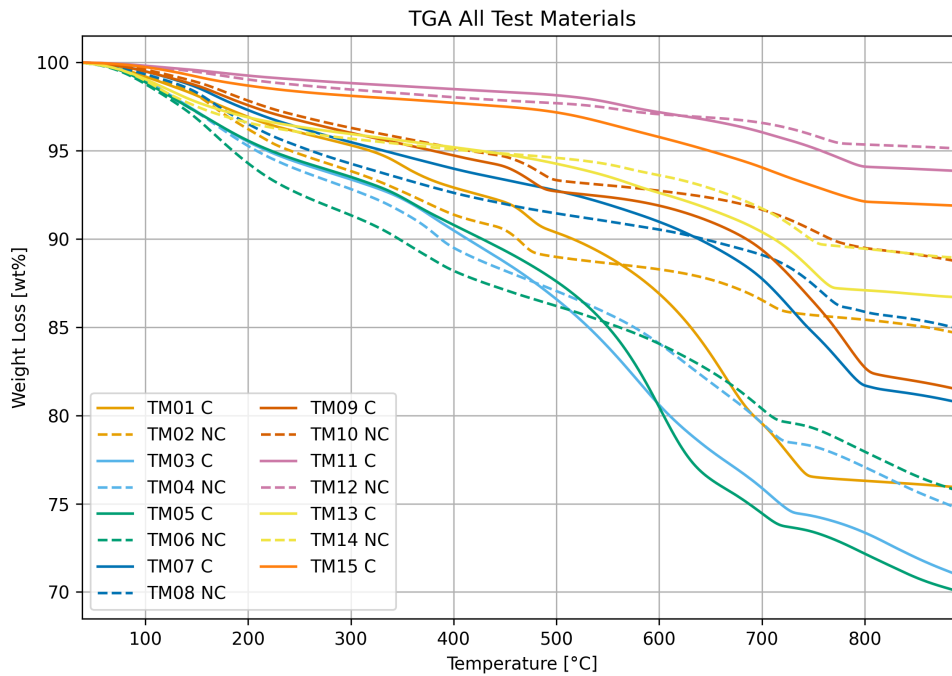
Figure 29: TGA results of TM01 - TM15.
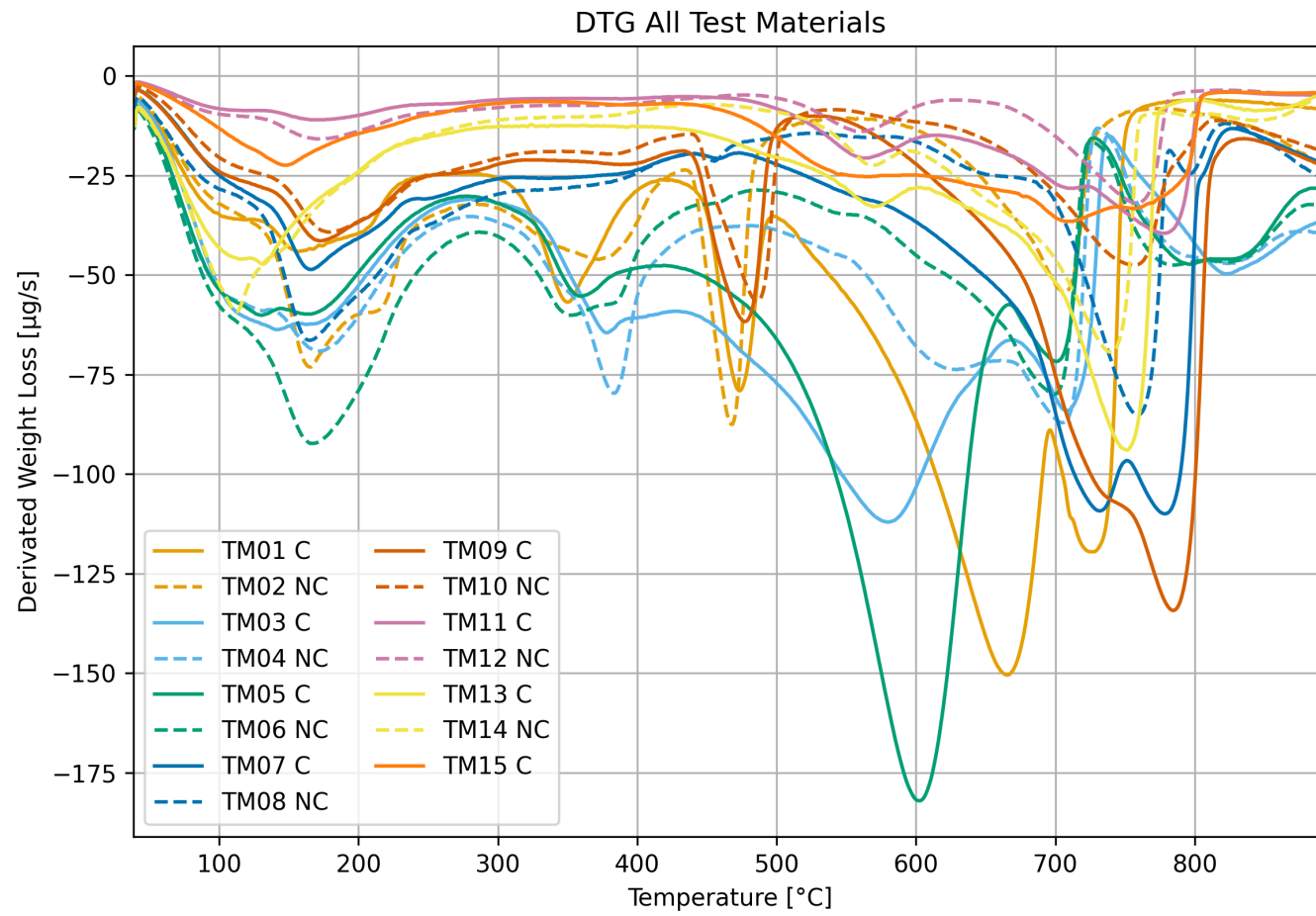
Figure 30: DTG results of TM01 - TM15.

Table 11: Calculated CO_2 uptake for the carbonated materials due to the carbonation, based on the temperature range 500 - 900 °C.

Carbonated Sample	CO_2 uptake [g CO_2/ g recycled fines]
TM01	0.10
TM03	0.03
TM05	0.07
TM07	0.05
TM09	0.07
TM11	0.02
TM13	0.02

The calculated CĈ contents are shown in Figure 31. In the figure it can be seen that TM05 has the largest amount CĈ with 39.9 %, followed by TM03 and TM01 with 35.6 and 32.8 %. It can be seen that TM02, TM10, TM11 and TM12 are the samples with the lowest calculated CĈ content. Figure 31 shows the values for the calculated CĈ content, and the difference between the carbonated and non-carbonated in percentage points. In the table it is shown that the CĈ content is higher for all the carbonated materials compared with the same non-carbonated material. TM01 is the sample with the largest increase in CĈ content compared with the same but non-carbonated material.
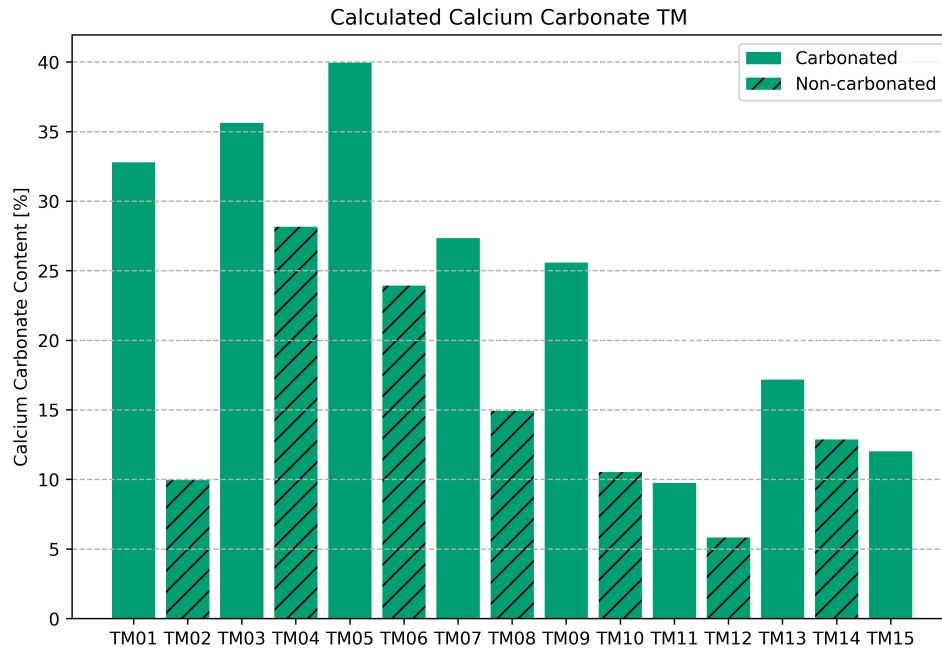
Figure 31: Calculated calcium carbonate content in % for the TM samples.

Table 12: Calculated amount CĈ based on weight loss between 500 - 900 ℃.

Test material	Calc. CaCO$_3$ [%]	Difference Carb./Non-carb. [pp]
TM01	32.8	22.9
TM02	9.9	
TM03	35.6	7.5
TM04	28.2	
TM05	39.9	16.0
TM06	23.9	
TM07	27.3	12.4
TM08	14.9	
TM09	25.6	15.1
TM10	10.5	
TM11	9.8	3.9
TM12	5.8	
TM13	17.2	4.3
TM14	12.9	
TM15	12.0	

4.3   Particle Size Distribution

The particle size distribution of the test materials TM01-TM15 are shown in Figure 32 together with FA. In the Figure it can be seen that there are both samples with larger and smaller particles size compared with FA. The median particle size for each TM sample is shown in Table 32 in the Appendix. Table 13 show the difference in particle size in μm, and in percent for the carbonated and non-carbonated couples. The data show that the carbonated samples consistent for all TM materials have smaller median particle size compared with same material but non-carbonated. The reduction in particle size is more than 20 % for TM02, TM04, TM10 and TM12. TM04 has the largest decrease with 5.66 μm and 42.4 %. TM08 and TM14 did not have that big decrease of the particle size, only 5-10 %. The 250 μm sieve residue is presented in Figure 34. It can be seen that most of the TM powders have sieve residue around 40 % or more, while TM11 and TM12 stands out with small sieve residue with around 10 %.
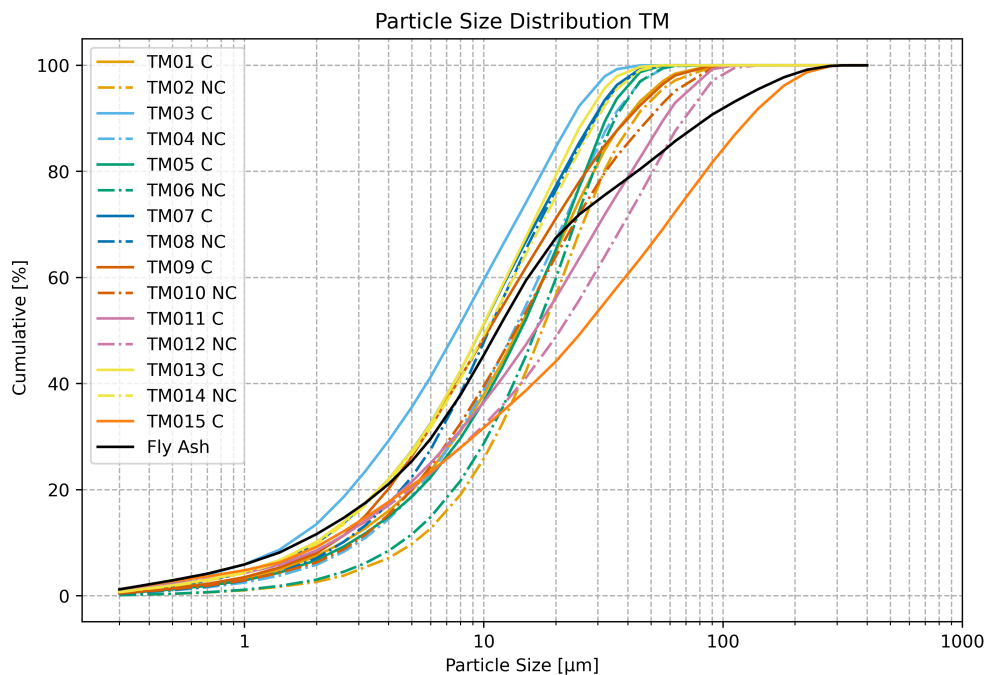
Figure 32: Particle size distribution of the TM samples and of FA.

Table 13: The differences in median particle size of carbonated and non-carbonated TM samples.

Test material	Difference in particle size [μm]	Percentage Decrease in Particle Size [%]
TM01 - TM02	- 3.59	20.5
TM03 - TM04	- 5.66	42.4
TM05 - TM06	- 2.38	14.4
TM07 - TM08	- 0.80	7.6
TM09 - TM10	- 3.14	23.1
TM11 - TM12	- 4.44	21.3
TM13 - TM14	- 0.55	5.4
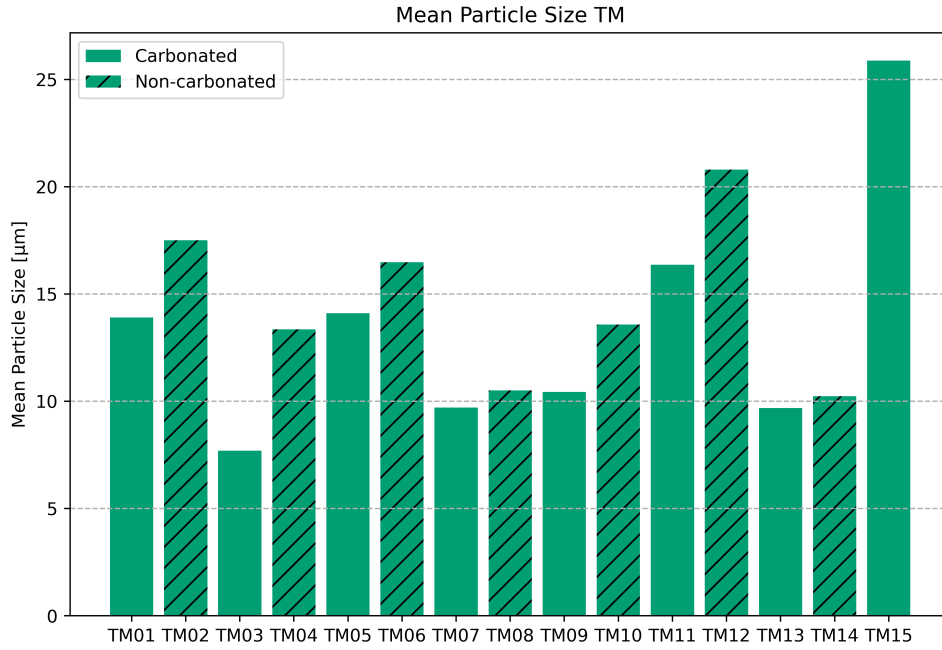
Figure 33: Mean particle size of TM01 - TM15.

Figure 34: Sieve residues of the TM samples given in percent.

The particle size distribution of the composite cement samples RB01 and RB09 - RB15 are shown in Figure 35. It can be seen that the industry reference sample has a lower particle size distribution compared with the RB samples. It can be observed that the RB samples are quite alike.

The Standard FA cement has a higher particle size distribution then the other samples. These observations are also visible for the median particle size in Figure 36. The median particle size values are shown in Table 33 in the Appendix. The RB samples and the industry reference sample have small deviations, less than 1.24 μm. It can also be seen that the Standard FA sample has about 1.5 μm larger median diameter than the RB samples. The 250 μm sieve residue to the RB samples are presented in Figure 37. It can be seen that the reference sample contained almost no particles larger than 250 μ. While RB01 and RB09-RB15 show sieve residues from about 10 % to about 25 %. RB10 stands out with almost 25 % sieve residue, and RB12 with the least amount less then 10 %.
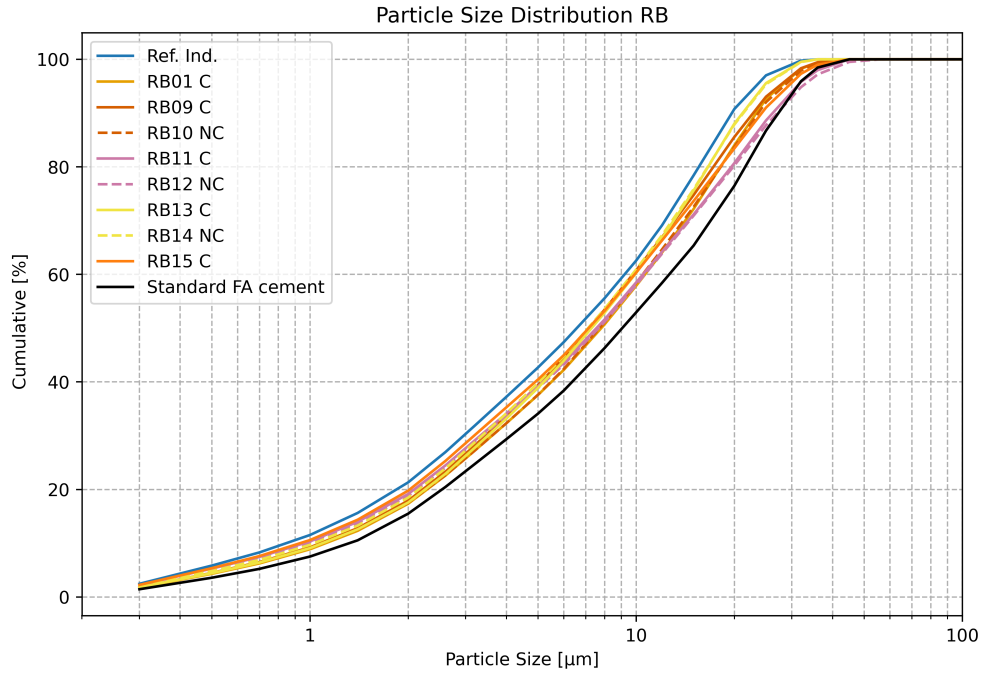
Figure 35: Particle size distribution or RB01, RB09 - RB15, the reference sample, and Standard FA cement.
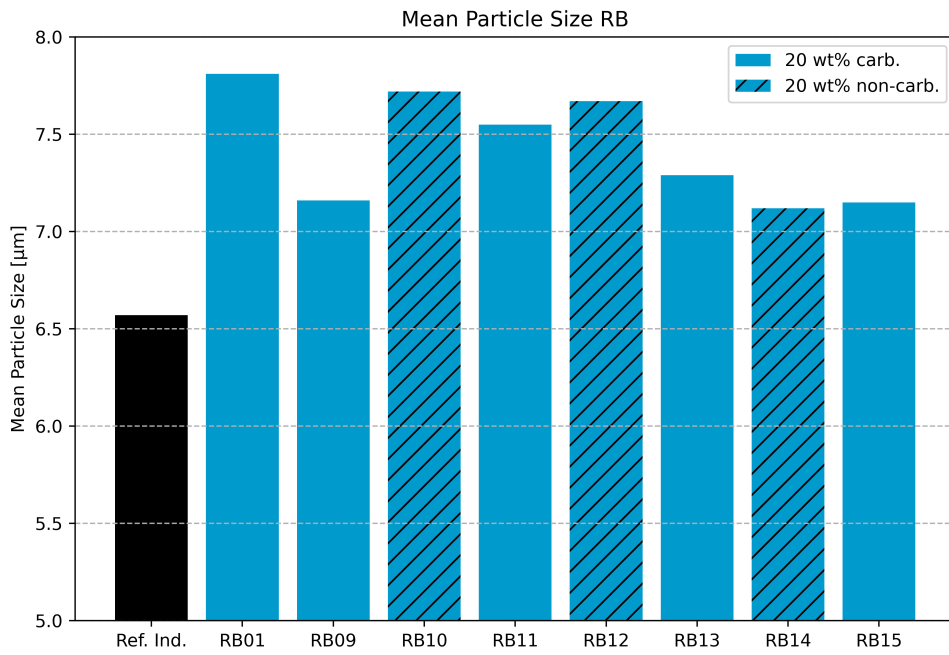
Figure 36: Mean particle size of RB01, RB09 - RB15, and the reference sample.
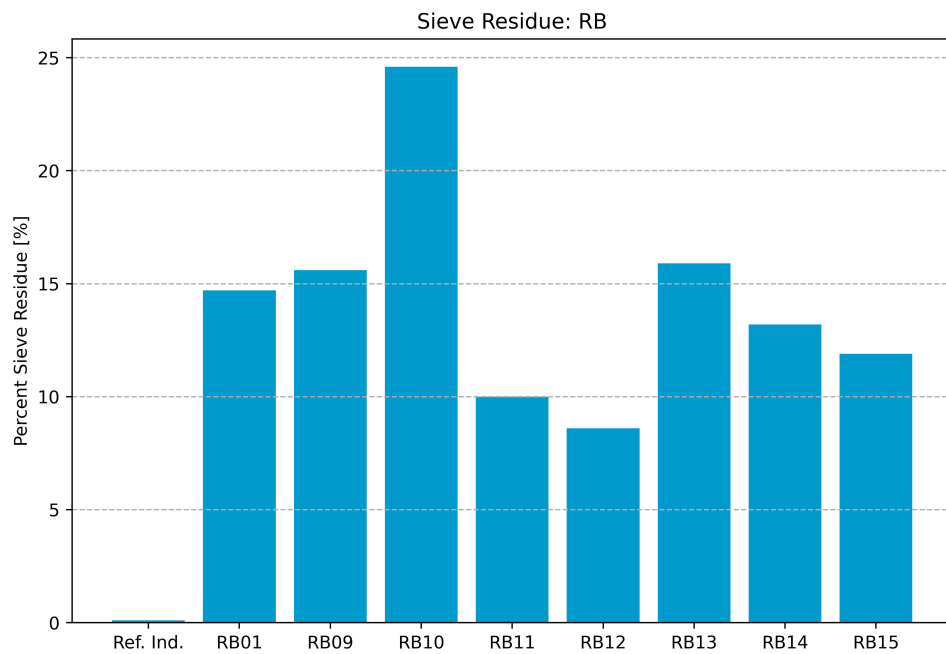
Figure 37: Sieve residues of RB01, RB09 - RB15, and the reference sample.

4.4 XRF

The XRF data to the TM samples are shown in Table 14. The table includes the oxides that are present in the largest extent, in addition to Loss On Ignition (LOI). The oxides and LOI are given in wt%. In Table 14 it can be seen that the amount CaO varies between 19.5 to 32.24 wt%, and the SiO_2 between 21.88 to 42.74 wt%. The CaO/SiO_2 - ratio is varying from 0.46 to 1.41 for the TM materials. The CaO and SiO_2 content, and the CaO/SiO_2 - ratio are also shown in Figure 38 for easier comparison. In the figure it is seen that the CaO/SiO_2 - ratio is greater than 1.0 for some samples, and less than 1.0 for some samples. The differences between the carbonated and non-carbonated materials for each oxide is small, and there is not possible to identify one clear trend for the small changes due to the carbonation. Three materials got higher CaO/SiO_2 - ratio after carbonation, two got lower and one stayed the same. Al_2O_3 content is varying from 5.67 to 10.01. The Fe_2O_3 content is significant higher for TM11 and TM12 compared with the other materials. TM03 and TM04 have some higher MgO content than the rest of the materials.

Table 14: The XRF result of TM01 - TM15 given in wt%.

| Test material	CaO	SiO_2	Al_2O_3	Fe_2O_3	MgO	Na_2O	K_2O	SO_3	L.O.I.	CaO /SiO_2
TM01	24.11	39.3	6.31	2.66	1.42	1.2	1.28	0.31	20.5	0.61
TM02	23.8	41.21	6.34	2.76	1.37	1.23	1.25	0.29	20.2	0.58
TM03	29.88	21.97	5.67	2.65	6.56	1.92	0.41	2.68	30.63	1.36
TM04	29.86	21.88	5.7	2.65	6.6	1.99	0.42	2.79	30.66	1.36
TM05	32.24	23.43	6.51	3.12	3.78	0.81	0.15	2.11	29.46	1.38
TM06	32.05	22.78	6.43	3.08	3.76	0.96	0.22	2.22	29.29	1.41
TM07	26.51	33.23	8.58	3.09	1.14	1.29	1.45	0.94	22.08	0.80
TM08	26.63	33.76	8.82	3.13	1.17	1.35	1.48	1.04	22.21	0.79
TM09	27.21	33.52	7.12	3.54	1.58	0.94	0.79	1.07	23.11	0.81
TM10	26.76	34.7	7.1	3.51	1.54	0.99	0.83	1.1	22.71	0.77
TM11	20.27	40.94	7.45	9.46	2.28	1.26	0.58	0.25	18.42	0.50
TM12	20.29	41.26	7.51	8.72	2.28	1.24	0.6	0.27	18.43	0.49
TM13	22.2	41.15	8.59	3.59	1.28	1.71	1.6	0.43	18.84	0.54
TM14	22.39	39.97	8.32	3.5	1.23	1.62	1.54	0.53	18.94	0.56
TM15	19.5	42.74	10.01	2.59	0.85	2.29	2.38	0.19	16.25	0.46

The XRF data for the RB01, RB09 - RB15 and the reference sample are shown in Table 15. The CaO and SiO_2 content, and CaO/ SiO_2 - ratio are also shown in Figure 39. In the figure a clear difference between the reference sample and the RB samples are seen. The CaO/ SiO_2 - ratio is about 3 for the reference sample, and about 2 for the RB samples.
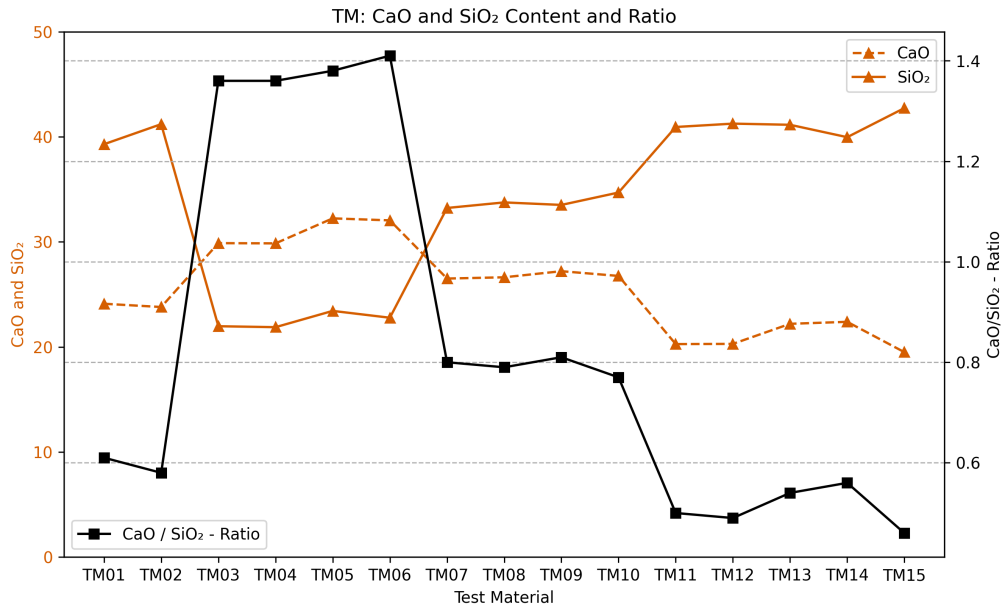
Figure 38: The amount CaO and SiO$_2$, and the CaO/ SiO$_2$ - ratio to TM01 - TM15. Amount CaO and SiO$_2$ are given in wt%.

Table 15: The XRF result of RB01, RB09 - RB15, and the reference sample. Amounts are given in wt%.

Test material	CaO	SiO$_2$	Al$_2$O$_3$	Fe$_2$O$_3$	MgO	Na$_2$O	K$_2$O	SO$_3$	L.O.I.	CaO /SiO$_2$
Ref Ind.	60.32	18.97	4.89	3.13	1.68	0.77	0.74	3.71	3.01	3.18
RB01	49.18	27.63	5.62	3.36	1.62	0.91	0.98	2.96	5.38	1.78
RB09	52.97	22.89	5.69	3.5	1.69	0.77	0.81	3.39	5.84	2.31
RB10	52.07	24.07	5.8	3.57	1.74	0.81	0.84	3.34	5.16	2.16
RB11	50.17	26.44	6	5.08	1.96	0.91	0.78	3.12	3.5	1.90
RB12	49.9	26.77	6	5.22	1.99	0.92	0.79	3.1	3.39	1.86
RB13	49.88	26.22	6.11	3.58	1.65	0.96	1.04	3.15	5.46	1.90
RB14	51.24	25.17	6.01	3.56	1.66	0.94	1.02	3.27	4.95	2.04
RB15	49.54	26.8	6.58	3.36	1.57	1.12	1.26	3.08	4.22	1.85
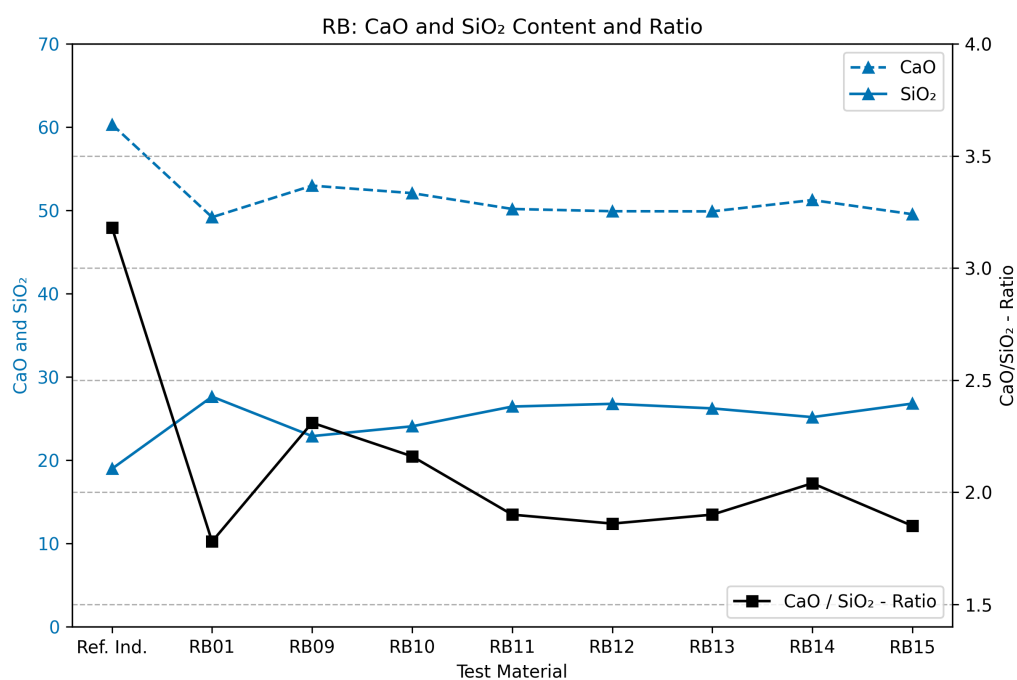
Figure 39: The amount CaO and SiO_2, and the CaO/ SiO_2 - ratio to RB01, RB09 - RB15, and the reference sample. Amount CaO and SiO_2 are given in wt%.

4.5 XRD

In Table 16 the identified phases from the XRD analysis of TM09-TM15 are shown. In the table it is seen that two different phases of $CaCO_3$ were identified, calcite and vaterite. Calcite was the most common phase. Portlandite was identified in TM09 and TM10, quartz was identified in all samples. Albite was identified in TM11-TM15.

In Figure 40 the XRD patterns for TM09 and TM10 are seen. Calcite, portlandite and quartz were identified. In Figure 41 are two peaks to TM09 and TM10. In Figure 41a at a reference peak for portlandite it can be seen that the non-carbonated sample TM10 has higher intensity than the carbonated sample TM09. In Figure 41b a calcite peak is shown, it is seen that the carbonated sample TM09 has higher intensity than the non-carbonated sample TM10.

In Figure 42 are the XRD patterns to TM11 and TM12. In the figure calcite, quartz and albite are identified, and no portlandite. The highest peaks for TM11 and TM12 are identified to be quartz. In Figure 43a one peak for albite, and 43b one for calcite are seen. In Figure 43a a small difference in intensity between carbonated TM11 an non-carbonated TM12 are seen. In Figure 43b a slightly higher intensity for carbonated TM11 than non-carbonated TM12 are seen.

The XRD result for TM13 and TM14 are seen in Figure 44. In the figure calcite, quartz and albite are identified, and the highest peak is quartz. In Figure 45a and 45b peaks for quartz and calcite are seen. The differences between the carbonated TM13 and non-carbonated TM14 are small.

In Figure 46 are the XRD result to carbonated TM15. In the figure it is seen that the highest peaks are quartz. Vaterite and albite are also identified.

Table 16: Identified phases by XRD analysis for TM09 - TM15.

	Calcite	Vaterite	Portlandite	Quartz	Albite
	$CaCO_3$		$Ca(OH)_2$	SiO_2	$NaAlSi_3O_8$
TM09 C	✓		✓	✓	
TM10 NC	✓		✓	✓	
TM11 C	Little			✓	✓
TM12 N	Little			✓	✓
TM13 C	✓			✓	✓
TM14 NC	✓			✓	✓
TM15 C	Little	✓		✓	✓
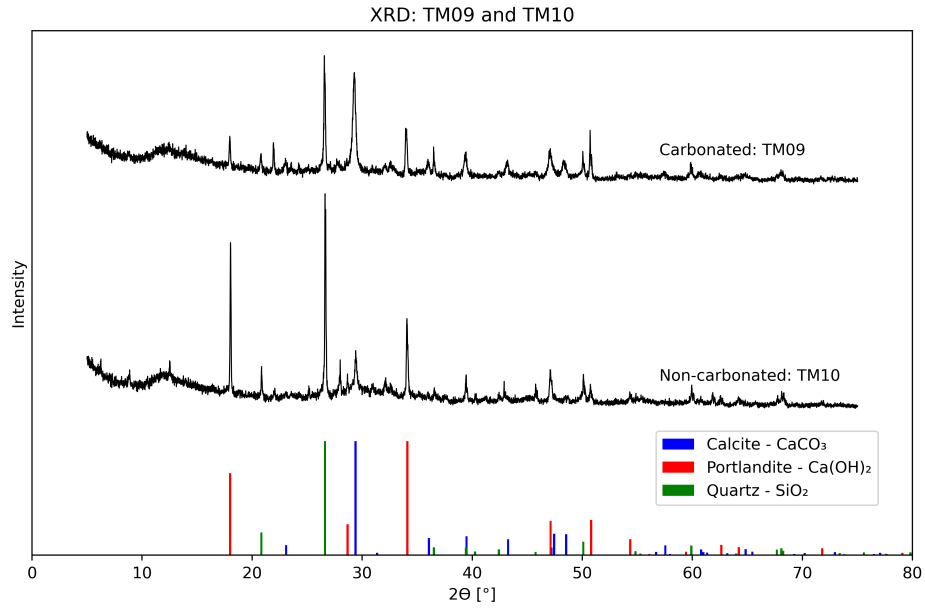
Figure 40: XRD pattern to TM09 and TM10, and identified phases calcite, portlandite, and quartz.

Figure 41: (a) Portlandite, and (b) Calcite.

Figure 42: XRD pattern to TM11 and TM12, and identified phases calcite, quartz, and albite.

<div style="text-align:center">(a)</div>

<div style="text-align:center">(b)</div>
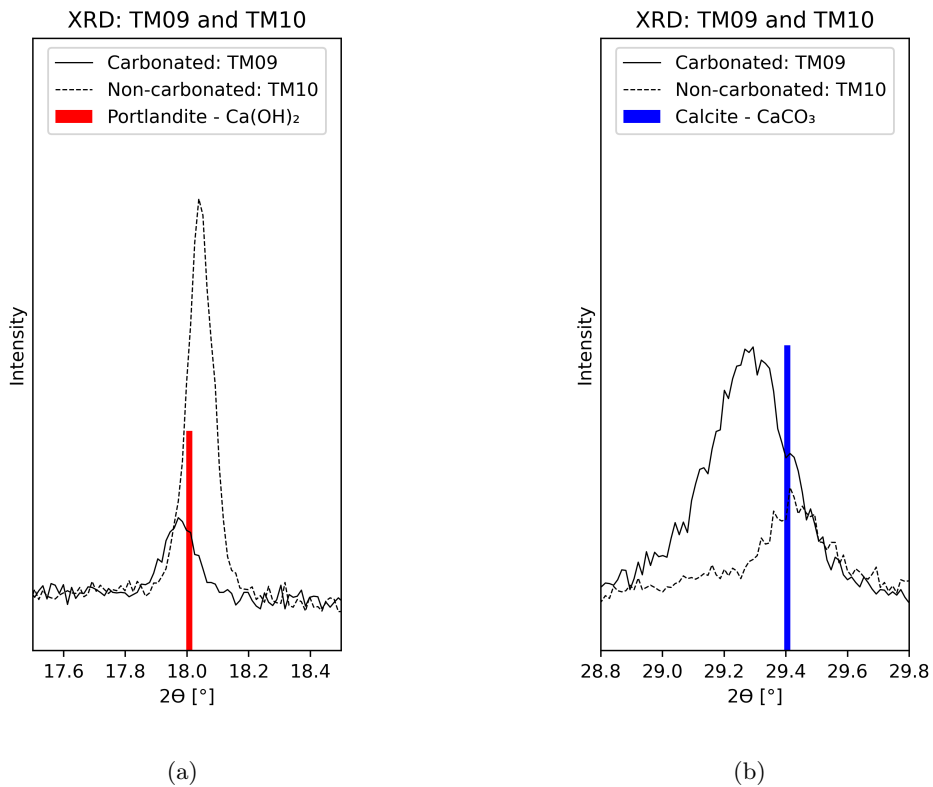
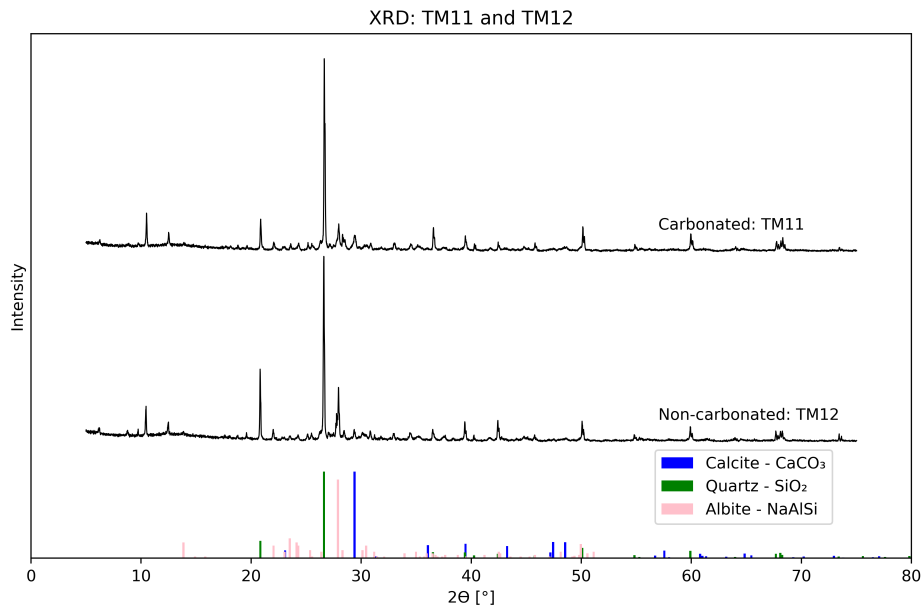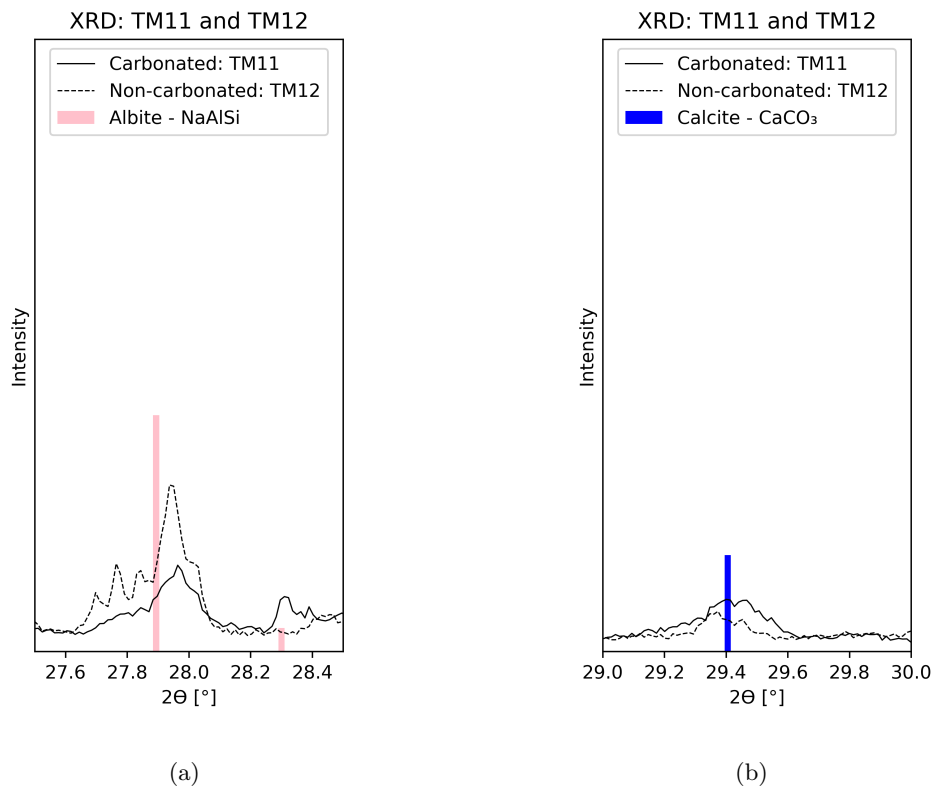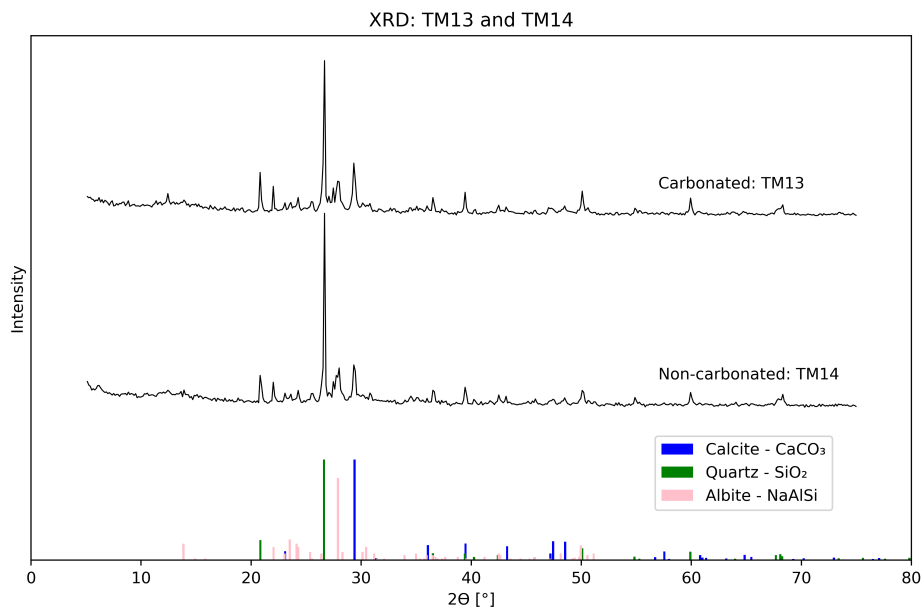Figure 43: (a) Albite, and (b) Calcite.

Figure 44: XRD pattern to TM13 and TM14, and identified phases calcite, quartz, and albite.

(a)

(b)
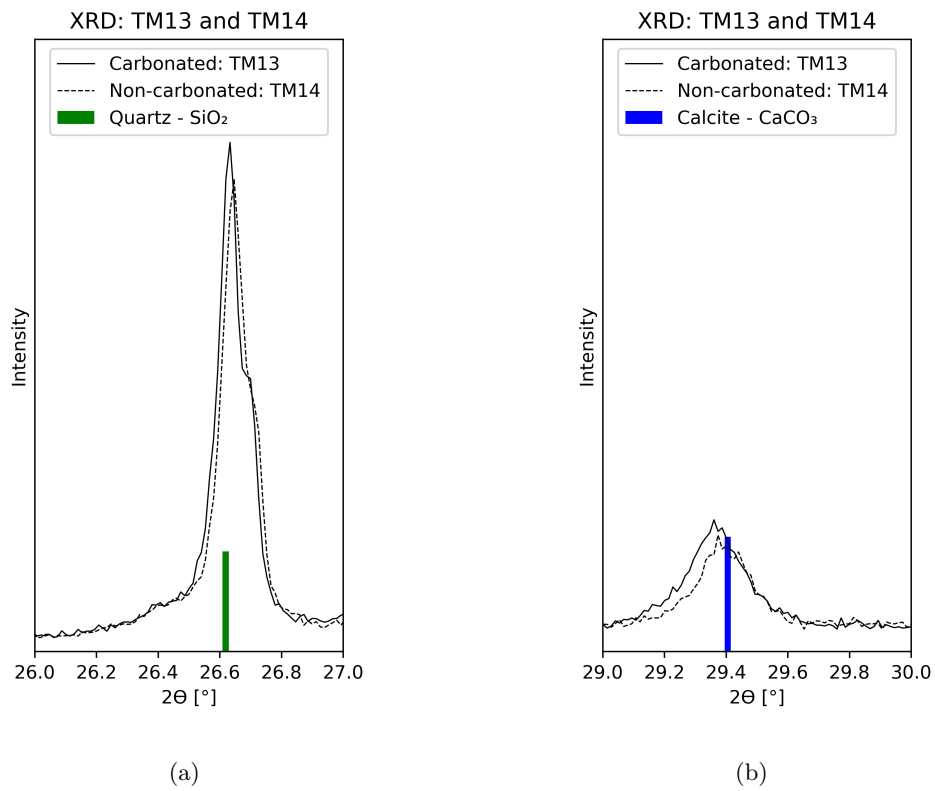
Figure 45: (a) Quartz, and (b) Calcite.
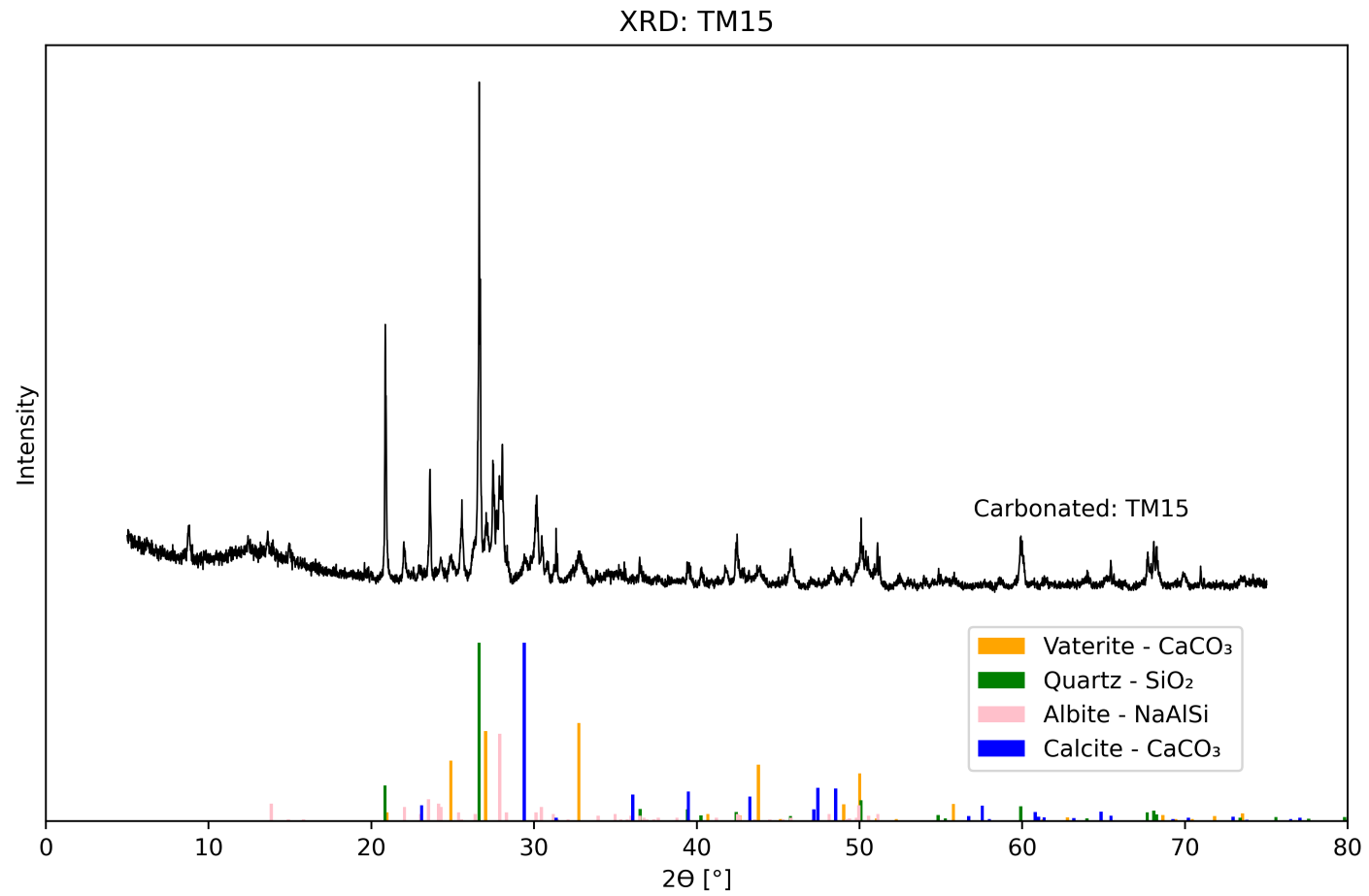
Figure 46: XRD pattern to TM15 and identified phases vaterite, quartz, albite, and calcite.

4.6   Isothermal Calorimetry

Results from the isothermal calorimetry of the composite cements and the reference sample can be seen in Figure 47. In the figure the result is presented as mW/ g powder, ie heat development per g powder. It can be seen that all the composite cements containing recycled concrete have less heat development compared with the reference sample. It is also seen that some samples have faster heat development in the start compared with the reference, especially RB02, RB03, RB13 and RB14. But the reference sample has the highest peak. The cumulative heat development are presented in Figure 48, also this figure shows heat per g powder. It is seen that the reference sample achieves the highest cumulative heat with 383 J/g powder after one week, ie 168 h. RB04, RB05 and RB06 achieves the lowest cumulative heat around 310 J/ g powder. The rest of the RB samples are quite alike within a 25 J interval. The achieved cumulative heat after 168 h are presented in Figure 49. In the figure it can be seen that RB04, RB05 and RB06 stands out with lower achieved cumulative heat than the other RB samples. The values are also presented in Table 34 in the Appendix. Figures with the calorimetry and cumulative heat development result for each sample pair containing carbonated material and non-carbonated material are show in Section 8.4 in the Appendix.

The difference in cumulative heat at 168 h between the sample containing carbonated material, and the sample containing same but non-carbonated material is seen in Table 17. In the table it is seen that all but one of the materials containing carbonated material achieves higher heat development compared with the samples containing the same but non-carbonated material. The increase is from 1 to 41 J / g powder for the different samples. RB05 and RB06 are the exception, where RB05 containing carbonated material show 2 J /g powder lower than RB06 containing non-carbonated material. It can also be mentioned that RB03 and RB04 stands out among the couples with the largest difference between their achieved heat, 41 J/g powder.
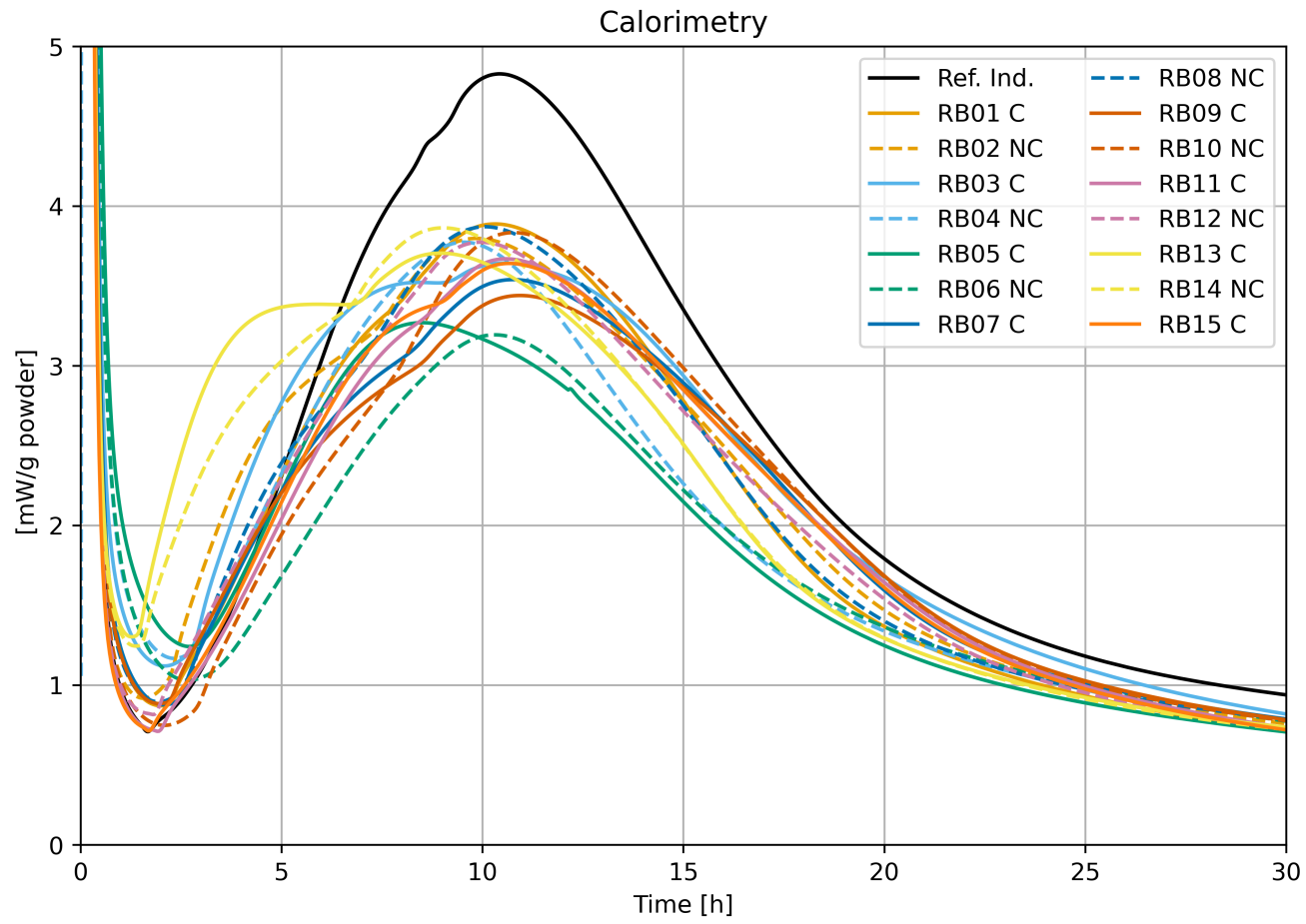
Figure 47: The heat development to RB01 - RB15 and the reference sample.
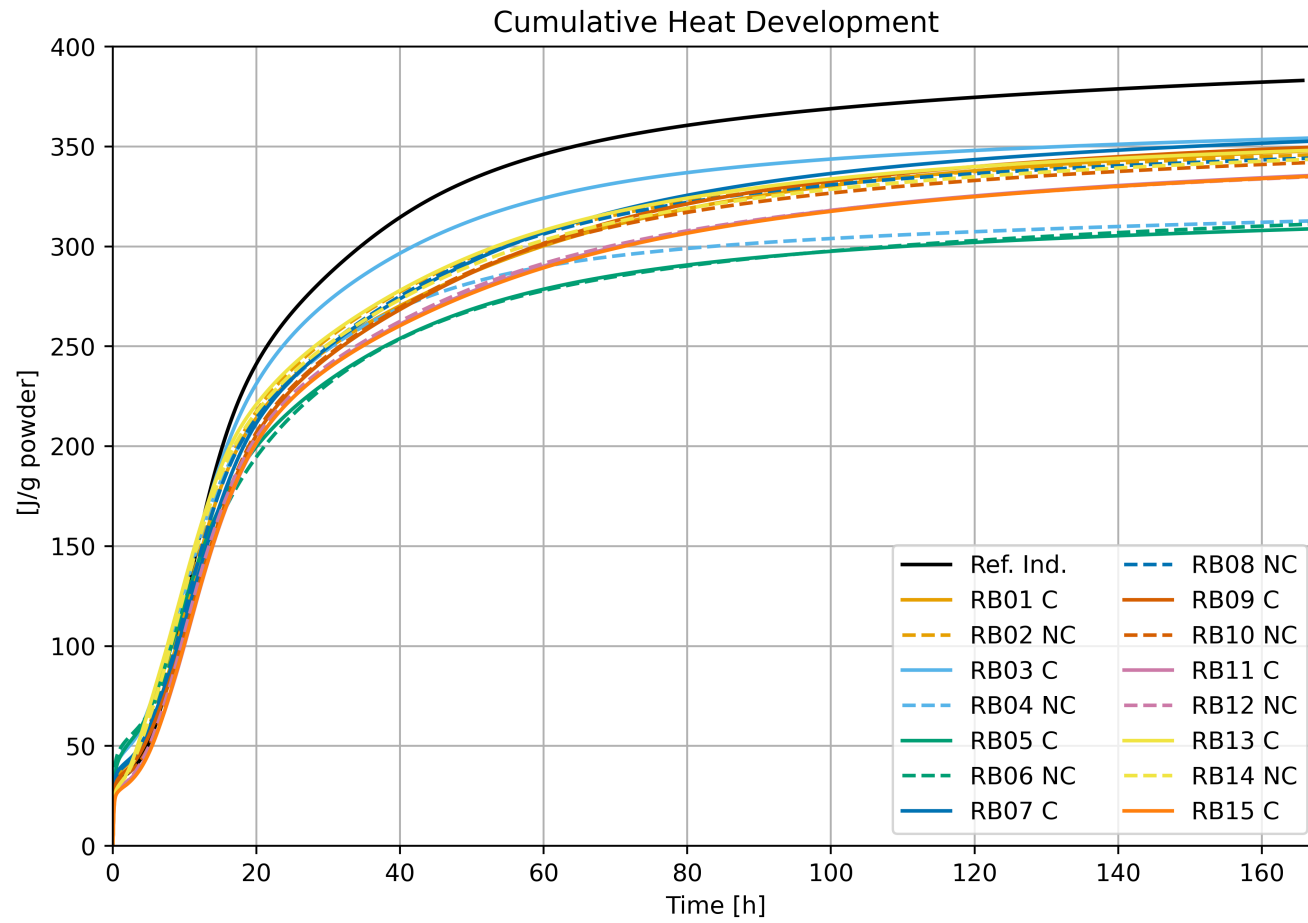
Figure 48: The cumulative heat development to RB01 - RB15 and the reference sample.
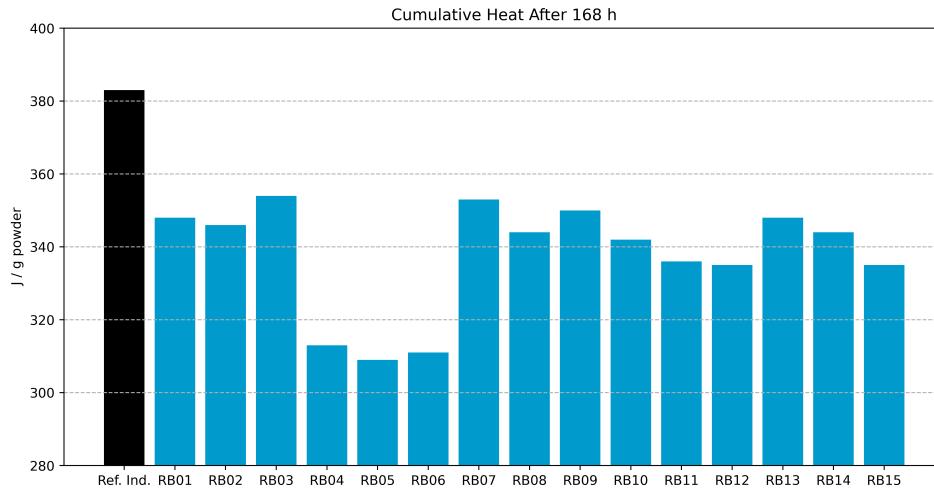
Figure 49: Achieved cumulative heat of RB01 - RB15 and the reference sample after 168 h. Given in J/ g powder.

Table 17: Difference in cumulative heat after 168 h between the composite cements containing carbonated and non-carbonated material.

Sample	Cumulative Heat diff. 168 h [J/ g powder]
RB01-RB02	2.0
RB03-RB04	41.5
RB05-RB06	-2.4
RB07-RB08	8.5
RB09-RB10	7.6
RB11-RB12	0.6
RB13-RB14	4.5

In Figure 50 the heat development has been divided by 0.8, to show heat development per g cement for the RB samples. In the figure it can be seen that the heat development of the reference sample are quite similar to the RB samples. It is also possible to identify several RB samples that show a higher early heat development compared with the reference sample. In Figure 51 the cumulative heat development with the RB samples divided by 0.8 are shown. It is shown in the figure that all the RB samples have higher cumulative heat after 168 h than the reference sample.
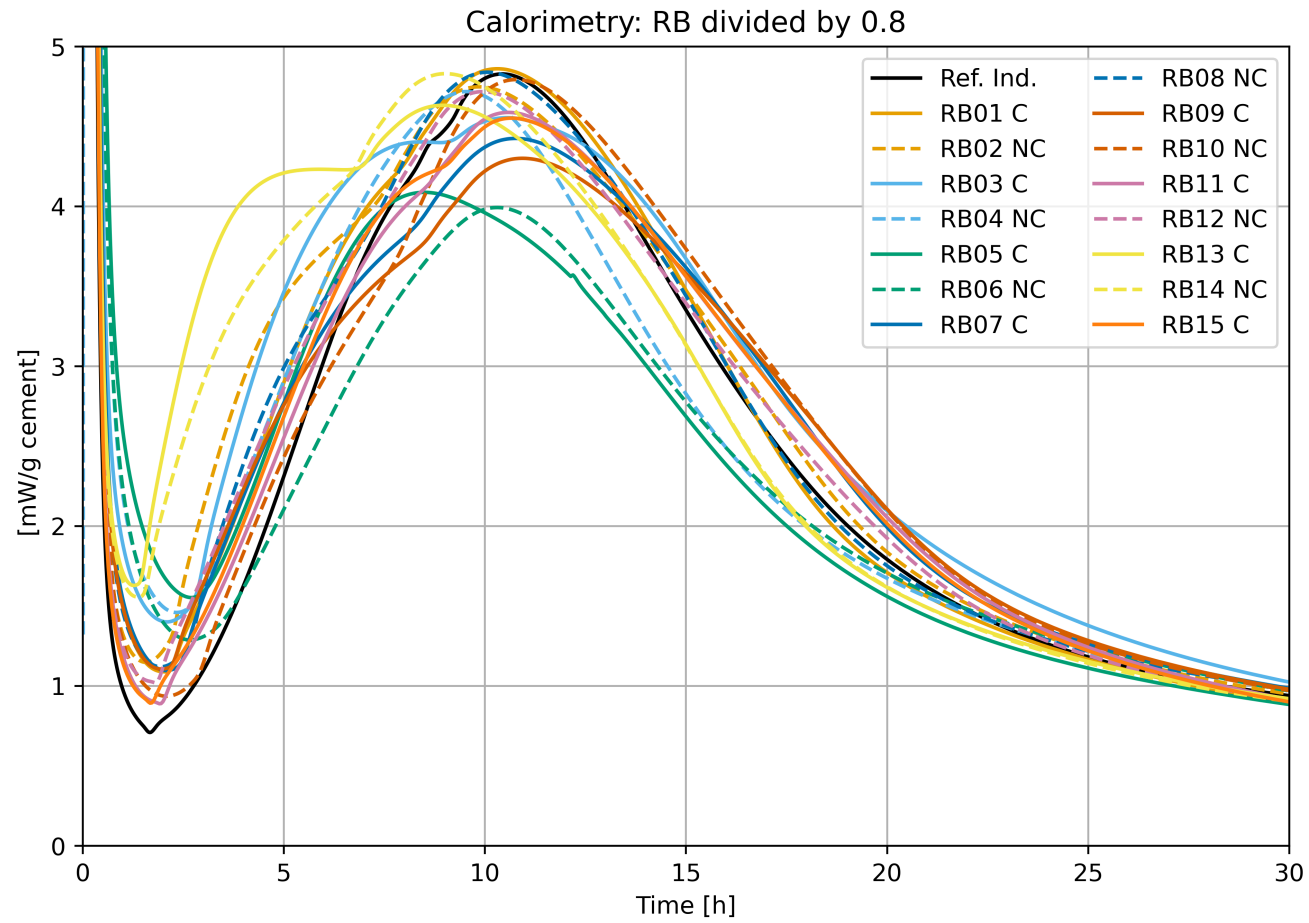
Figure 50: The heat development to RB01 - RB15 and the reference sample divided by 0.8. Given in mW/g cement.
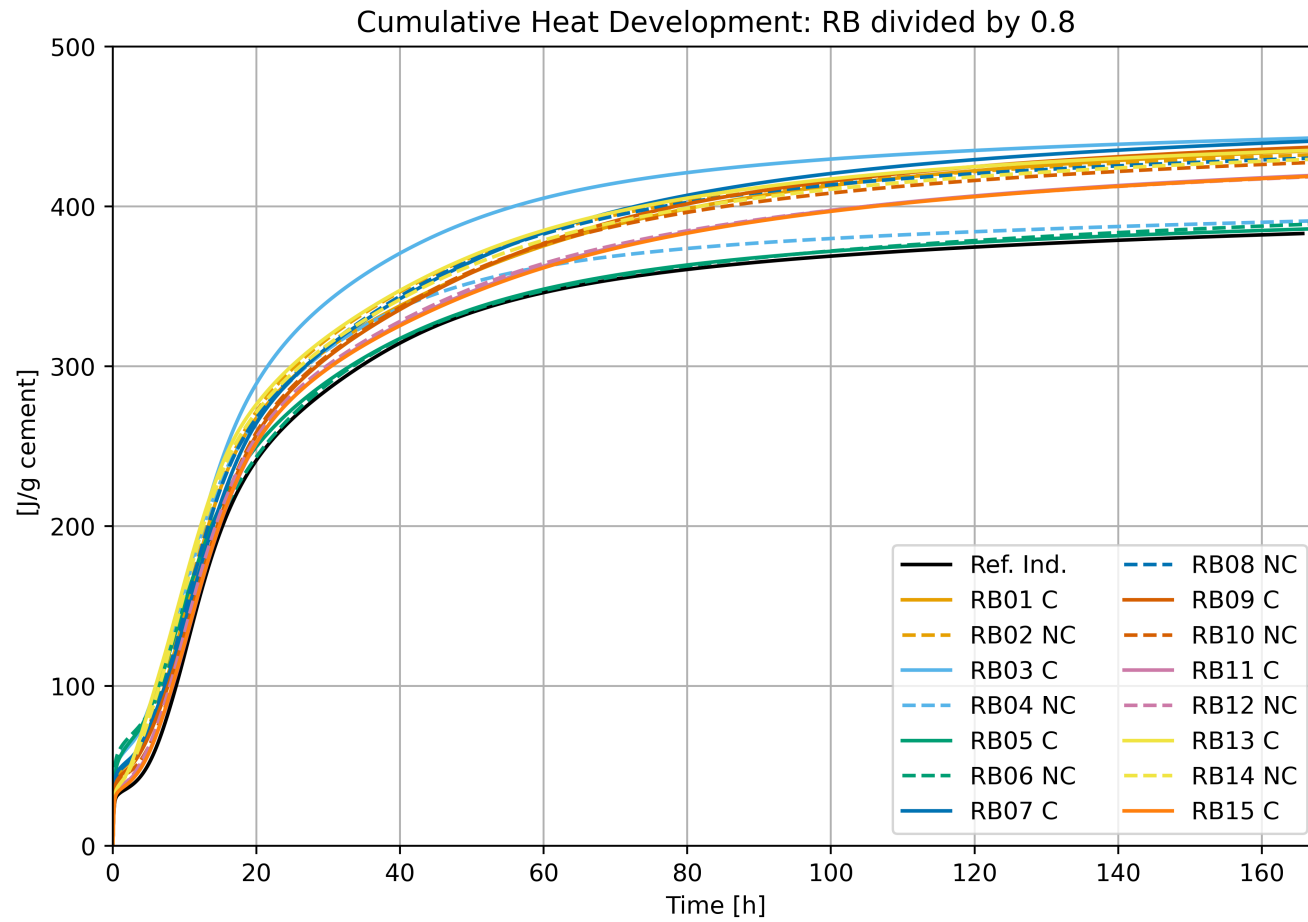
Figure 51: The cumulative heat development to RB01 - RB15 and the reference sample divided by 0.8. Given in J/g cement.

4.7 Standard Consistency

The water percent from the standard consistency test is presented in Figure 52. In the figure it is seen that all the RB materials have water percent over 30 %. RB13 and RB14 have the highest water percent. RB15 has the lowest water percent. The water percent are also shown in Table 35 in the Appendix.
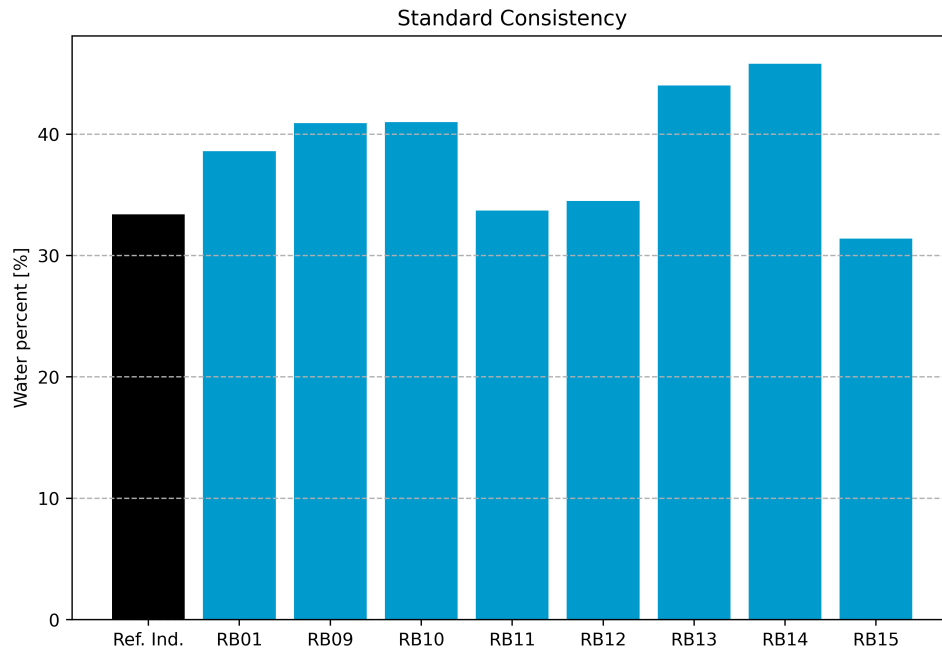
Figure 52: Water demand of RB01 - RB15 and the reference sample from the standard consistency test, given in %.

4.8 Expansion

The result from the expansion test of RB01, RB09-RB15 and the reference sample are shown in Table 18. In the table it is seen that the maximum expansion was 0.9 mm and that the minimum expansion was 0.1 mm.

4.9 Setting time

The setting time development for all the RB samples are seen in Figure 53. In the figure it is seen that the reference sample has the earliest setting time and development, close followed by RB13. RB10 had the longest setting time. In the figure it can also be observed that the all the samples containing carbonated material (solid line) have shorter setting time, compared with the sample containing same but non-carbonated material (dashed line). The initial and final setting time for RB01 and RB09 - RB15, and the reference sample is seen in Table 19. The measurements for each sample is seen in Subsection 8.5 in the Appendix.

Table 18: Result from the expansion test of RB01, RB09 - RB15, and the reference sample.

Sample	Expansion [mm]
Ref. Ind.	0.5
RB01	0.3
RB09	0.3
RB10	0.9
RB11	0.4
RB12	0.5
RB13	0.4
RB14	0.2
RB15	0.1
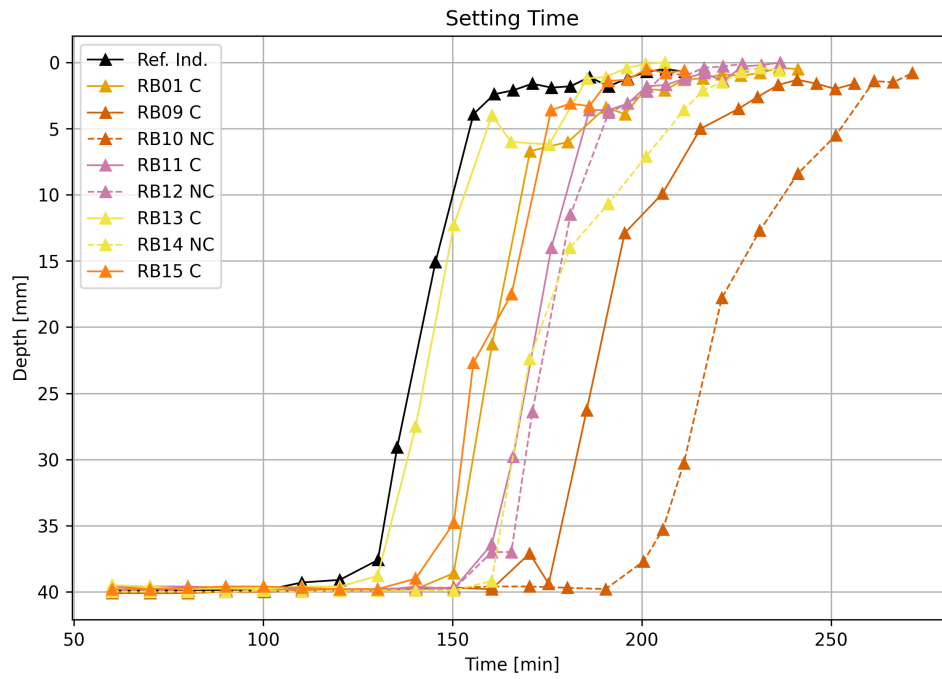
Figure 53: Setting time of RB01, RB09 - RB15, and the reference sample.

Table 19: Initial and final setting time of RB01, RB09 - RB15, and the reference sample.

Test material	Initial setting time [min]	Final setting time [min]
Ref. Ind.	131	160
RB01	150	184
RB09	177	237
RB10	205	261
RB11	160	193
RB12	165	194
RB13	135	187
RB14	161	217
RB15	148	183

5 Discussion

In following section the results from the analyses are discussed and compared to theory and findings from other studies. The compressive strength is also plotted against cumulative heat, CaO/SiO_2 - ratio, and $C\hat{C}$ for discussion of possible trends. And the relationship between the origin of the concrete powder and the properties are discussed. The Industrisement used in the composite cement samples for the isothermal calorimetry was from one batch Industrisement. The cement used in the RB samples tested for compressive strength, standard consistence, setting time and expansion tests was from another batch but same type Industrisement. In the following discussion the difference between the two cement batches are assumed to be negligible when results are compared and discussed.

5.1 Compressive Strength

In Figure 54 the strength results are shown together with the requirements for strength class 52.5 R, 42.5 R and 32.5 according to NS-EN 197-01 standard. It can be seen that the compressive strength of all the RB samples are greater than strength class 42.5 R and 32.5 R. The RB samples does however not full fill the requirement according to the 52.5 R standard at 28 days, which also is the strength class to the reference sample. The compressive strength of the RB composite cements can thus be considered as approved at 28 days within strength class 42.5 R and 32.5 R. The strength development at longer time is however unknown and should be further examined.

Figure 54: Compressive strength of RB01, RB09 - RB15, and the reference sample together with the requirements for strength class 32.5 R, 42.5 R and 52.5 R.

Lower obtained strength for the RB samples containing 20 wt% carbonated material compared with the reference sample as presented in Section 4.1, agrees with the results on mortar by Kumar

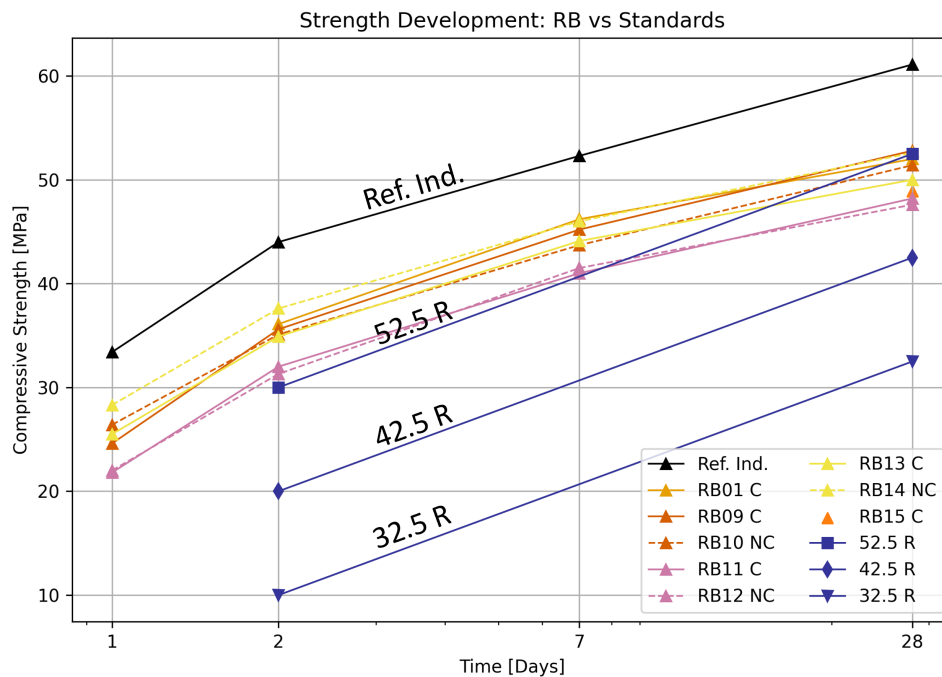Kaliyavaradhan et al. [15]. And disagrees with the result by Lu et al. who experienced higher compressive strength on cement paste containing 20 wt% carbonated concrete fines than the reference up to 28 days, and equal compressive strength as the reference after 90 days. [19] The non-existing clear difference in compressive strength between the samples containing carbonated or non-carbonated materials in Figure 27 differs from the conclusions by Kumar Kaliyavaradhan et al. and Lu et al., who both experienced an increase in strength with the carbonated powder in comparison with the non-carbonated powder. [15] [19]

From the compressive strength result in Table 20 at 28 days it is not possible to distinguish one source for concrete fines that showed more potential than the others. Since the 2 composite cement with highest strength RB09, and RB14 originated from two different process steps washing water and sawing sludge.

It should be mentioned that the high early strength at 1 day for RB10 in Figure 66 partly can be affected by 15 min to late execution of the compressive strength test.

With 20 wt% cement replaced with carbonated or non-carbonated material, it was seen that several RB samples exceeded 80 % in relative compressive strength in Figure 28. It can thus be suggested that the replaced material in some way contribute to the achieved strength in the mortars for sample RB01, RB09, RB10, RB13 and RB14. Since RB11 and RB12 had less than, and RB15 equal to 80 % of the reference strength, the concrete fines could be considered to not be contributing to the strength.

Standardsement FA and Anleggsement FA are cement types on the Norwegian market, and their strength development are presented in Figure 55 together with the RB samples, and the reference sample. Between day 1 and 7 the strength development of the RB samples and especially RB11 and RB12, are quite similar to the Standardsement FA. But the strength development of Standardsement FA are increasing more after 7 days compared with the RB samples. All the RB samples have a higher strength than the Anleggsement FA cement between 1 and 7 days. Anleggsement FA however increase the compressive strength more than all the RB samples after 28 days. These observations indicate that the the RB samples contribute with mores strength development during early times, up to 7 days, compared with other composite cements on the market.
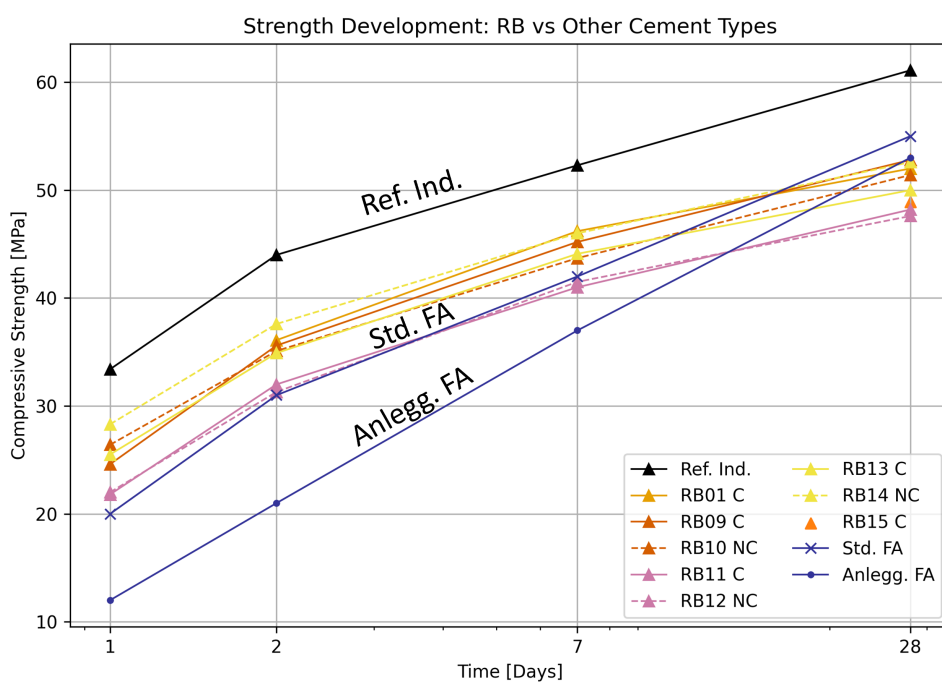
Figure 55: Compressive strength development of the RB samples and referenace sample against Standardsement FA and Anleggsement FA. [30][28]

5.2 TGA and DTG

The lowerings in Figure 30 between 105-420 °C are assumed to be due to decomposition of CSH and AFt. [34] The lowering at 450 - 500 °C is clearly visible for TM01, TM02, TM09 and TM10, and is most likely mass loss due to decomposition of $Ca(OH)_2$, in short notation CH. [24][35] The mass loss around 500 - 900 °C are assumed to be due to decomposition of $CaCO_3$. For some samples it is possible to identify two different lowerings within this temperature range. It is possible that the lowerings at the lower temperature are due to decomposition of unstable $CaCO_3$ phases as aragonite and vaterite, and the higher temperature is due to decomposition of the stable phase calcite. [40] The identified phases are seen in Figure 56.
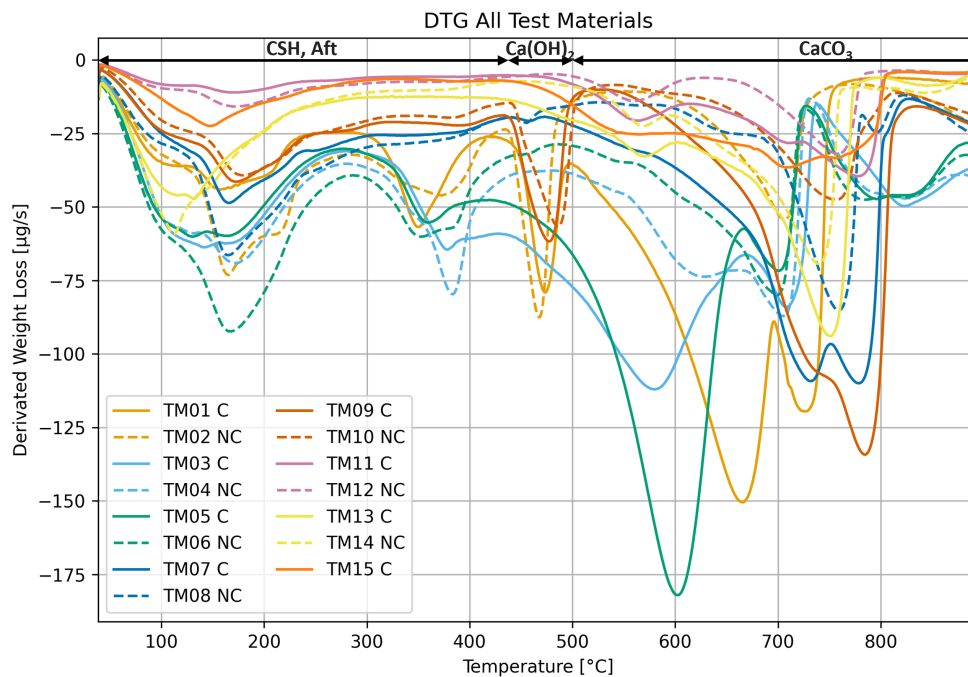
Figure 56: DTG result of TM01 - TM15 together with identified phases.

The chosen temperature interval of 500 - 900 °C for the calculation of weight loss due to CO_2 was motivated by the temperature range 500 - 800 °C for where $CaCO_3$ decompose. [40] The start temperature was also motivated by the early weight loss by especially TM05, TM01 and TM03 at 500 - 700 °C seen in Figure 30. The finish temperature was also motivated by the late weight loss for several samples at 800 - 900 °C, see Figure 30. The samples most probably also contained some content calcite independently of the carbonation, since limestone is added to the cement as described in Section 2.1. [12] This is however assumed to not affect the calculated CO_2 uptake by the carbonated samples, since the CO_2 uptake by the non-carbonated sample was subtracted according to Equation 10. It is however also possible that the samples were carbonated even before the carbonation treatment was preformed for this study.

According to the maximum calculated CO_2 uptake in Table 11 the carbonation method in this study show potential to capture 0.10 g CO_2/ g recycled fines, which equals 10 % of the generated CO_2 from the clinker production. This is less than the 0.13 g CO_2/g concrete fines, Ho et al. captured with their method, [11] but the result in this study still shows the potential of easy CO_2
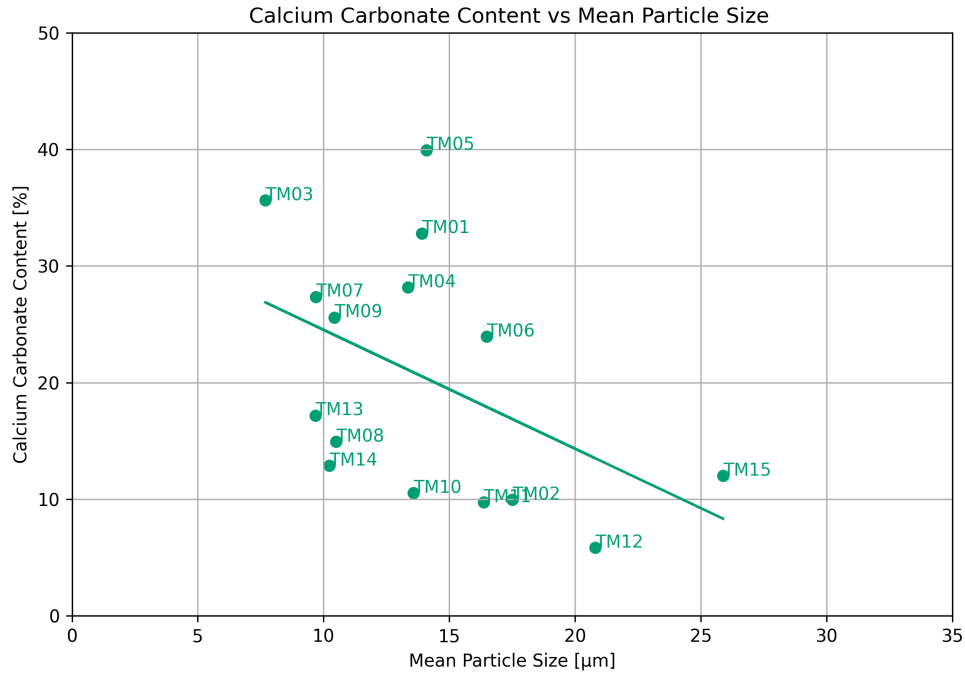
Figure 57: Calcium carbonate content vs median particle size for the TM samples.

capturing. It should also be mentioned that TM13 and TM15 were carbonated in advance by another method, and the potential of the materials can thus be higher than the result shown in the table.

As discussed above was the weight loss between 500 - 900 °C assumed to be associated with $C\hat{C}$ decomposition. The calculated CO_2 in Table 11 were then used according to Equation 9 to calculate amount $C\hat{C}$.

5.3 Particle Size Distribution

The decrease in particle size of the concrete powders after carbonation complies with the observations by Lu et at. [19] But disagrees with Kumar Kaliyavaradhan et al. who got coarser particles after carbonation due to agglomeration. [15] It is possible that different carbonation methods influence the particle size differently.

The large sieve residues seen in Figure 34 and 37 for the TM and RB samples, means that a large proportion of the particles are larger than 250 μm. The particle size distribution in Section 4.3 therefore do not present the reality. It is likely that the larger particles origin from the stone aggregates in the concrete. These particles were experienced difficult to mill together with the porous dried cement during the preparation of test material for the experiments.

In Figure 57 the $C\hat{C}$ content is plotted against the median particle size for the TM samples. The figure shows a trend for decreasing particle size with increasing calcium carbonate content. The scatter is however widely dispersed.

5.4 XRF

As was seen in Figure 38 did the TM samples mainly contain of CaO and SiO_2, which agrees with the XRF data on carbonated cement paste (cCP) in Table 6 by Zajac et al. The TM samples however generally had lower CaO content and higher SiO_2 content compared with the carbonated cement paste in the Table and the content in the concrete slurry to Kumar Kaliyavaradhan et al. [41][15]

TM01 - TM06 originates washing sludge from different sediments basins. TM01 and TM02 contain more SiO_2 and is probably from an basin with more aggregates. While TM03 - TM06 are from a basin containing more cement paste than aggregates since the CaO content is higher. TM09 and TM10 also originates from washing sludge, but not from a specific basin. TM11 - TM15 originated from drilling and sawing sludge, and demolished concrete. These materials had a high content of SiO_2, which probably is due to the aggregates in the concrete. The higher Fe_2O_3 content in TM11 and TM12 compared with the other TM samples could be due to the drilling process and wear from the equipment. It could also be due to other variations in the cement or aggregates. The origin and process of the material thus have a big influence on the chemical composition.

The LOI was also varying between the materials. The highest LOI is obtained by TM03 and TM04 on 30.63 respective 30.66 wt%. Lowest LOI is obtained by TM15 with 16.25 wt%.

5.5 XRD

The higher respective lower intensity for portlandite and calcite for the non-carbonated sample TM10 and carbonated sample TM09 in Figure 41a and 41b, agrees with the theory in Section 2.3 that $Ca(OH)_2$ carbonates to $CaCO_3$. The increase of calcite and decrease of portlandite also align with the XRD result from studies mentioned in Section 2.4. This also agrees with the DTG result in Figure 58 which showed a significantly deeper lowering due to $CaCO_3$ between 600 - 800 °C for the carbonated sample TM09 compared with the non-carbonated sample TM10. And in the higher calculated $CaCO_3$ in Table 31.

The XRD result for TM11 and TM12 in Figure 42 showed high intensity for quartz, and low for calcite. This agrees with the XRF result in Figure 38 which showed a low CaO / SiO_2 - ratio. The small difference in intensity for calcite between the carbonated sample TM11 and non-carbonated sample TM12 in Figure 43b also agrees with the small difference in calculated $C\hat{C}$ in Table 31. The peak at 10.5 was not identified for TM11 and TM12.

The small difference in intensity for calcite was also seen in Figure 45b for the carbonated sample TM13 and non-carbonated sample TM14. The small difference in $C\hat{C}$ intensity also agrees with the small difference in calculated $C\hat{C}$ content in Table 31. The peak at 12.5 for TM13 and TM14 was not identified.

The XRD result in Figure 46 showed that the carbonated sample TM15 contained two phases of CaO_3, vaterite and calcite. This can agree with the DTG result in 59, which shows a quite equal weight loss between 500 - 800 °C. The lower weight loss up to about 700 is prbably due to vaterite, and higher than 700 is probably due to calcite. [40]

$Ca(OH)_2$ was expected to be identified in the non-carbonated samples TM12 and TM14, this was not seen and can be due to that the samples were naturally carbonated.
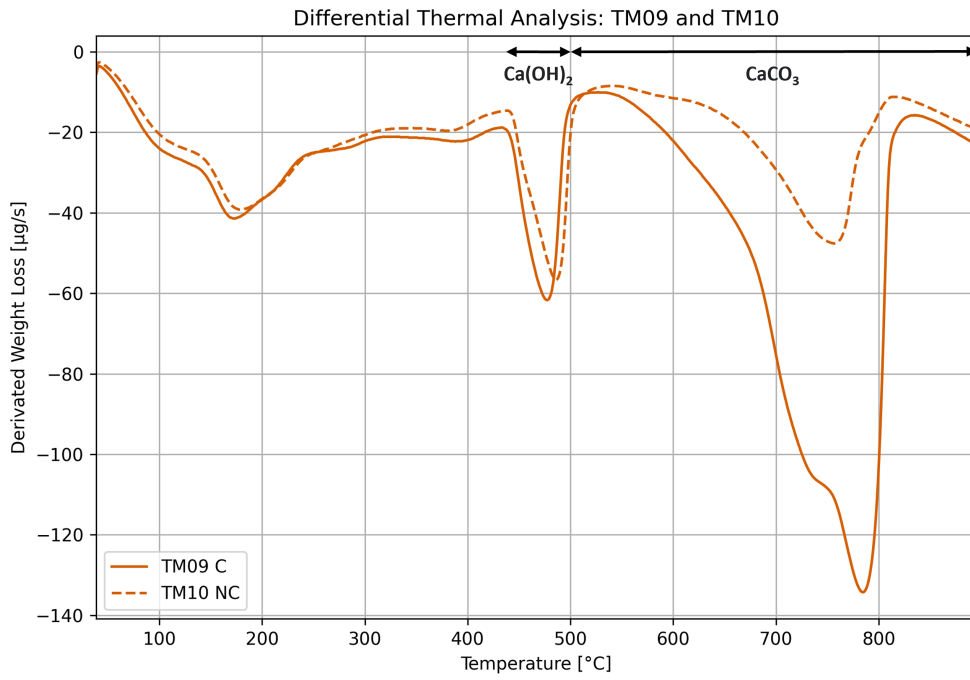
Figure 58: DTG result of TM09 and TM10 together with identified phases.
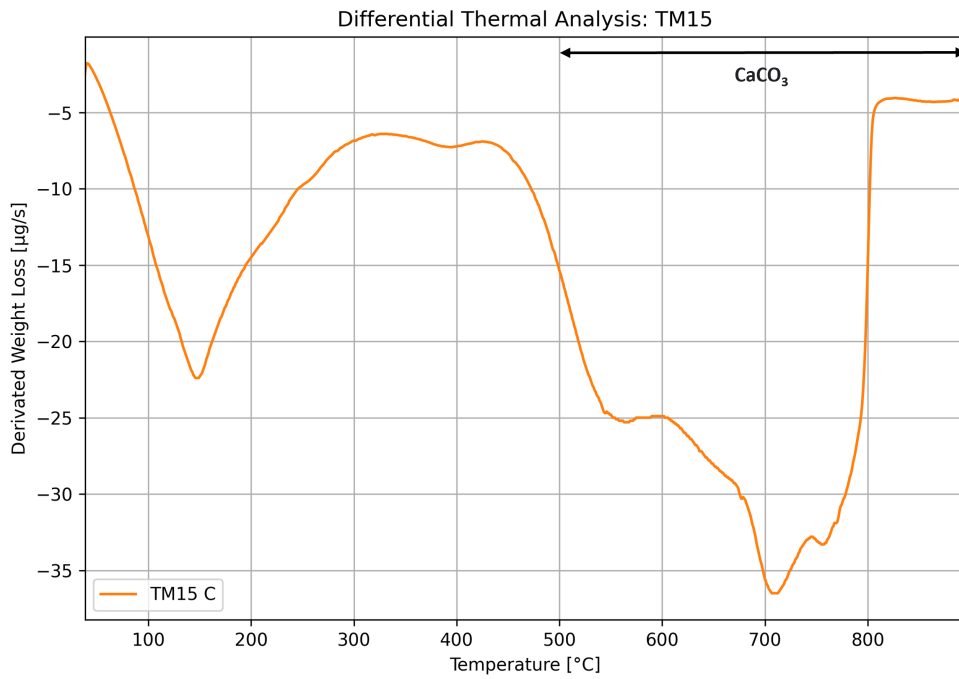

Figure 59: DTG result to TM15 together with identified phase.

5.6 Isothermal Calorimetry

The higher cumulative heat development for the carbonated samples as were seen in Table 17 can be a result of the smaller particle size for the carbonated materials as were seen in Table 13. This suggestion agrees with the theory in Section 2.6, which says that smaller particle size increase the reactivity, heat development and early strength. [12] The smaller achieved cumulative heat for RB05 containing carbonated material compared with RB06 containing non-carbonated material however can not be explained by non existing decrease in particle size. It is also possible that the decrease in cumulative heat for RB05 is a result of other mechanisms. The biggest increase in cumulative heat by RB03 - RB04 however also had the largest percent decrease in particle size, which again agrees with the higher reactivity mechanism for smaller particles mentioned in Section 2.6. The RB samples showed a lower heat development compared with the reference sample in Figure 48. Low heat development can however be a beneficial property while casting thick dimensions to avoid cracks, as mentioned in Section 2.1.

The distinct early heat development between 0 and 5 h for RB13, RB14 and RB03 compared with the other RB samples in Figure 47, can agree with the median particle size result in Figure 33. Where it is shown that RB13, RB14 and RB03 have smaller particle size compared with other samples. This early heat development effect is however not seen for RB07, RB08 and RB09 which also contains recycled fines with similar particle size. The absence of early heat development for RB07, RB08 and RB09 compared to the reference sample can be seen in Figure 91 and 93 in the Appendix.

The adjusted cumulative heat in Figure 51 showed that the RB samples obtained higher heat compared with the reference. This can motivate that both 20 wt% carbonated or non-carbonated material contribute to the heat development in some way.

5.7 Setting Time and Standard Consistency

The initial setting times of the composite cements presented in Table 19 were approved according to the NS-EN 197-01 standard, as the initial setting times were lower than the requirements in Table 4. Figure 60 show the setting time vs the water demand for the RB samples. In the figure trends for both higher initial, and final setting time with increased water demand are seen. The figure also show that the setting time for the different samples are quite dispersed. Long initial setting time can be a disadvantage for some usage, for example within the precast-industry. [12]

5.8 Expansion

As was seen in Table 18 did all the composite materials have less expansion than the required $\leq$ 10 mm in Table 4. The composite cements are thus approved regarding the expansions standards in NS-EN 197-01.

5.9 Influences on Strength

The strength development vs the cumulative heat development is shown in Figure 61 for RB01, RB09 - RB15, and the reference. The points are from 1, 2 and 7 days compressive strength, and
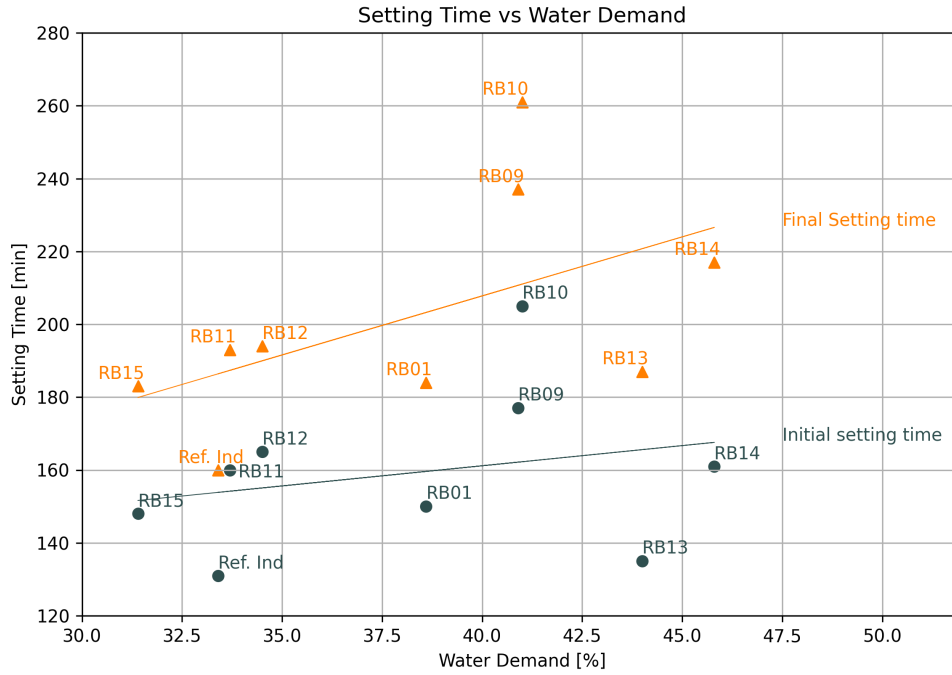
Figure 60: Initial and final setting time vs water demand for RB01, RB09 - RB15 and the reference sample.

cumulative heat at 24, 48 and 168 h. In the figure it is seen that the RB samples generally have lower compressive strength than generated heat in comparison with the reference. RB14 are on top of the reference and thus have similar strength increase with heat as the reference sample, but slower.

In Figure 62 the compressive strength at 28 days is plotted against the CaO / SiO$_2$ - ratio for each RB sample. In the figure a trend for the RB samples indicating higher compressive strength with higher CaO / SiO$_2$ - ratio are seen. This trend aligns with the reference sample which has both higher CaO / SiO$_2$ - ratio and compressive strength.

In Figure 63 the compressive strength at 28 days for the RB samples are plotted against the calculated CĈ content in the of the TM samples. The figures show a clear trend for increased compressive strength with higher content CĈ.

Figure 64 show the compressive strength vs the median particle size for RB01, RB09 - RB10, and the reference sample. In the figure a trend for increasing compressive strength for decreasing median particle size is seen for the RB samples.

These observed trends promoting higher compressive strength aligns with the conclusion by Zajac et al.. Who experienced high surface area, and the chemical composition as responsible mechanisms for the pozzolanic properties, and increased compressive strength in their composite cements containing carbonated recycled cement paste. [41]

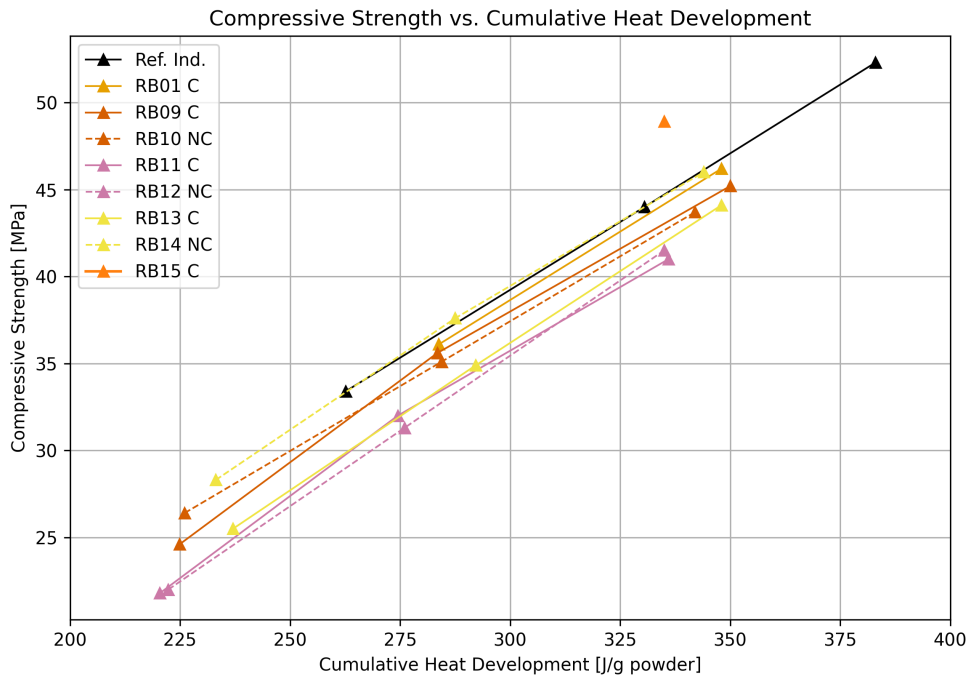Figure 61: Strength development vs cumulative heat development for the RB01, RB09-RB15 and the reference sample.
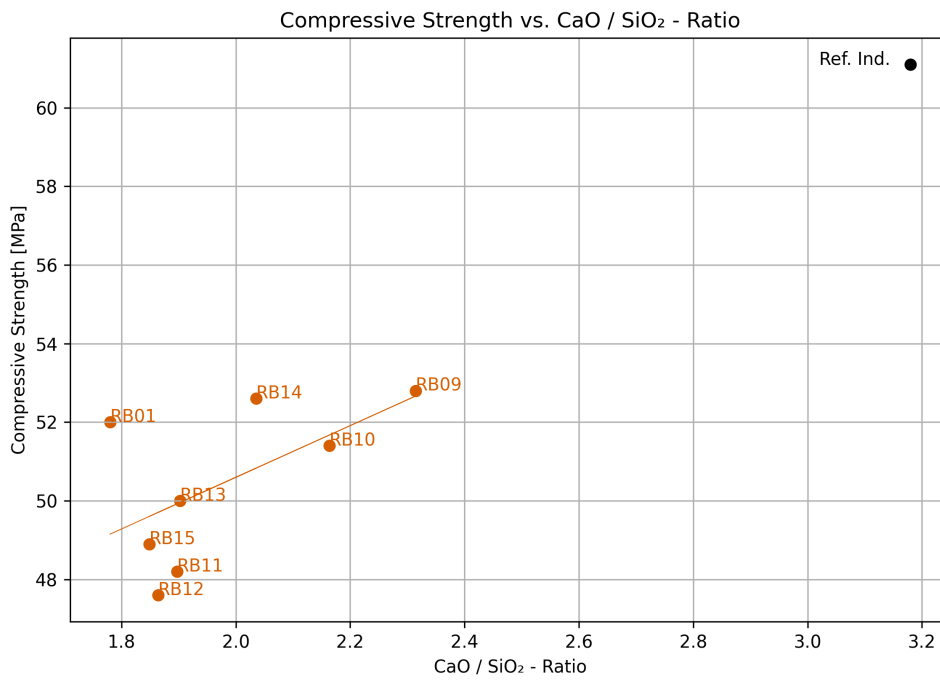

Figure 62: Strength vs CaO / SiO$_2$ - ratio for RB01, RB09 - RB10, and the reference sample.
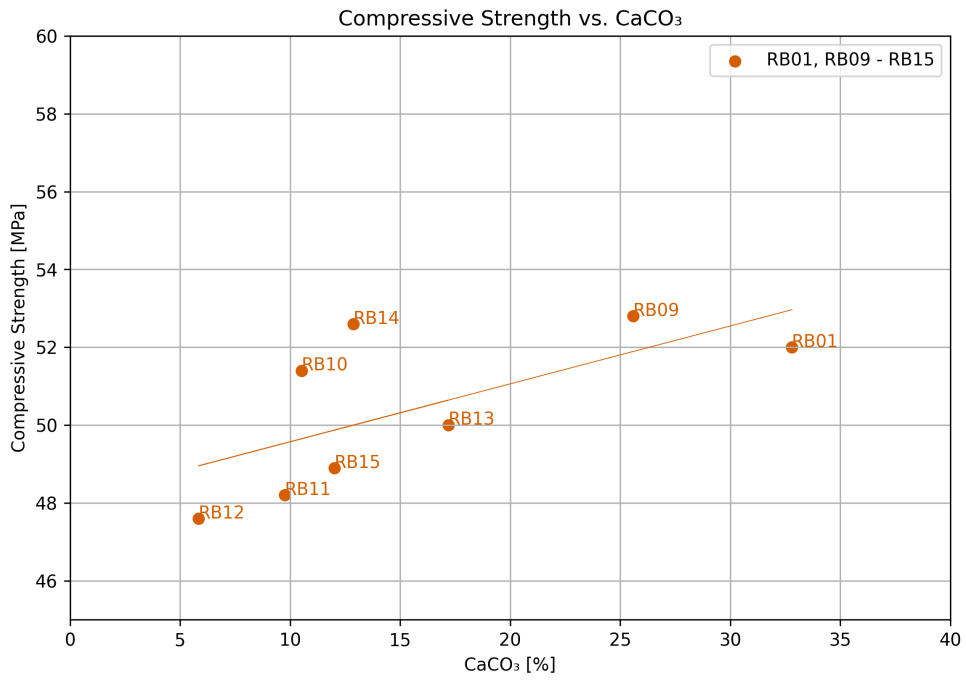
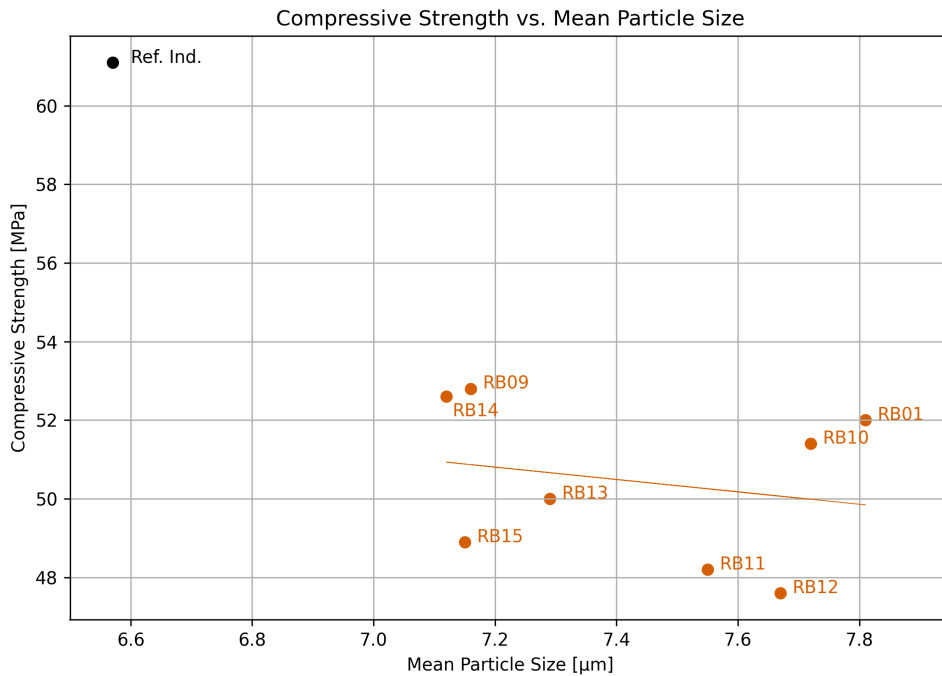Figure 63: Compressive strength vs $\hat{CC}$ content for RB01, and RB09 - RB10.

Figure 64: Compressive strength vs median particle size for RB01, RB09 - RB10, and the reference sample.

6 Conclusion

In this master thesis different kinds of concrete waste were tested by several methods to investigate if the materials can be used in composite cement. In addition, it explored if the recycled concrete waste has potential to capture CO_2, and how this affects the properties of the material. The composition of the tested cements were 80 wt% Industrisement CEM I 52,5 R from Norcem AS, and 20 wt% carbonated recycled fines. A sample containing only Industrisement, and samples containing 20 wt% non-carbonated test material were used as reference.

- Compressive strength testing of mortar prisms according to standard NS-EN 196-1 showed that composite cement containing 20 wt% recycled concrete fines can achieve the requirements for strength class 32,5 R and 42,5 R after 28 days. Both composite cements containing carbonated or non-carbonated recycled concrete fines showed potential.

- TGA analysis showed that the recycled concrete fines have potential to capture 0.1 gram CO_2 per gram concrete fines, which implies that around 10 % of the produced CO_2 emissions from the clinker production potentially can be captured and stored.

- From the perspective of compressive strength, the substitution of 20 wt% recycled concrete fines did not give an increase compared with only Industrisement. 20 wt% carbonated material did not increase compressive strength compared with 20 wt% non-carbonated material. However, the relative compressive strength indicated that 20 wt% concrete fines contribute to the strength in some way.

- Isothermal calorimetry showed a lower heat development for samples containing 20 wt% concrete fines, in comparison with only Industrisement. However, the cumulative heat development divided by 0.8 indicated that the fines contribute to the heat development in some way. Isothermal calorimetry further indicated that the cumulative heat development was higher for samples containing 20 wt% carbonated concrete fines compared with samples containing 20 wt% non-carbonated concrete fines. Most of the samples containing 20 wt% concrete fines showed less strength at a given heat development, compared with the sample containing only Industrisement.

- The initial and final setting time increased along with increasing water demand for the composite cements.

- Higher CaO/SiO_2 - ratio, higher content $C\hat{C}$, and smaller particle size showed increasing effect on the compressive strength for the composite cements containing 20 wt% recycled concrete fines.

7 Further Work

The following areas should be investigated further.

- Composite cement containing recycled concrete fines should be further tested to make ensure it achieve the compressive strength, durability, and workability properties required by the industry.

- A development of an industrial and optimised carbonation method should be further investigated.

- The amount of available concrete waste should be mapped. This could provide an estimate on the potential economical savings and environmental benefits of applying CO_2 capture and storage methods.

References

[1] Cementa AB. *Cementa och HeidelbergCement ett steg närmare etableringen av klimatpositiv cementfabrik i Sverige.* URL: https://www.cementa.se/sv/cementa-och-heidelbergcement-ett-steg-narmare-etableringen-av-klimatpositiv-cementfabrik-i-sverige. (accessed:06.12.2022).

[2] Norcem AS. *Karbonfangst ved Norcem Brevik.* URL: https://www.norcem.no/no/CCS_Brevik. (accessed:06.12.2022).

[3] Norcem AS. *Sirkulær økonomi.* URL: https://www.norcem.no/no/sirkulaer_oekonomi. (accessed:06.12.2022).

[4] Paul Barnes and John Bensted. *Structure and performance of cements.* Spon Press, 2002.

[5] Allan Blackman. *Aylward and Findlay's SI Chemical Data.* eng. Milton, 2014.

[6] Yosra Briki et al. 'Impact of limestone fineness on cement hydration at early age'. In: *Cement and Concrete Research* 147 (2021), p. 106515. ISSN: 0008-8846. DOI: https://doi.org/10.1016/j.cemconres.2021.106515. URL: https://www.sciencedirect.com/science/article/pii/S0008884621001642.

[7] Cementa. *Cementproduktion steg-för-steg.* URL: https://www.cementa.se/sv/cementproduktion-steg-f%C3%B6r-steg. (accessed: 24.01.2022).

[8] EU Construction and Demolition Waste Management. *Guidelines for the waste audits before demolition and renovation works of buildings.* Information. May 2018. URL: https://ec.europa.eu/docsroom/documents/29203/attachments/1/translations/en/renditions/native.

[9] Olje- og energidepartementet. *Støtter gjennomføring av Langskip og Northern Lights.* URL: https://www.regjeringen.no/no/dokumentarkiv/regjeringen-solberg/aktuelt-regjeringen-solberg/oed/pressemeldinger/2020/stotter-gjennomforing-av-langskip-og-northern-lights/id2791729/. (accessed:06.12.2022).

[10] Xiaoliang Fang et al. 'A novel upcycling technique of recycled cement paste powder by a two-step carbonation process'. In: *Journal of Cleaner Production* 290 (2021), p. 125192. ISSN: 0959-6526. DOI: https://doi.org/10.1016/j.jclepro.2020.125192. URL: https://www.sciencedirect.com/science/article/pii/S0959652620352367.

[11] Hsing-Jung Ho et al. 'Utilization of CO2 in direct aqueous carbonation of concrete fines generated from aggregate recycling: Influences of the solid–liquid ratio and CO2 concentration'. In: *Journal of Cleaner Production* 312 (2021), p. 127832. ISSN: 0959-6526. DOI: https://doi.org/10.1016/j.jclepro.2021.127832. URL: https://www.sciencedirect.com/science/article/pii/S0959652621020503.

[12] Stefan Jacobsen et al. *Concrete Technology.* Institutt for konstruksjonsteknikk, NTNU, 2016. ISBN: 82-7482-098-3.

[13] Harald Justnes. 'Chemical composition and reactivity of Portland Cement and the Influence of Alternative Raw materials (AR)'. In: ().

[14] Harald Justnes. 'Performance of SCMs - Chemical and Physical Principles'. In: 17 (2019), pp. 11–12.

[15] Senthil Kumar Kaliyavaradhan, Tung-Chai Ling and Kim Hung Mo. 'CO2 sequestration of fresh concrete slurry waste: Optimization of CO2 uptake and feasible use as a potential cement binder'. In: *Journal of CO2 Utilization* 42 (2020), p. 101330. ISSN: 2212-9820. DOI: https://doi.org/10.1016/j.jcou.2020.101330. URL: https://www.sciencedirect.com/science/article/pii/S2212982020309604.

[16] Norcem AS Kjøpsvik. *CEM I, Industrisement (CEM I 52,5 R)*. ENVIRONMENTAL PRODUCT DECLARATION. Jan. 2018. URL: https://www.norcem.no/no/system/files_force/assets/document/nepd-1483-489_cem-i-industrisement-cem-i-52-5-r-i-bulk_kjopsvik.pdf?download=1.

[17] Norcem AS Kjøpsvik. *CEM II, Standardsement FA (CEM II/B-M)*. ENVIRONMENTAL PRODUCT DECLARATION. Nov. 2016. URL: https://www.norcem.no/no/system/files_force/assets/document/nepd-1195-357_cem-ii-standardsement-fa-cem-ii-b-m_kjv.pdf?download=1.

[18] Wolfgang Kunther, Sergio Ferreiro and Jørgen Skibsted. 'Influence of the Ca/Si ratio on the compressive strength of cementitious calcium–silicate–hydrate binders'. In: *J. Mater. Chem. A* 5 (33 2017), pp. 17401–17412. DOI: 10.1039/C7TA06104H. URL: http://dx.doi.org/10.1039/C7TA06104H.

[19] Bao Lu et al. 'Effects of carbonated hardened cement paste powder on hydration and microstructure of Portland cement'. In: *Construction and Building Materials* 186 (2018), pp. 699–708. ISSN: 0950-0618. DOI: https://doi.org/10.1016/j.conbuildmat.2018.07.159. URL: https://www.sciencedirect.com/science/article/pii/S0950061818318324.

[20] Xiaodong Ma et al. 'Hydration reaction and compressive strength of small amount of silica fume on cement-fly ash matrix'. In: *Case Studies in Construction Materials* 16 (2022), e00989. ISSN: 2214-5095. DOI: https://doi.org/10.1016/j.cscm.2022.e00989. URL: https://www.sciencedirect.com/science/article/pii/S2214509522001218.

[21] Department of Materials Science and Engineering. *TMT4905 - Materials Technology, Master's Thesis*. URL: https://www.ntnu.edu/studies/courses/TMT4905#tab=omEmnet. (accessed: 21.01.2022).

[22] Miljødirektoratet. *Betong- og teglavfall*. URL: https://miljostatus.miljodirektoratet.no/tema/avfall/avfallstyper/betong--og-teglavfall/ (visited on 13th June 2022).

[23] IVL - Svenska Miljöinstitutet. *Carbonation of concrete*. URL: https://www.ivl.se/projektwebbar/co2-concrete-uptake/carbonation-of-concrete.html. (accessed: 25.05.2022).

[24] Liwu Mo, Feng Zhang and Min Deng. 'Mechanical performance and microstructure of the calcium carbonate binders produced by carbonating steel slag paste under CO2 curing'. In: *Cement and Concrete Research* 88 (2016), pp. 217–226. ISSN: 0008-8846. DOI: https://doi.org/10.1016/j.cemconres.2016.05.013. URL: https://www.sciencedirect.com/science/article/pii/S000888461630120X.

[25] Chenxin Ni et al. 'Hydration of Portland cement paste mixed with densified silica fume: From the point of view of fineness'. In: *Construction and Building Materials* 272 (2021), p. 121906. ISSN: 0950-0618. DOI: https://doi.org/10.1016/j.conbuildmat.2020.121906. URL: https://www.sciencedirect.com/science/article/pii/S0950061820339106.

[26] Norcem. *Cement production and emissions*. URL: https://www.norcem.no/en/Cement_and_CCS. (accessed: 06.06.2022).

[27] Norcem. *Flygeaske*. URL: https://www.norcem.no/no/FlyAsh. (accessed: 06.13.2022).

[28] Norcem. *Norcem Anleggsement FA*. URL: https://www.norcem.no/en/anleggsement_FA. (accessed: 25.01.2022).

[29] Norcem. *Norcem Industrisement*. URL: https://www.norcem.no/en/industrisement. (accessed: 25.01.2022).

[30] Norcem. *Norcem Standardsement FA*. URL: https://www.norcem.no/en/standardsement_fa. (accessed: 25.01.2022).

[31] Brevik Norcem AS. *Fakta om flygeaske*. Information. URL: https://www.norcem.no/no/system/files_force/assets/document/a5/86/fakta_om_flygeaske.docx?download=1.

[32] Brevik Norcem AS. *Norcem Industrisement, Brevik - CEM I 52,5 R*. ENVIRONMENTAL PRODUCT DECLARATION. 2020. URL: https://www.norcem.no/no/system/files_force/assets/document/52/15/2020_nepd-2276-1028_epd_19358-norcem-industrisement-brevik-cem-i-52-5r.pdf?download=1.

[33] Brevik Norcem AS. *Norcem Standardsement FA, Brevik - CEM II/B-M 42,5 R*. ENVIRONMENTAL PRODUCT DECLARATION. Aug. 2020. URL: https://www.norcem.no/no/system/files_force/assets/document/84/50/2020_nepd-2275-1028_epd_19343-norcem-standardsement-fa-brevik-cem-ii-b-m-42-5r.pdf?download=1.

[34] Ling Qin and Xiaojian Gao. 'Properties of coal gangue-Portland cement mixture with carbonation'. In: *Fuel* 245 (2019), pp. 1–12. ISSN: 0016-2361. DOI: https://doi.org/10.1016/j.fuel.2019.02.067. URL: https://www.sciencedirect.com/science/article/pii/S0016236119302704.

[35] Vahid Rostami et al. 'Microstructure of cement paste subject to early carbonation curing'. In: *Cement and Concrete Research* 42.1 (2012), pp. 186–193. ISSN: 0008-8846. DOI: https://doi.org/10.1016/j.cemconres.2011.09.010. URL: https://www.sciencedirect.com/science/article/pii/S0008884611002559.

[36] *Sement Del 1: Sammensetning, krav og samsvarskriterier for ordinære sementtyper*. Norsk Standard NS-EN 197-1:2011. Dec. 2011. URL: https://www.standard.no/no/Nettbutikk/produktkatalogen/Produktpresentasjon/?ProductID=507733.

[37] Statistisk Sentralbyrå. *Avfallsregnskapet*. URL: https://www.ssb.no/natur-og-miljo/avfall/statistikk/avfallsregnskapet (visited on 13th June 2022).

[38] Nils Spjeldnæs. *kalkstein*. URL: https://snl.no/kalkstein. (accessed: 24.01.2022).

[39] European Union. *Construction and demolition waste*. URL: https://ec.europa.eu/environment/topics/waste-and-recycling/construction-and-demolition-waste_en. (accessed:06.12.2022).

[40] Géraldine Villain, Mickaël Thiery and Gérard Platret. 'Measurement methods of carbonation profiles in concrete: Thermogravimetry, chemical analysis and gammadensimetry'. In: *Cement and Concrete Research* 37.8 (2007), pp. 1182–1192. ISSN: 0008-8846. DOI: https://doi.org/10.1016/j.cemconres.2007.04.015. URL: https://www.sciencedirect.com/science/article/pii/S0008884607001044.

[41] Maciej Zajac et al. 'Effect of carbonated cement paste on composite cement hydration and performance'. In: *Cement and Concrete Research* 134 (2020), p. 106090. ISSN: 0008-8846. DOI: https://doi.org/10.1016/j.cemconres.2020.106090. URL: https://www.sciencedirect.com/science/article/pii/S0008884619314413.

[42] Maciej Zajac et al. 'Kinetics of enforced carbonation of cement paste'. In: *Cement and Concrete Research* 131 (2020), p. 106013. ISSN: 0008-8846. DOI: https://doi.org/10.1016/j.cemconres.2020.106013. URL: https://www.sciencedirect.com/science/article/pii/S0008884619312578.

[43]   Maciej Zajac et al. 'Phase assemblage and microstructure of cement paste subjected to enforced, wet carbonation'. In: *Cement and Concrete Research* 130 (2020), p. 105990. ISSN: 0008-8846. DOI: https://doi.org/10.1016/j.cemconres.2020.105990. URL: https://www.sciencedirect.com/science/article/pii/S0008884619309500.

8 Appendix

8.1 Flexural and Compressive Strength

Average compressive strength are shown in Table 20, and relative compressive strength are shown in Table 21. The strength development for RB01, RB09 - RB10, RB11 - RB12 and RB13 - RB14 are shown in Figure 65, 66, 67 and 68. The weight of all the prisms are seen in Table 22. All flexural and compressive strength values are seen in Table 23, 24, 25, 26, 27, 28, 29, 30 and 31.
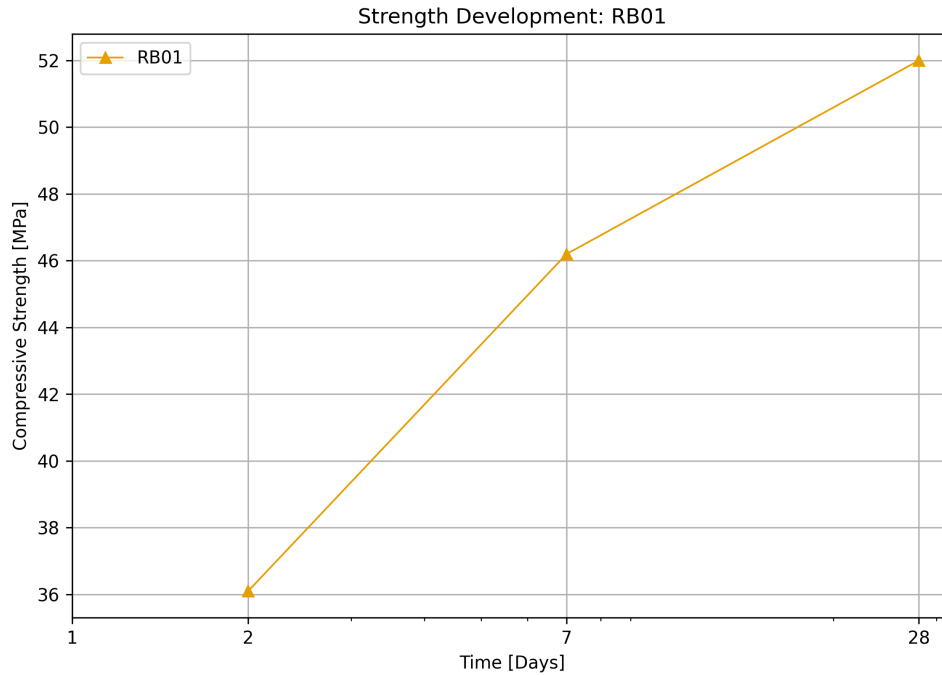
Figure 65: Strength development to RB01.

Table 20: Average compressive strength [MPa] for the reference sample and the 8 different samples containing composite cement after 1-28 days.

Test material	1 day	2 days	7 days	28 days
Ref. Ind.	33.4	44.0	52.3	61.1
RB01	-	36.1	46.2	52.0
RB09	24.6	35.6	45.2	52.8
RB10	26.4	35.1	43.7	51.4
RB11	21.8	32.0	41.0	48.2
RB12	22.0	31.3	41.5	47.6
RB13	25.5	34.9	44.1	50.0
RB14	28.3	37.6	46.0	52.6
RB15	-	-	-	48.9
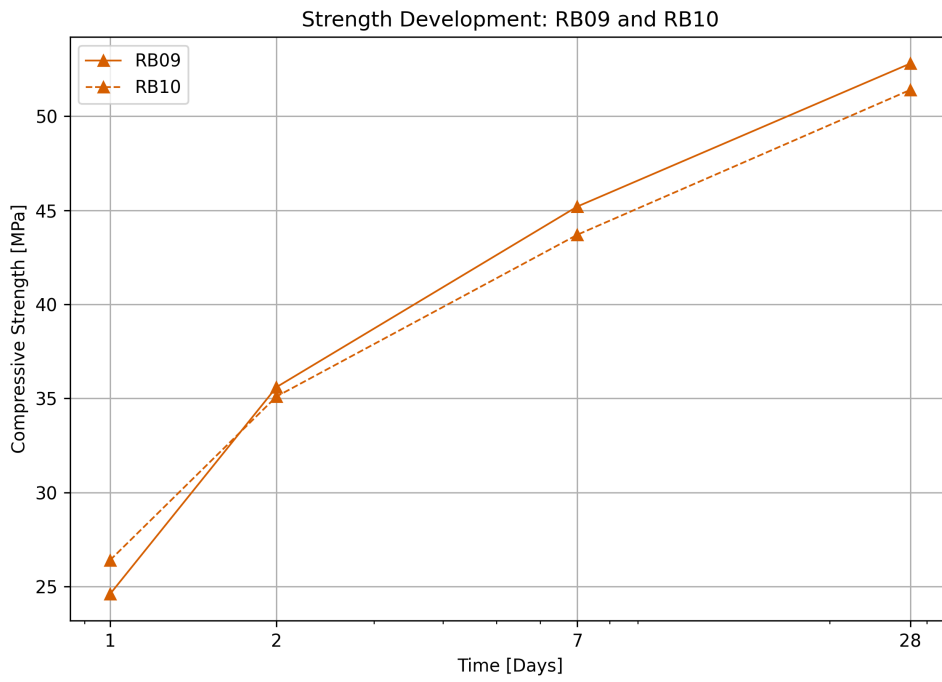
Figure 66: Strength development to RB09 and RB10.
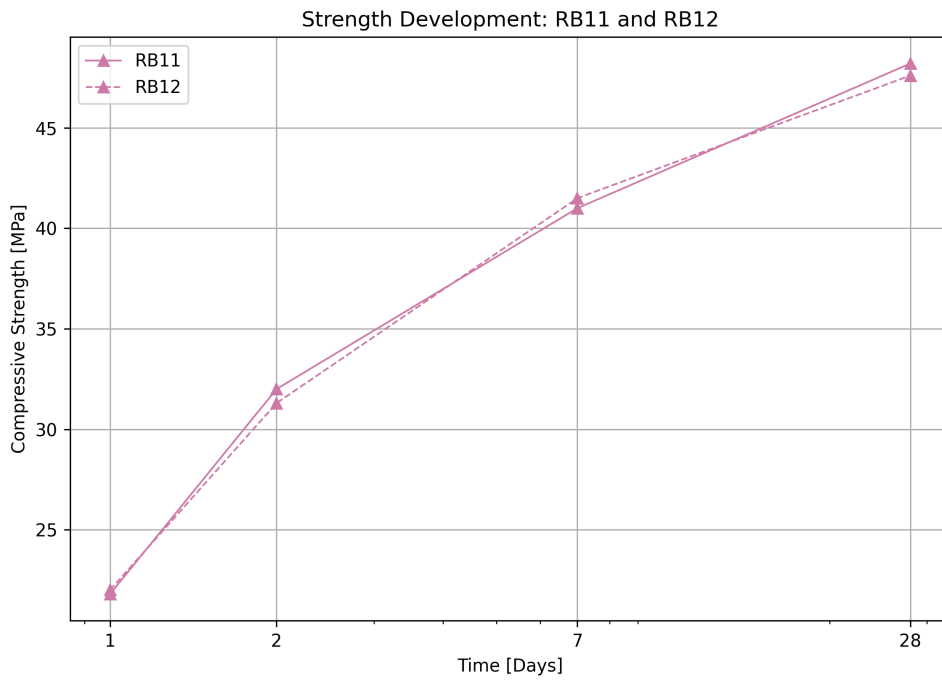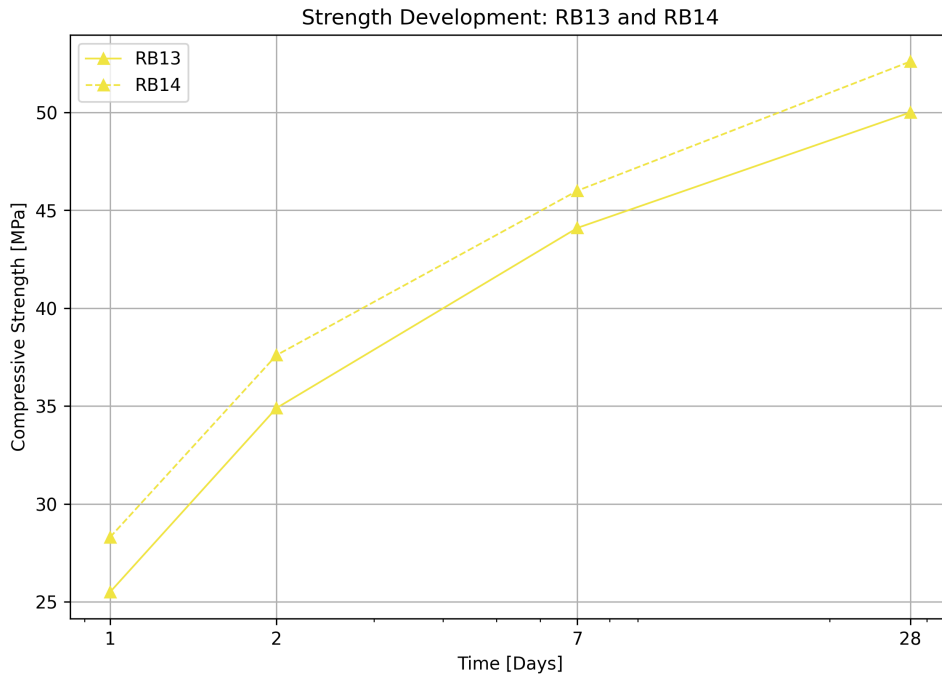

Figure 67: Strength development to RB11 and RB12.

Figure 68: Strength development to RB13 and RB14.

Table 21: Relative compressive strength [%] for the reference sample and the 8 different samples containing composite cement after 1-28 days.

Test material	1 day	2 days	7 days	28 days
Ind. Ref.	100.0	100.0	100.0	100.0
RB01	-	82.0	88.3	85.1
RB09	73.7	80.9	86.4	86.4
RB10	79.0	79.8	83.6	84.1
RB11	65.3	72.7	78.4	78.9
RB12	65.9	71.1	79.3	77.9
RB13	76.3	79.3	84.3	81.8
RB14	84.7	85.5	88.0	86.1
RB15	-	-	-	80.0

Table 22: Weight of compression strength prisms, given in grams.

	1 day	2 days	7 days	28 days	Average
Ind. Ref.	558	559	560	567	
	567	569	568	570	
	571	566	565	568	566
RB01	-	552	550	551	
	-	553	556	552	
	-	556	559	559	554
RB09	561	563	560	566	
	562	565	565	568	
	568	560	559	563	563
RB10	568	565	564	560	
	558	565	561	566	
	565	563	561	561	563
RB11	556	561	563	554	
	558	556	558	558	
	559	558	558	561	558
RB12	559	560	563	565	
	565	561	567	562	
	563	566	562	567	563
RB13	554	557	557	551	
	551	557	551	559	
	560	553	553	555	555
RB14	562	564	562	566	
	567	562	566	566	
	566	562	564	563	564
RB15	-	-	-	556	
	-	-	-	559	
	-	-	-	561	559

Table 23: Flexural and compressive strength results to reference industry sample.

Specimen	Flexural strength (MPa)				Compressive strength (MPa)			
	1 day	2 days	7 days	28 days	1 days	2 days	7 days	28 days
1 a	7.58	-	7.4	8.3	33.5	42.8	51.5	60.7
1 b					32.5	43.6	52.3	61.6
2 a	6.95	7.0	7.7	8.2	34.0	44.4	52.4	59.9
2 b					33.3	44.4	52.4	61.1
3 a	7.14	6.4	8.7	8.9	33.5	44.7	52.7	62.3
3 b					33.6	44.3	52.4	61.2
Average	7.2	6.7	7.9	8.5	33.4	44.0	52.3	61.1

Table 24: Flexural and compressive strength results of RB01.

Specimen	Flexural strength (MPa)			Compressive strength (MPa)		
	2 days	7 days	28 days	2 days	7 days	28 days
1 a	6.1	7.1	7.4	36.1	45.4	50.7
1 b				35.8	45.1	51.4
2 a	6.3	6.9	7.6	34.9	46.4	54.6
2 b				37.1	46.7	50.9
3 a	5.8	-	7.7	35.2	46.8	52.1
3 b				37.4	46.7	52.5
Average	6.1	7.0	7.6	36.1	46.2	52.0

Table 25: Flexural and compressive strength results of RB09.

Specimen	Flexural strength (MPa)				Compressive strength (MPa)			
	1 day	2 days	7 days	28 days	1 days	2 days	7 days	28 days
1 a	5.7	6.2	6.4	7.3	24.8	35.7	45.8	52.5
1 b					24.1	35.7	44.3	51.8
2 a	5.7	6.1	-	8.1	24.0	35.2	45.9	53.7
2 b					24.3	36.3	45.7	54.0
3 a	5.6	6.0	7.0	-	25.3	35.0	45.7	52.3
3 b					25.0	35.4	43.6	52.7
Average	5.7	6.1	6.7	7.7	24.6	35.6	45.2	52.8

Table 26: Flexural and compressive strength results of RB10.

Specimen	Flexural strength (MPa)				Compressive strength (MPa)			
	1 day	2 days	7 days	28 days	1 days	2 days	7 days	28 days
1 a	6.1	5.7	6.3	7.5	25.9	35.2	43.2	51.5
1 b					26.4	34.3	43.3	51.0
2 a	6.0	6.2	6.6	7.7	26.5	35.1	43.6	51.2
2 b					26.1	35.7	43.8	52.3
3 a	5.7	5.9	6.8	7.7	26.8	35.0	44.5	50.8
3 b					26.7	35.4	43.5	51.4
Average	5.9	5.9	6.5	7.6	26.4	35.1	43.7	51.4

Table 27: Flexural and compressive strength results of RB11.

Specimen	Flexural strength (MPa)				Compressive strength (MPa)			
	1 day	2 days	7 days	28 days	1 days	2 days	7 days	28 days
1 a	4.8	5.7	6.5	7.9	21.5	31.9	41.2	47.2
1 b					21.7	32.1	40.3	46.3
2 a	5.0	5.4	6.7	7.4	21.9	32.0	39.7	48.5
2 b					21.9	31.6	40.8	49.3
3 a	4.6	5.6	6.8	8.1	21.8	32.0	42.2	49.7
3 b					21.9	32.2	41.7	48.4
Average	4.8	5.6	6.7	7.8	21.8	32.0	41.0	48.2

Table 28: Flexural and compressive strength results of RB12.

Specimen	Flexural strength (MPa)				Compressive strength (MPa)			
	1 day	2 days	7 days	28 days	1 days	2 days	7 days	28 days
1 a	4.7	5.4	7.1	7.3	23.0	32.2	41.7	47.5
1 b					22.9	32.1	41.8	48.3
2 a	4.6	5.4	6.8	7.6	21.8	29.9	41.8	45.8
2 b					22.2	29.5	41.9	46.3
3 a	4.6	5.6	6.8	7.9	20.9	32.7	41.1	48.7
3 b					21.1	31.3	40.9	49.2
Average	4.6	5.5	6.9	7.6	22.0	31.3	41.5	47.6

Table 29: Flexural and compressive strength results of RB13.

Specimen	Flexural strength (MPa)				Compressive strength (MPa)			
	1 day	2 days	7 days	28 days	1 days	2 days	7 days	28 days
1 a	5.1	5.9	6.0	8.2	25.3	35.4	43.8	48.9
1 b					25.2	35.3	43.6	48.9
2 a	5.4	6.2	6.4	7.3	25.6	34.1	45.2	50.5
2 b					25.5	34.0	44.1	50.0
3 a	5.3	5.8	6.1	7.3	25.6	34.8	43.8	50.6
3 b					26.0	35.6	44.1	51.1
Average	5.3	6.0	6.1	7.6	25.5	34.9	44.1	50.0

Table 30: Flexural and compressive strength results of RB14.

Specimen	Flexural strength (MPa)				Compressive strength (MPa)			
	1 day	2 days	7 days	28 days	1 days	2 days	7 days	28 days
1 a	5.8	6.3	-	-	28.2	37.5	45.8	51.8
1 b					27.8	38.3	45.8	52.4
2 a	5.7	6.8	7.3	8.3	28.9	37.7	45.4	54.3
2 b					28.5	37.9	45.0	54.1
3 a	5.8	6.0	6.8	7.9	27.8	37.1	46.5	50.6
3 b					28.3	37.3	47.5	52.5
Average	5.8	6.4	7.1	8.1	28.3	37.6	46.0	52.6

Table 31: Flexural and compressive strength results of RB15.

Sample	Flexural strength (MPa) 28 days	Compressive strength (MPa) 28 days
1 a	8.8	48.9
1 b		48.9
2 a	7.3	49.3
2 b		49.2
3 a	7.8	48.5
3 b		48.3
Average	8.0	48.9

8.2 TGA and DTG

The TGA and DTG result for RB01, RB09 - RB10, RB11 - RB12 and RB13 - RB14 are shown in Figure 69 - 84.
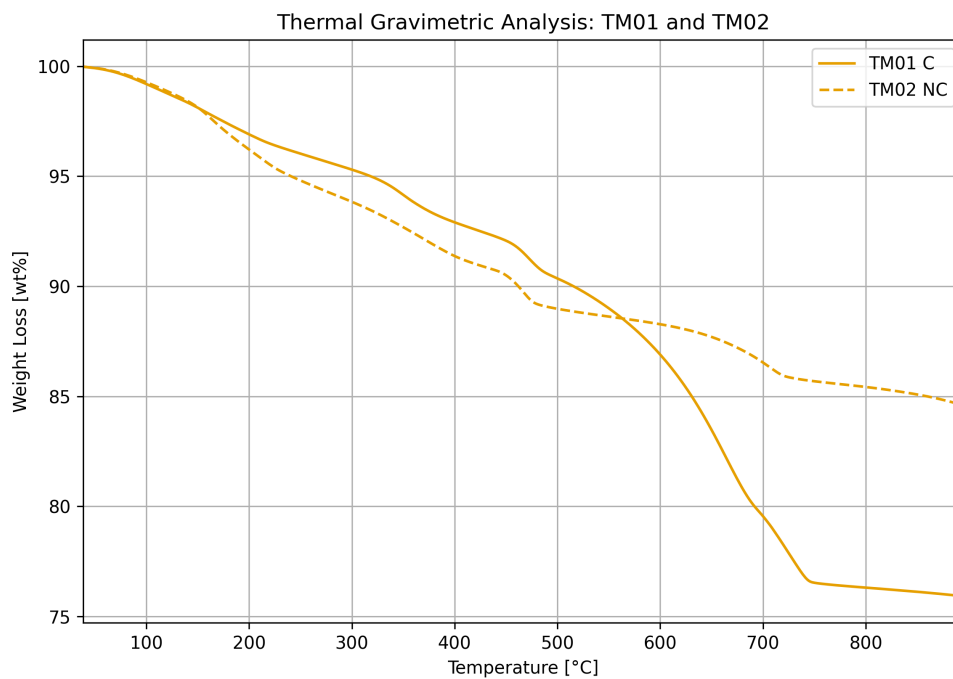
Figure 69: TGA to TM01 and TM02.
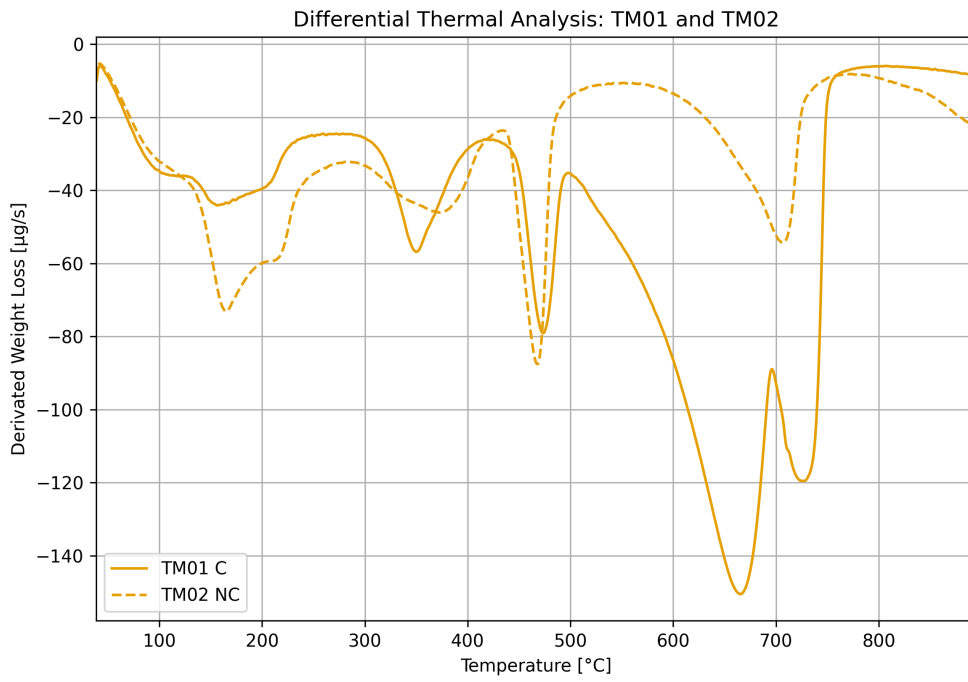
Figure 70: DTG to TM01 and TM02.
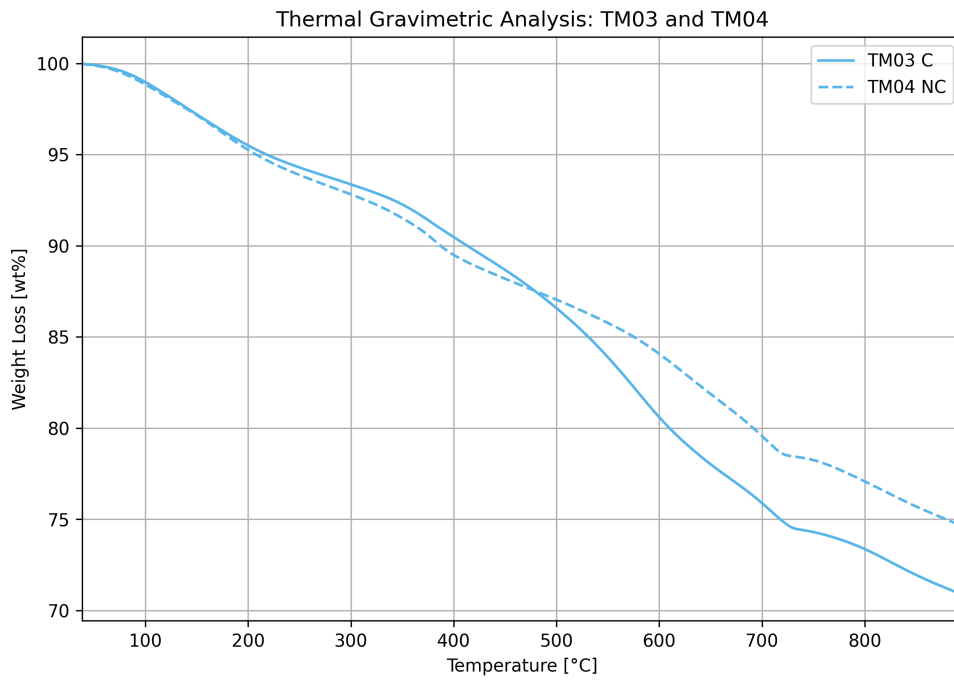
Figure 71: TGA to TM03 and TM04.
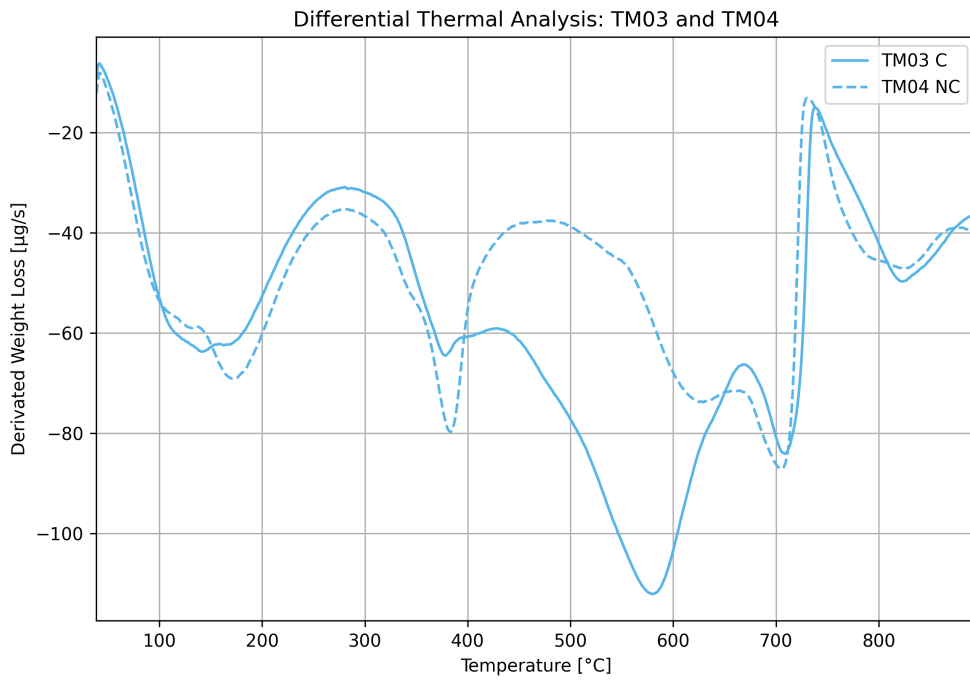
Figure 72: DTG to TM03 and TM04.
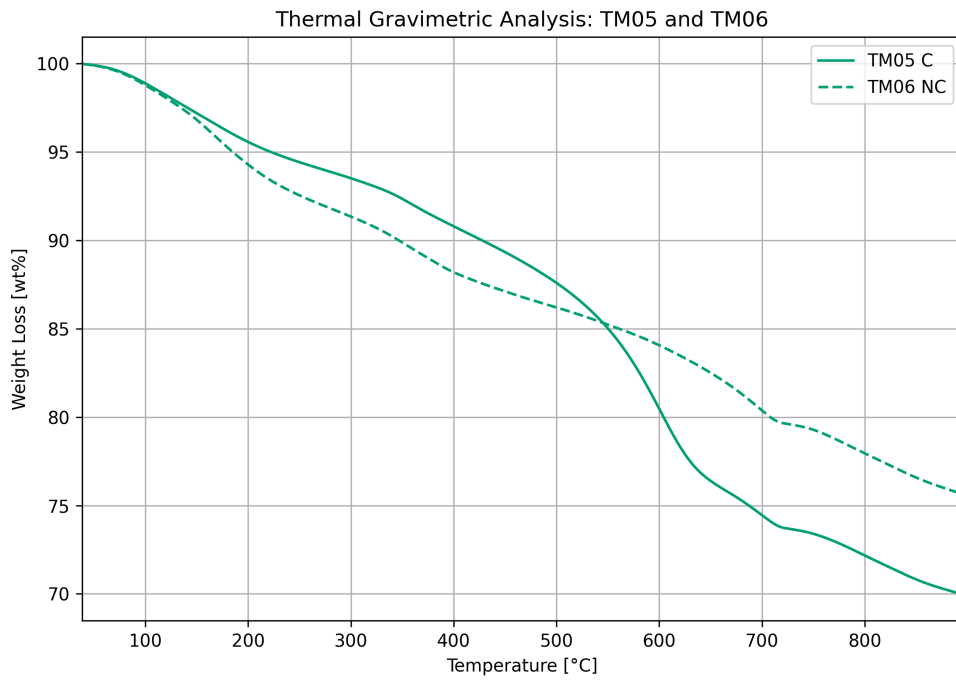
Figure 73: TGA to TM05 and TM06.
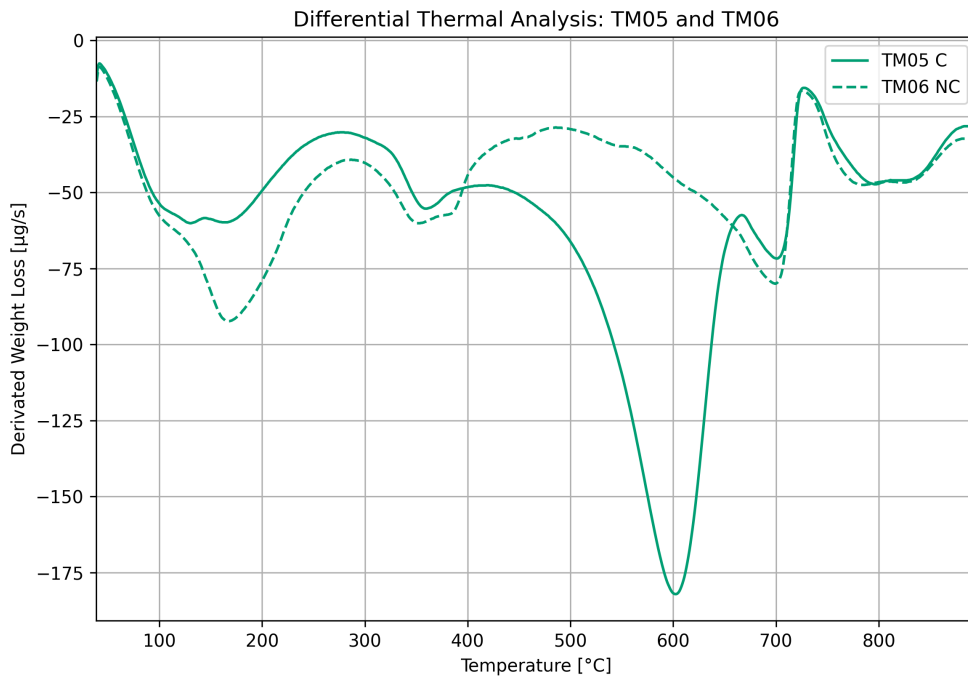
Figure 74: DTG to TM05 and TM06.
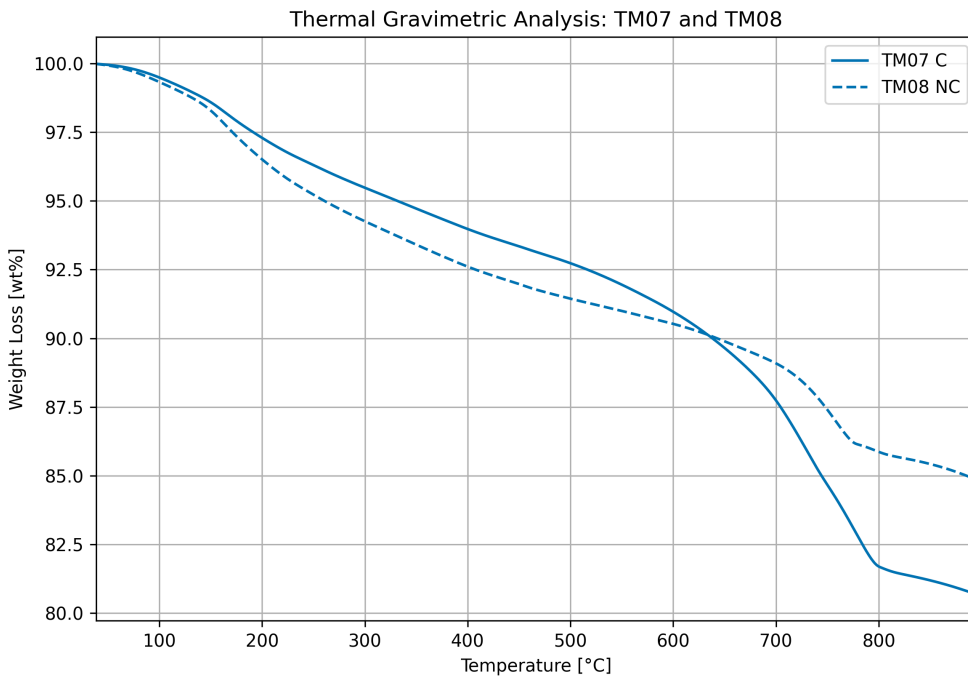
Figure 75: TGA to TM07 and TM08.
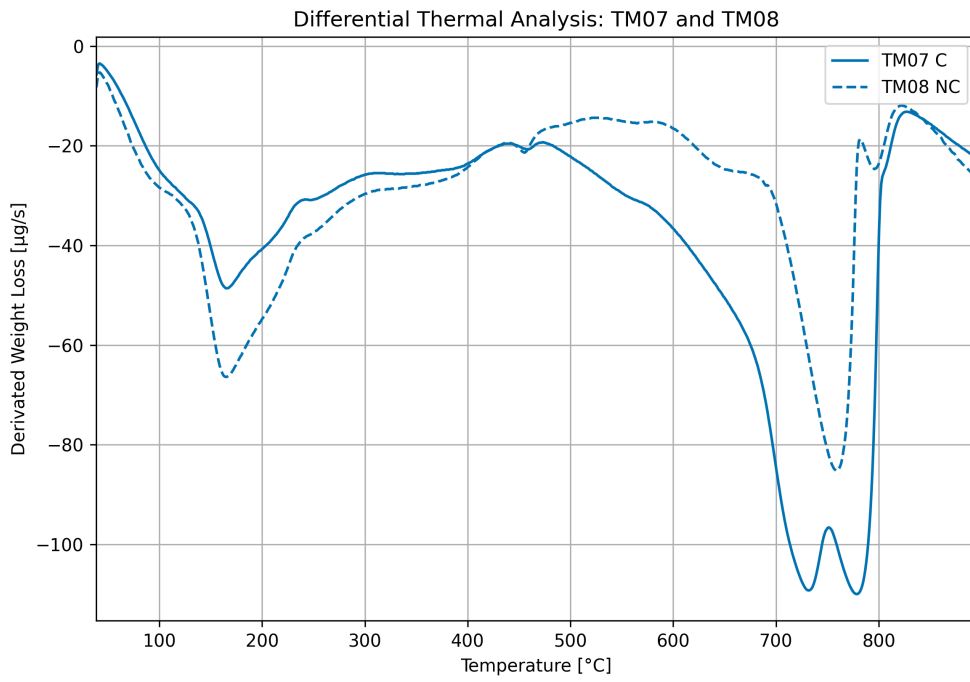
Figure 76: DTG to TM07 and TM08.
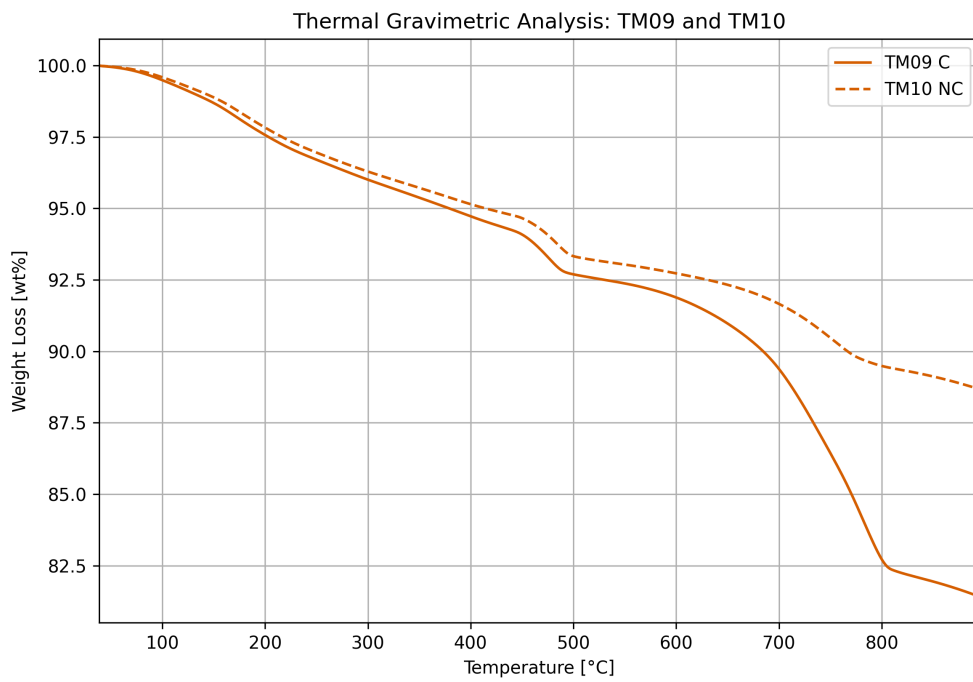
Figure 77: TGA to TM09 and TM10.
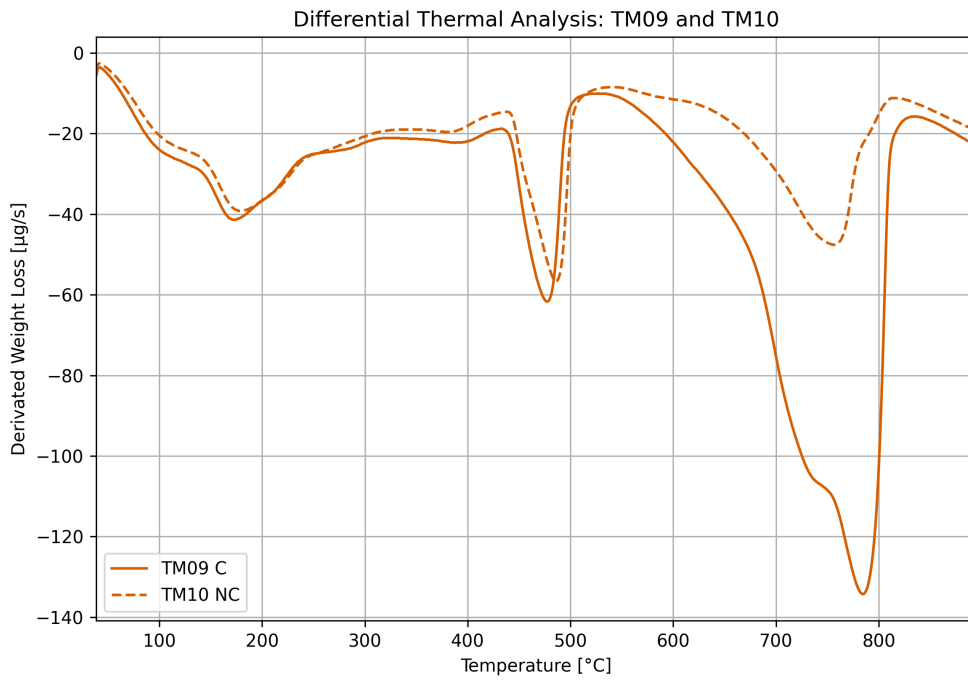
Figure 78: DTG to TM09 and TM10.
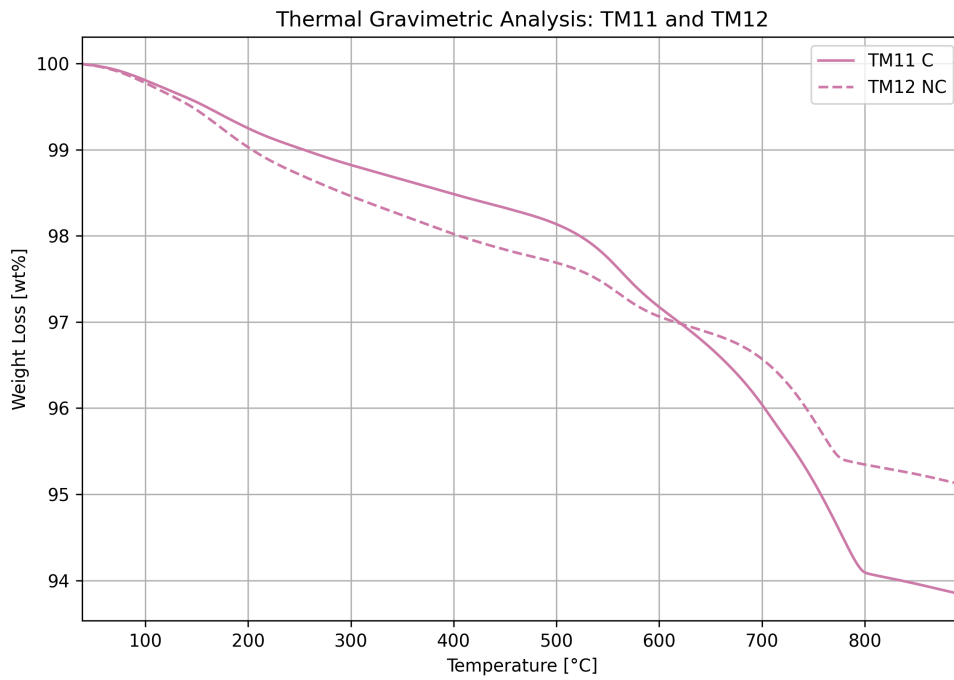
Figure 79: TGA to TM11 and TM12.
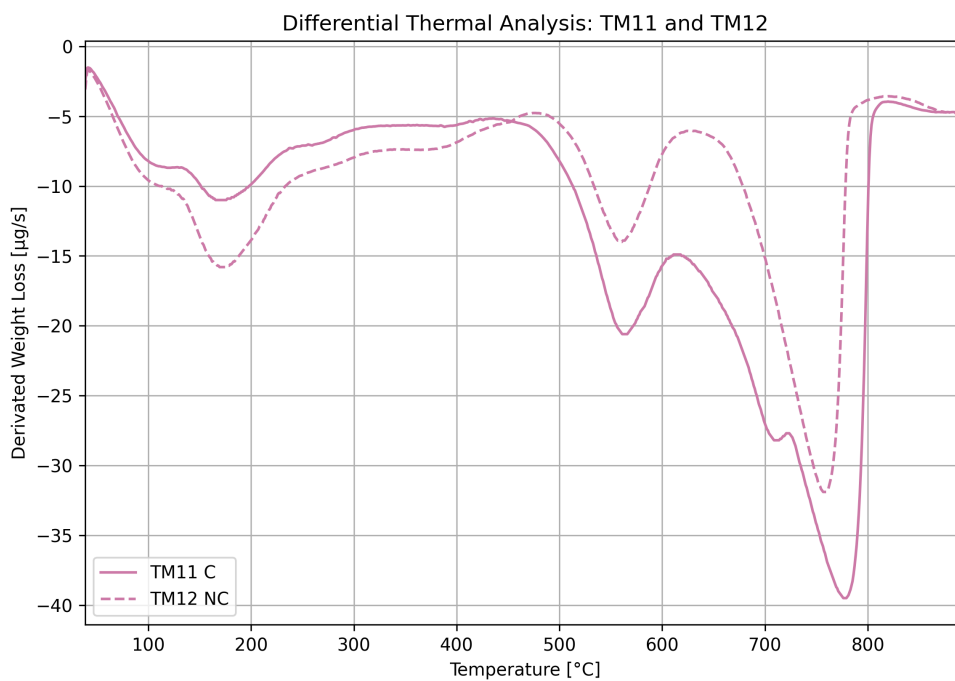
Figure 80: DTG to TM11 and TM12.
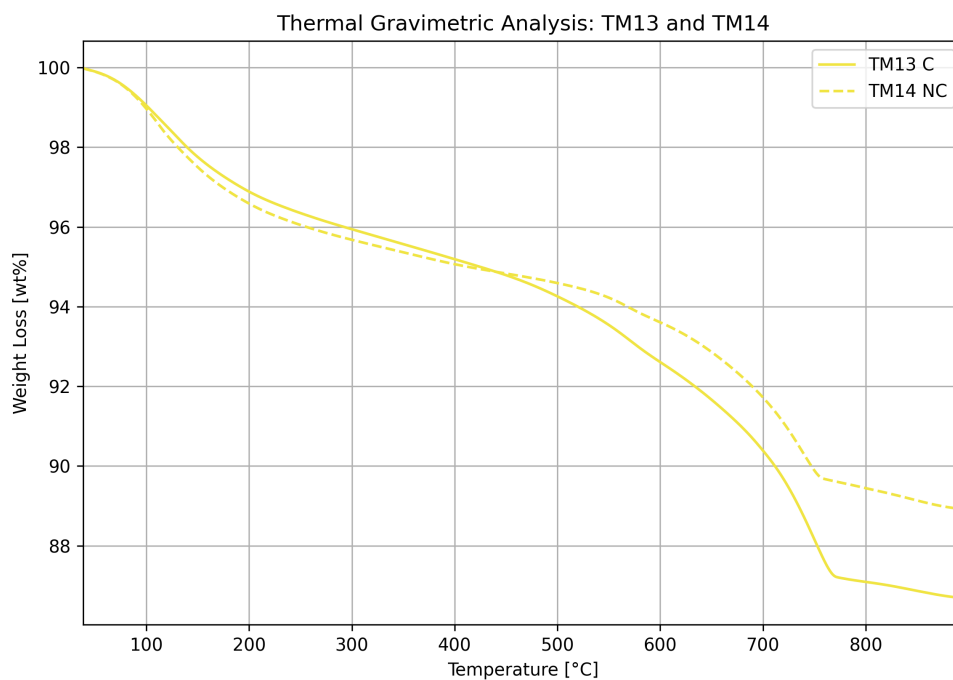
Figure 81: TGA to TM13 and TM14.
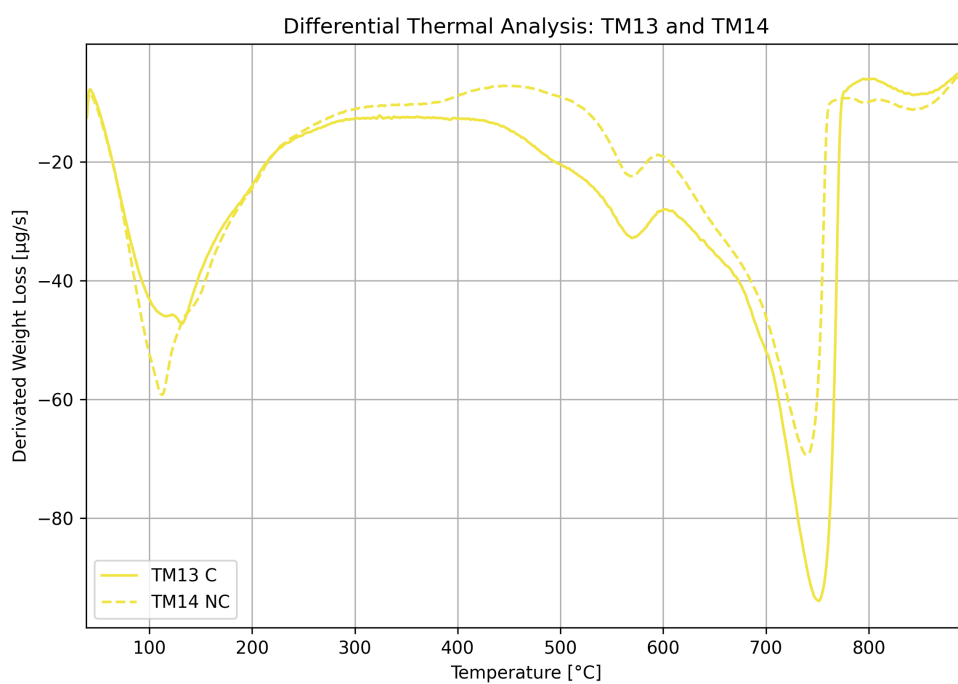
Figure 82: DTG to TM13 and TM14.
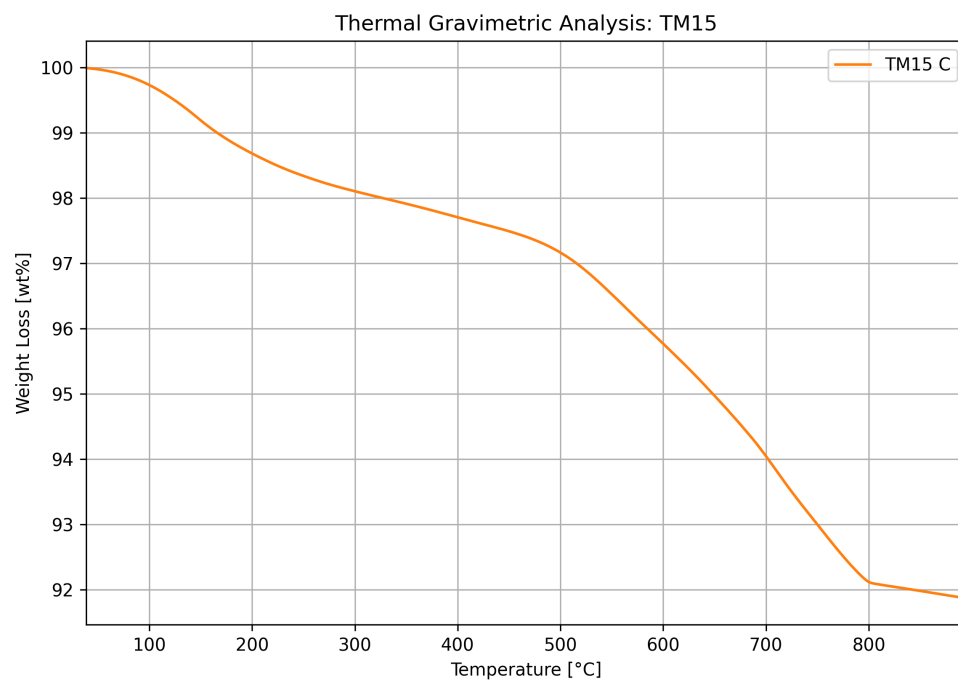
Figure 83: TGA to TM15.
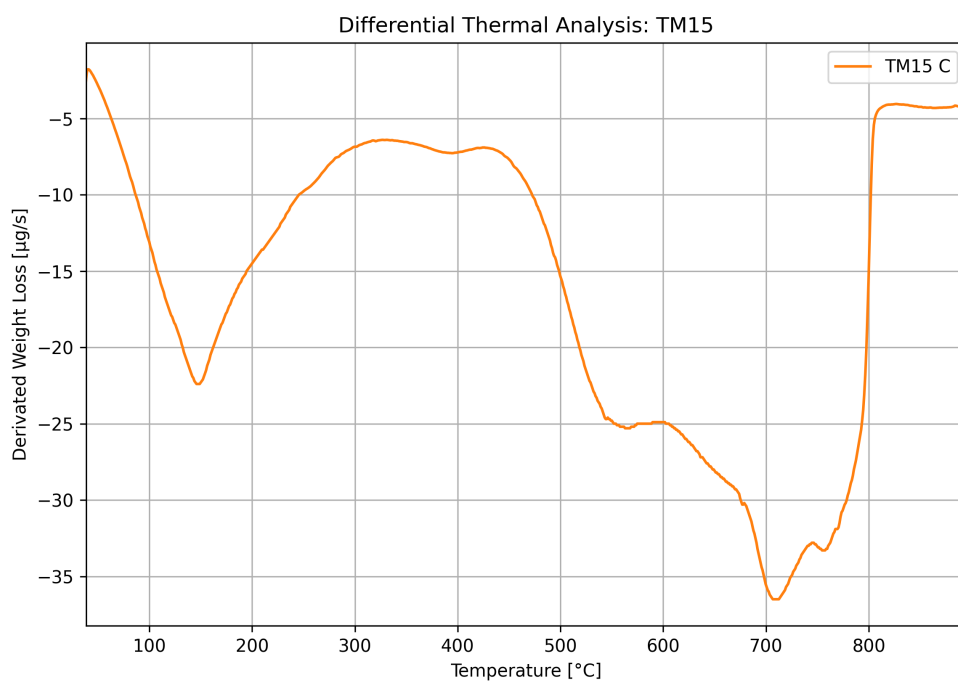
Figure 84: DTG to TM15.

8.3 Particle Size Distribution

The median particle size for the TM samples are shown in Table 32, and the RB samples are seen in Figure 33.

Table 32: TM samples, median diameter and sieve residue.

Test material	D_{50} [μm]
TM01	13.91
TM02	17.5
TM03	7.69
TM04	13.35
TM05	14.1
TM06	16.48
TM07	9.7
TM08	10.5
TM09	10.43
TM10	13.57
TM11	16.36
TM12	20.8
TM13	9.68
TM14	10.23
TM15	25.88
Fly Ash	11.39

Table 33: RB samples, median diameter and sieve residue.

Cement Sample	D_{50} [μm]
Ref. Ind.	6.57
RB01	7.81
RB09	7.16
RB10	7.72
RB11	7.55
RB12	7.67
RB13	7.29
RB14	7.12
RB15	7.15
Standard FA cement	9,06

8.4 Isothermal Calorimetry

The cumulative heat development after 168 h are shown in Table 34.

Table 34: Cumulative heat after 168 h for all the composite cement samples and reference sample.

Sample	Cumulative Heat [J/g powder]
Ref. Ind.	383
RB01	348
RB02	346
RB03	354
RB04	313
RB05	309
RB06	311
RB07	353
RB08	344
RB09	350
RB10	342
RB11	336
RB12	335
RB13	348
RB14	344
RB15	335

Following are the heat development and cumulative heat development for the RB pairs containing carbonated and non-carbonated material. Each pair is shown together with the reference sample. RB01 and RB02 in Figure 85 and 86. RB03 and RB04 in Figure 87 and 88. RB05 and RB06 in Figure 89 and 90. RB07 and RB08 in Figure 91 and 92. RB09 and RB10 in Figure 93 and 94. RB11 and RB12 in Figure 95 and 96. RB13 and RB14 in Figure 97 and 98. RB15 in Figure 99 and 100.
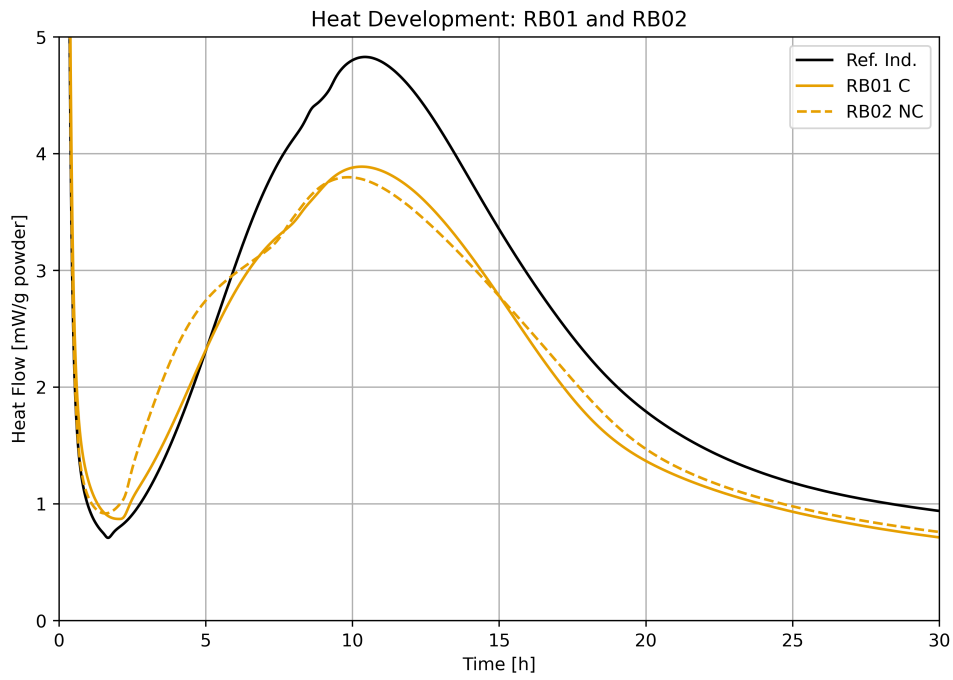
Figure 85: Heat development for RB01 and RB02, together with the reference sample.
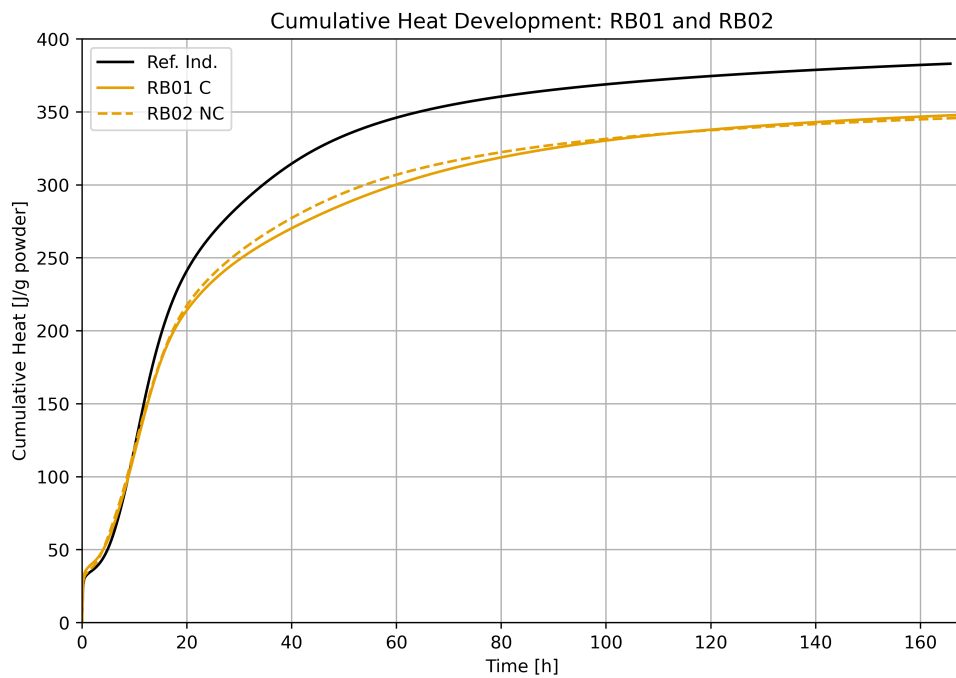
Figure 86: Cumulative heat development for RB01 and RB02, together with the reference sample.
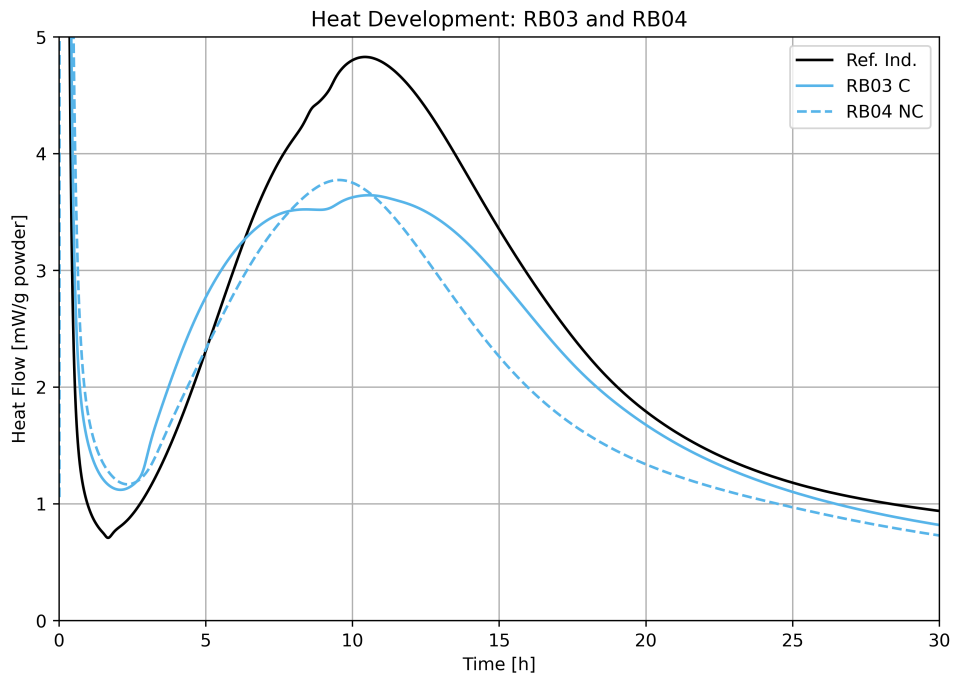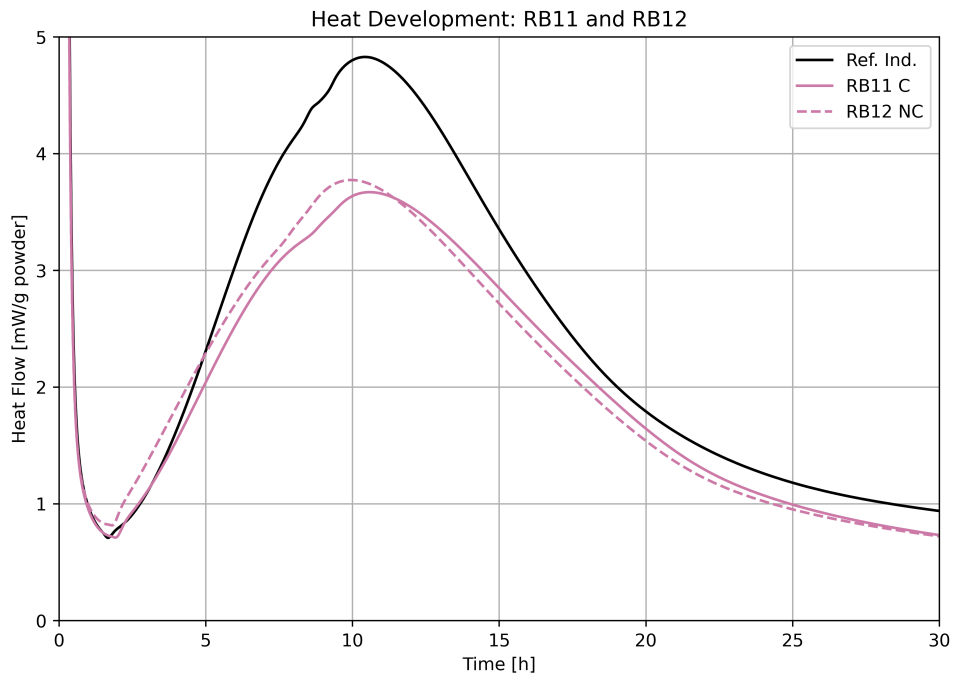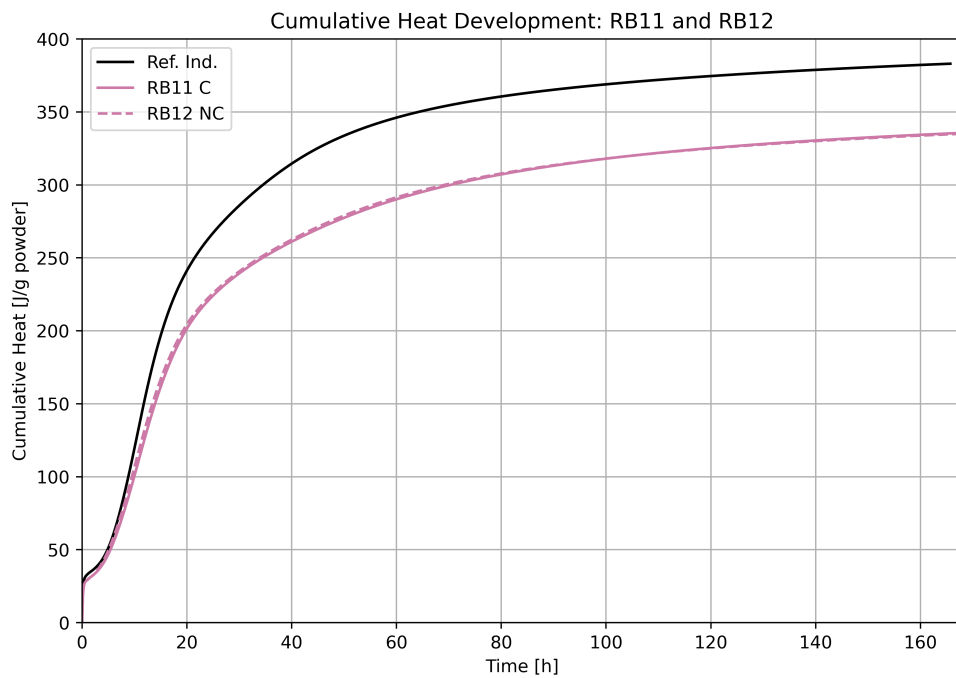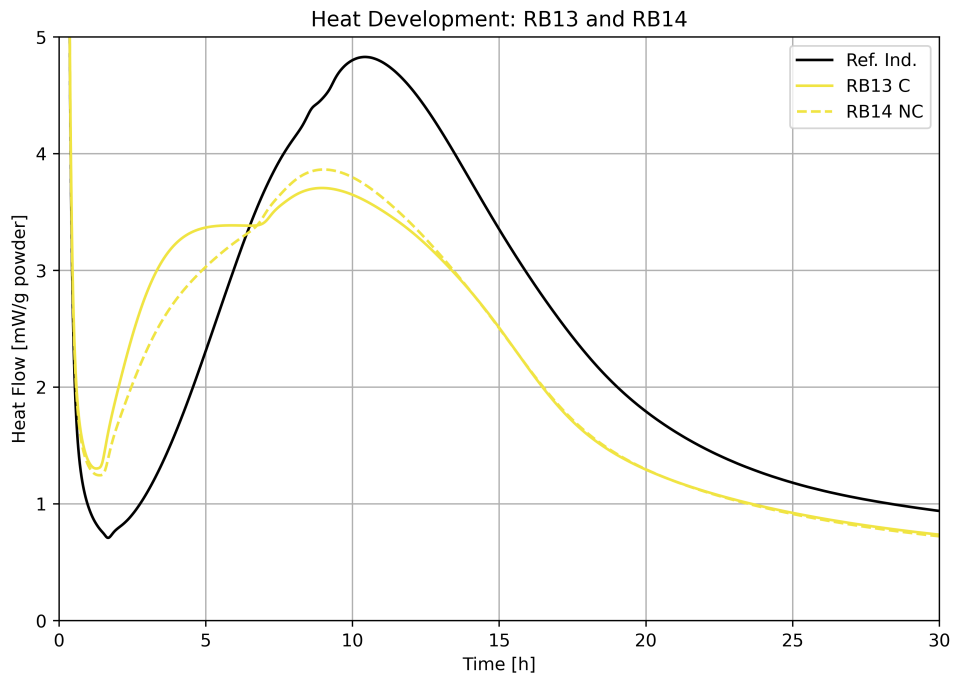
Figure 87: Heat development for RB03 and RB04, together with the reference sample.
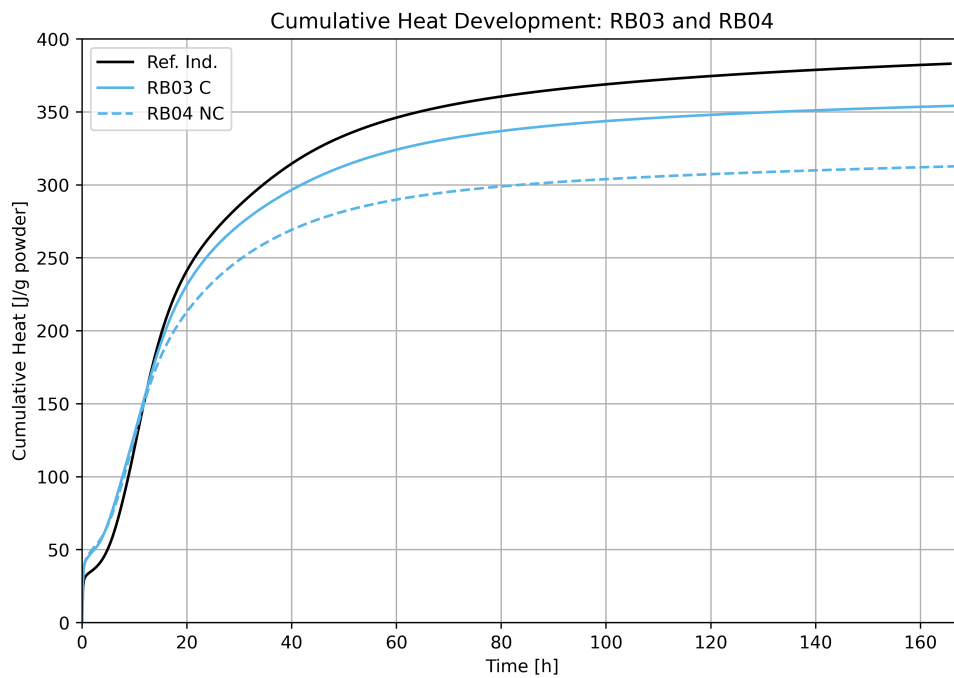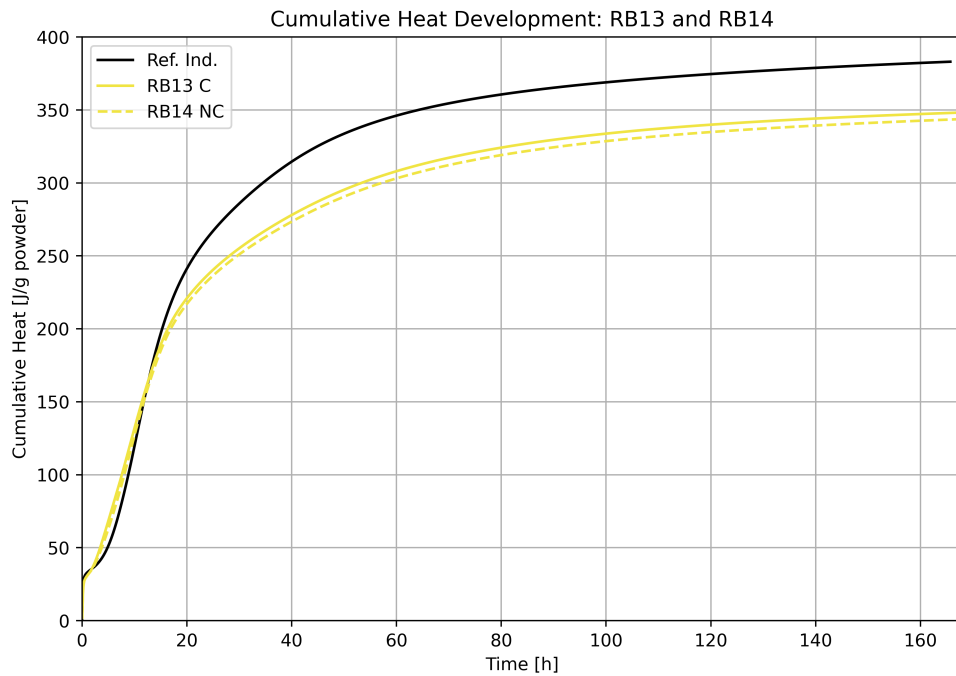

Figure 88: Cumulative heat development for RB03 and RB04, together with the reference sample.
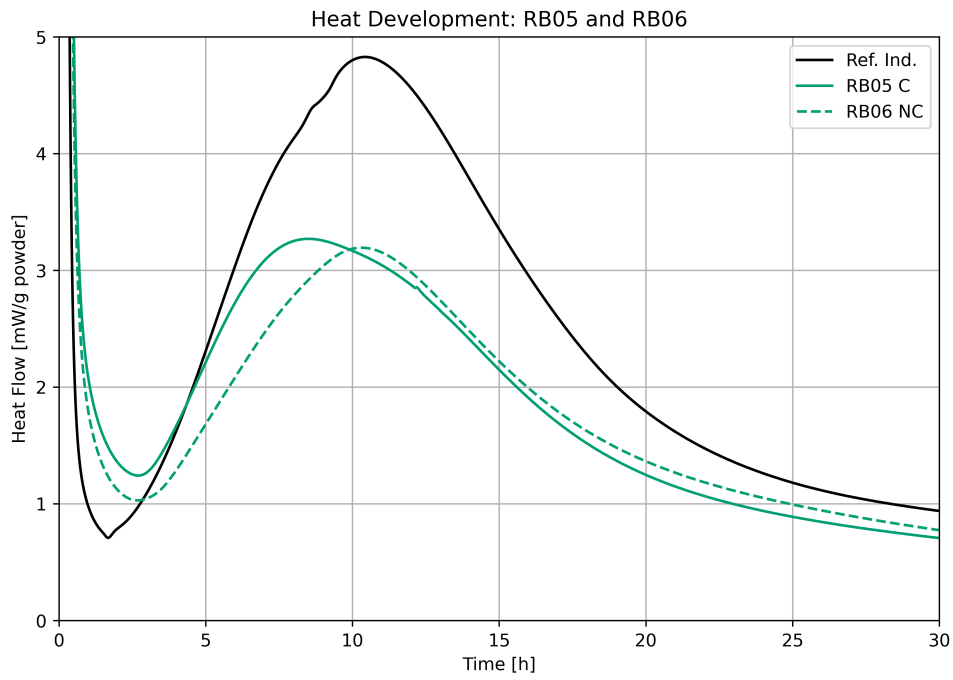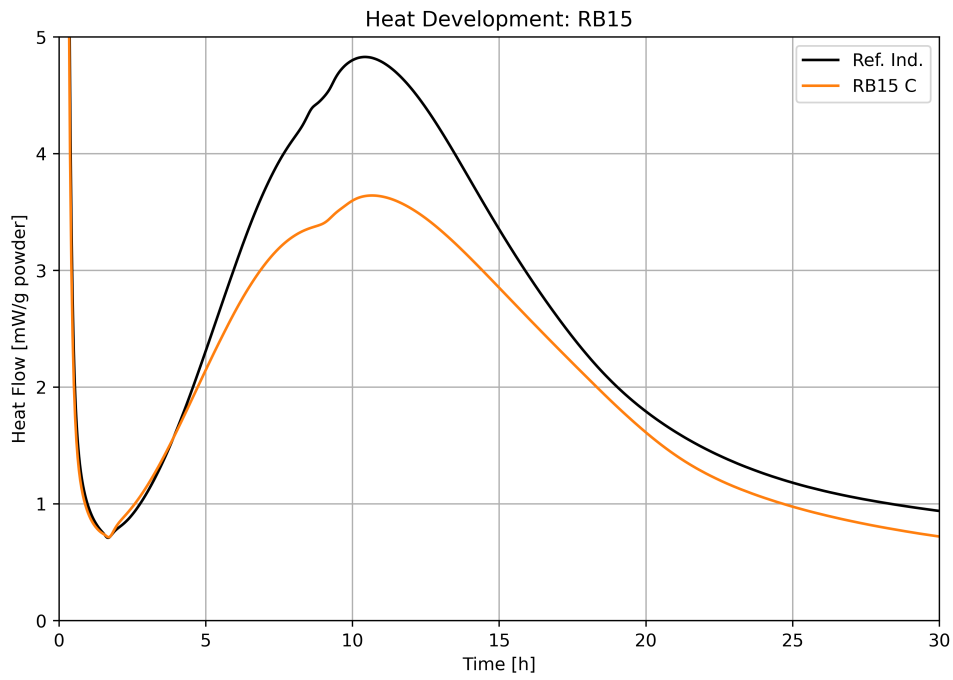
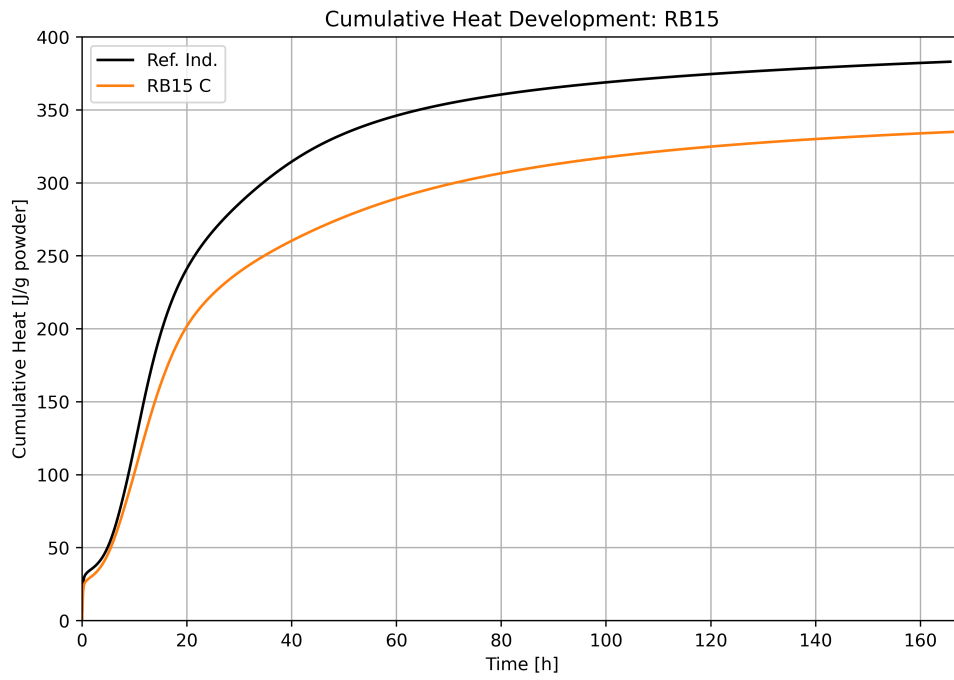Figure 89: Heat development for RB05 and RB06, together with the reference sample.
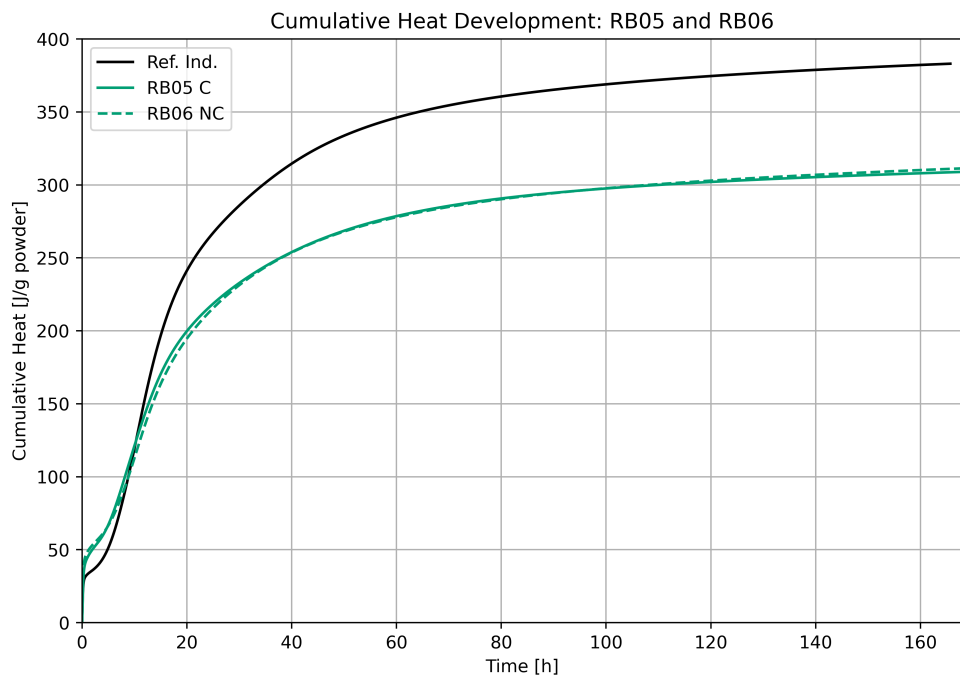
Figure 90: Cumulative heat development for RB05 and RB06, together with the reference sample.
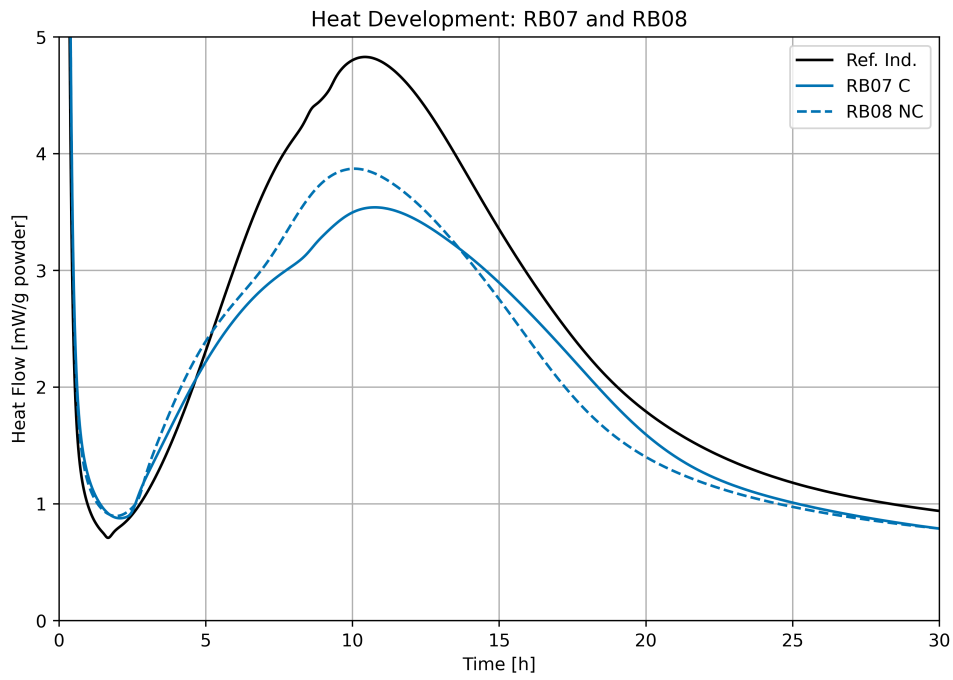
Figure 91: Heat development for RB07 and RB08, together with the reference sample.
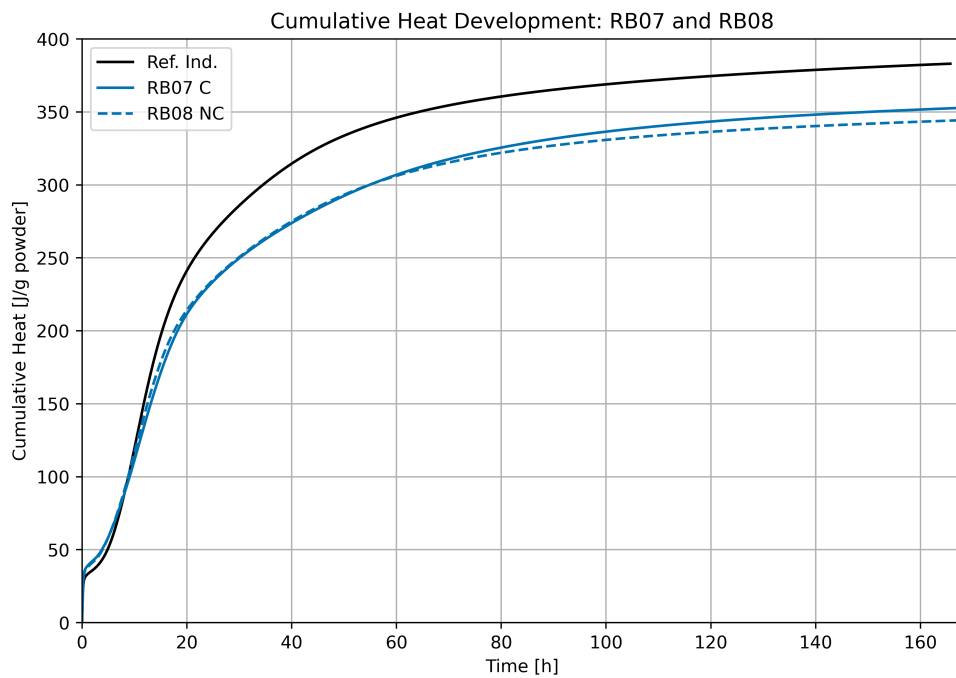
Figure 92: Cumulative heat development for RB07 and RB08, together with the reference sample.
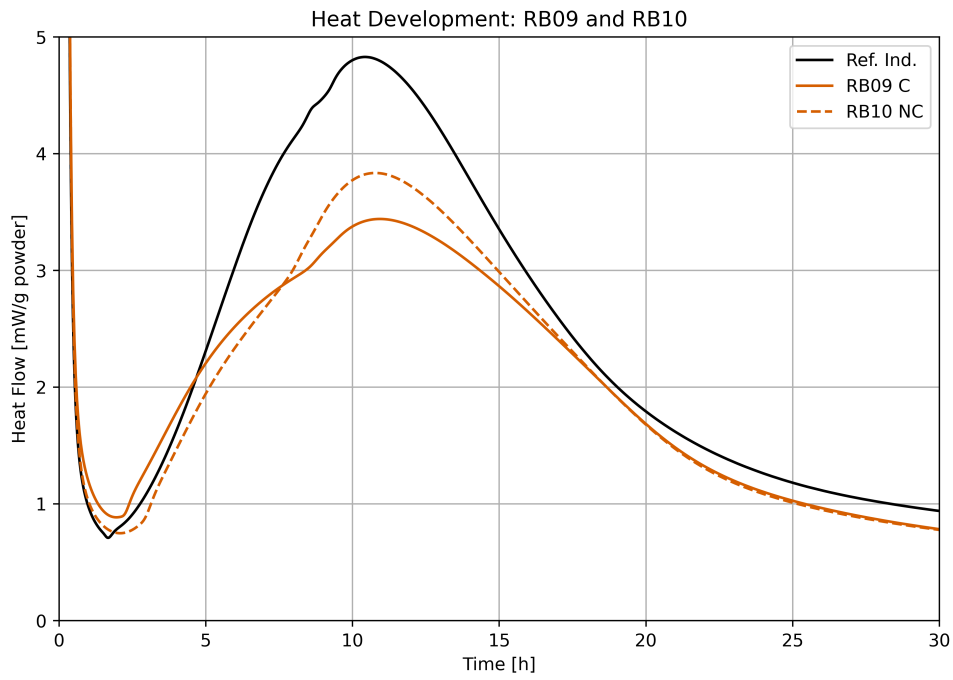
Figure 93: Heat development for RB09 and RB10, together with the reference sample.
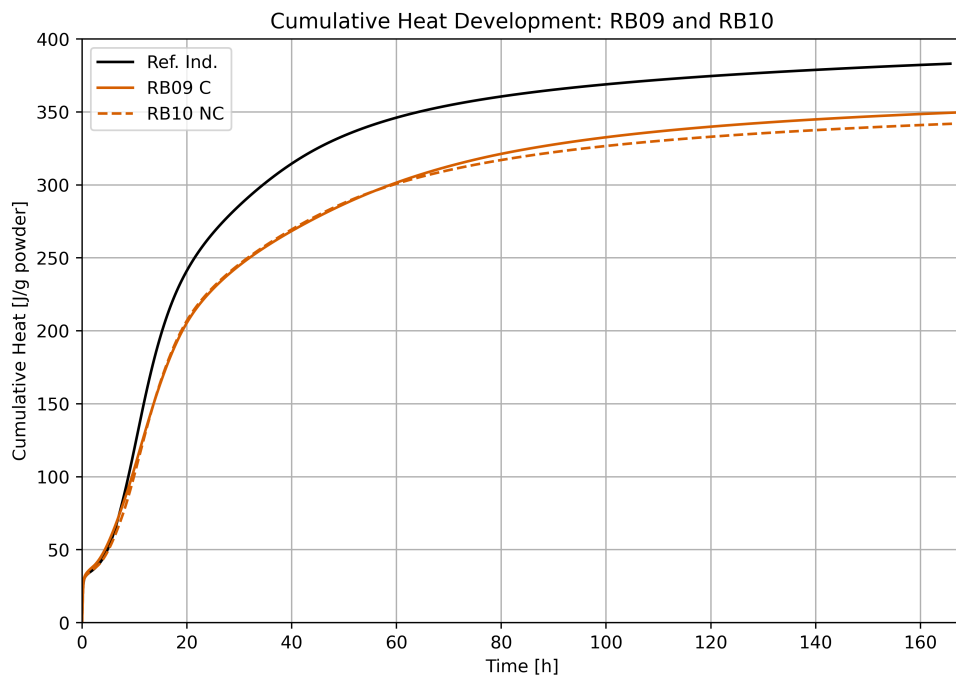
Figure 94: Cumulative heat development for RB09 and RB10, together with the reference sample.

Figure 95: Heat development for RB11 and RB12, together with the reference sample.

Figure 96: Cumulative heat development for RB11 and RB12, together with the reference sample.

Figure 97: Heat development for RB13 and RB14, together with the reference sample.

Figure 98: Cumulative heat development for RB13 and RB14, together with the reference sample.

Figure 99: Heat development for RB15, together with the reference sample.

Figure 100: Cumulative heat development for RB15 together with the reference sample.

8.5   Setting Time

The measurement for each sample is seen in Figure 101 - 109.
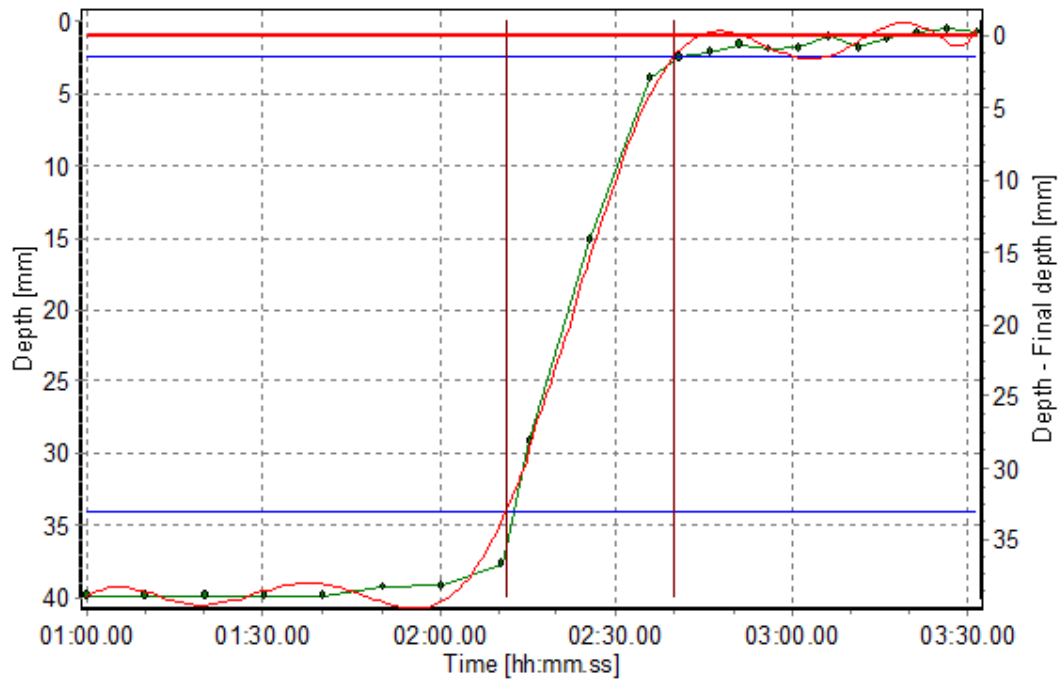
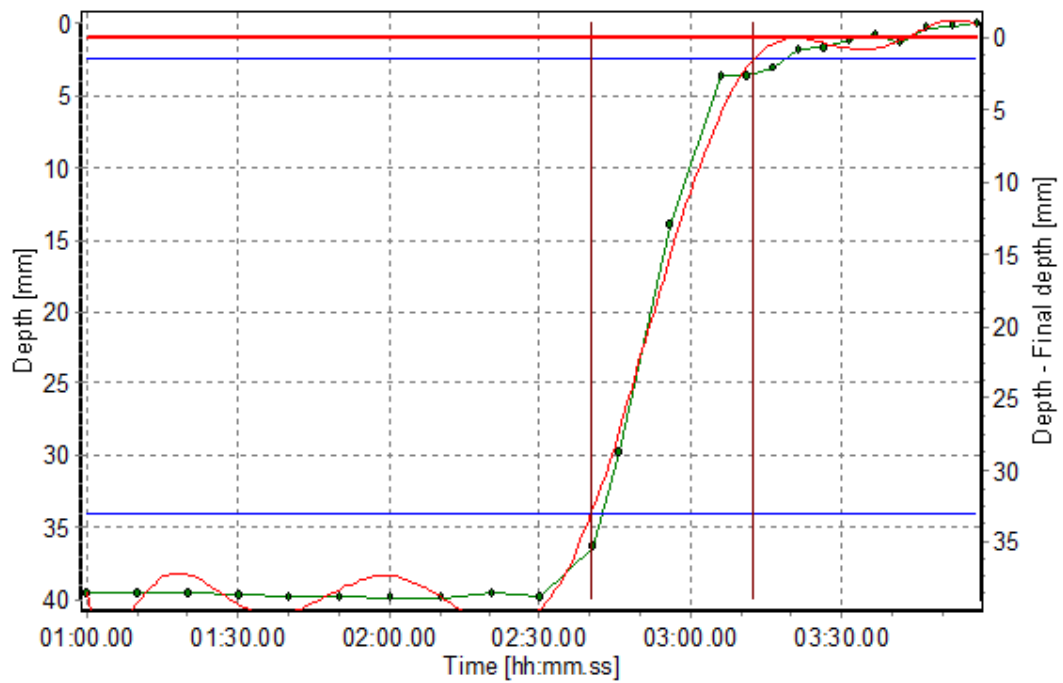Figure 101: Setting time curve of Reference Industry sample, consisting of only Industrisement.
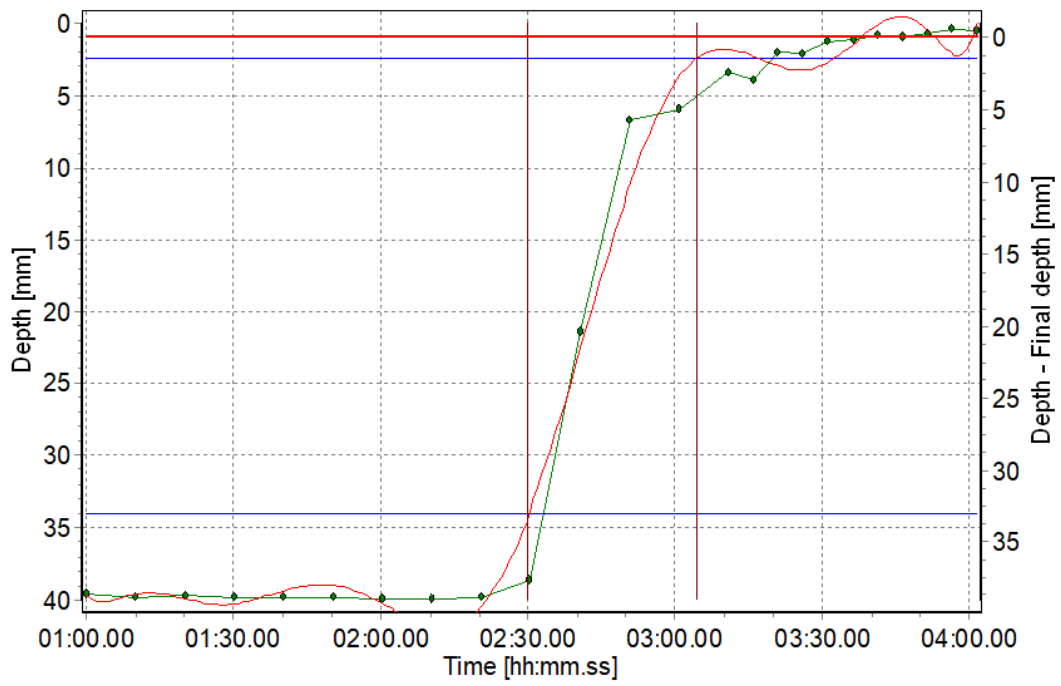
Figure 102: Setting time curve of RB01.
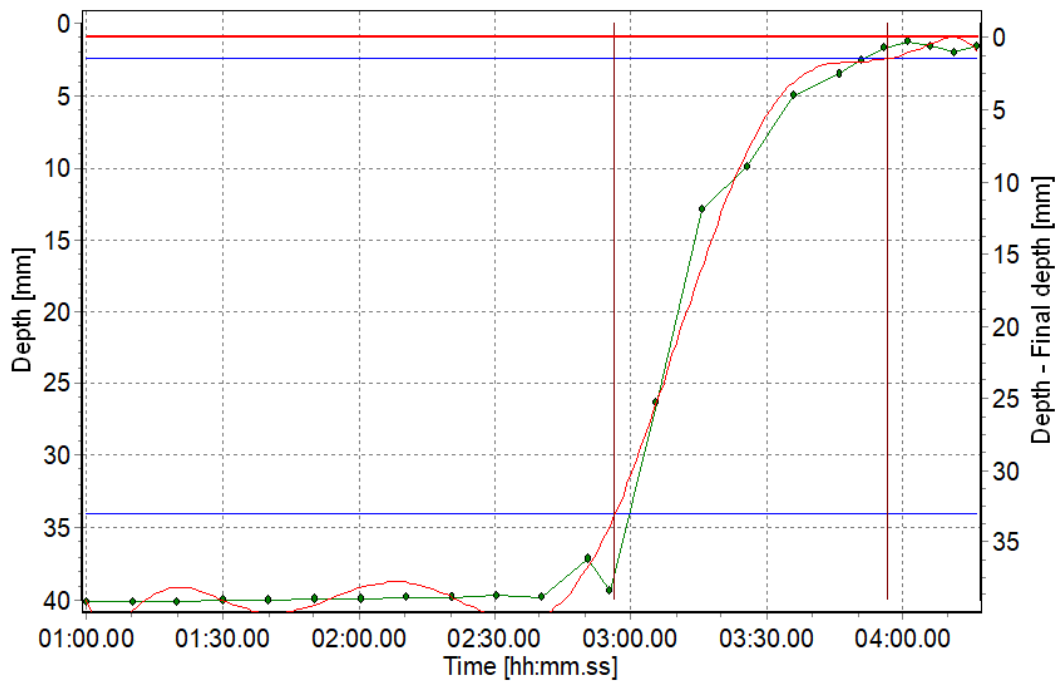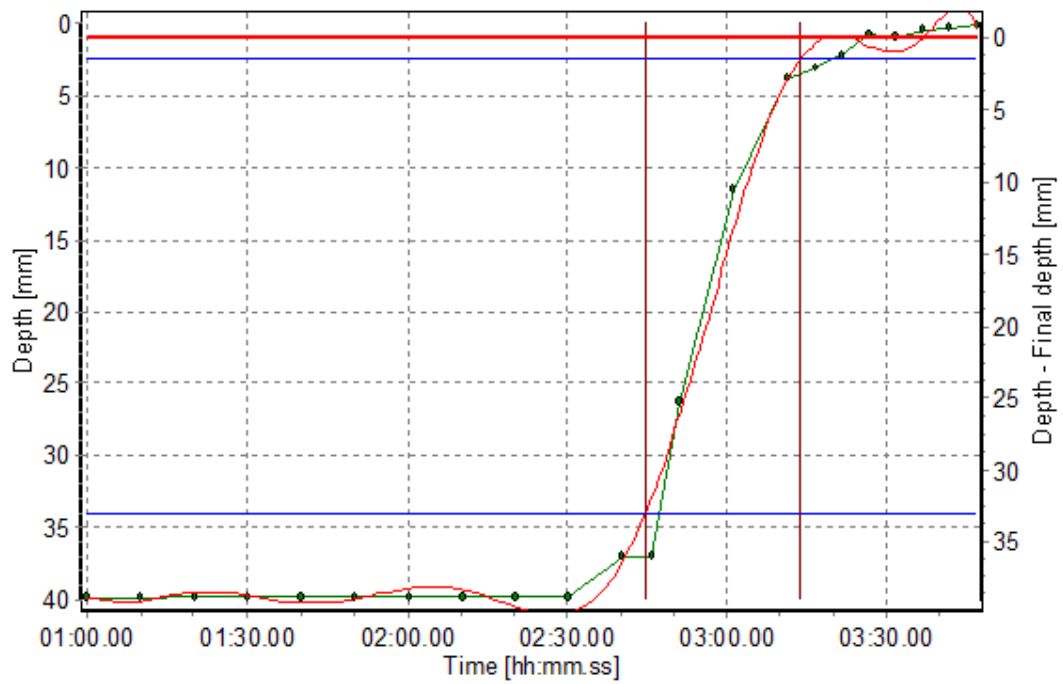

Figure 103: Setting time curve of RB09.
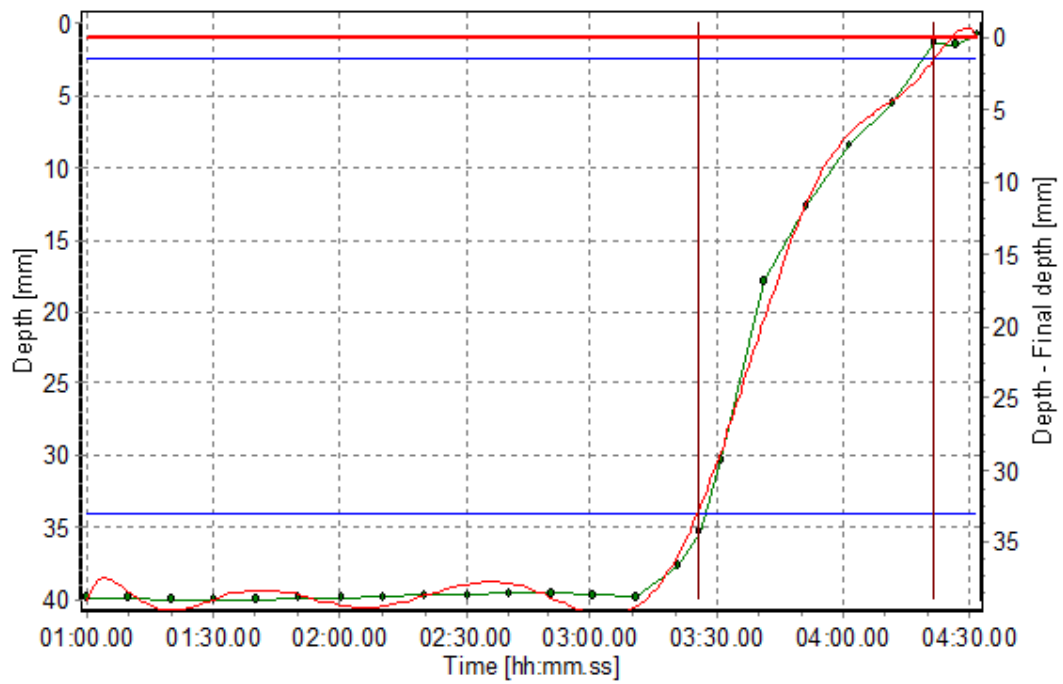
Figure 104: Setting time curve of RB10.

Figure 105: Setting time curve of RB11.
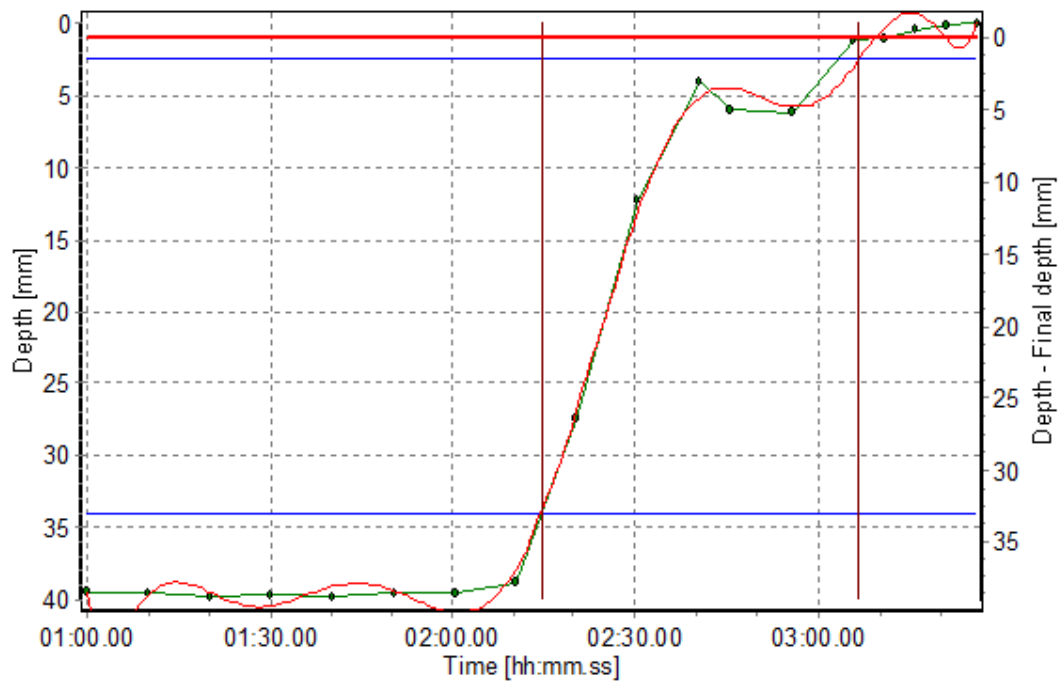
Figure 106: Setting time curve of RB12.

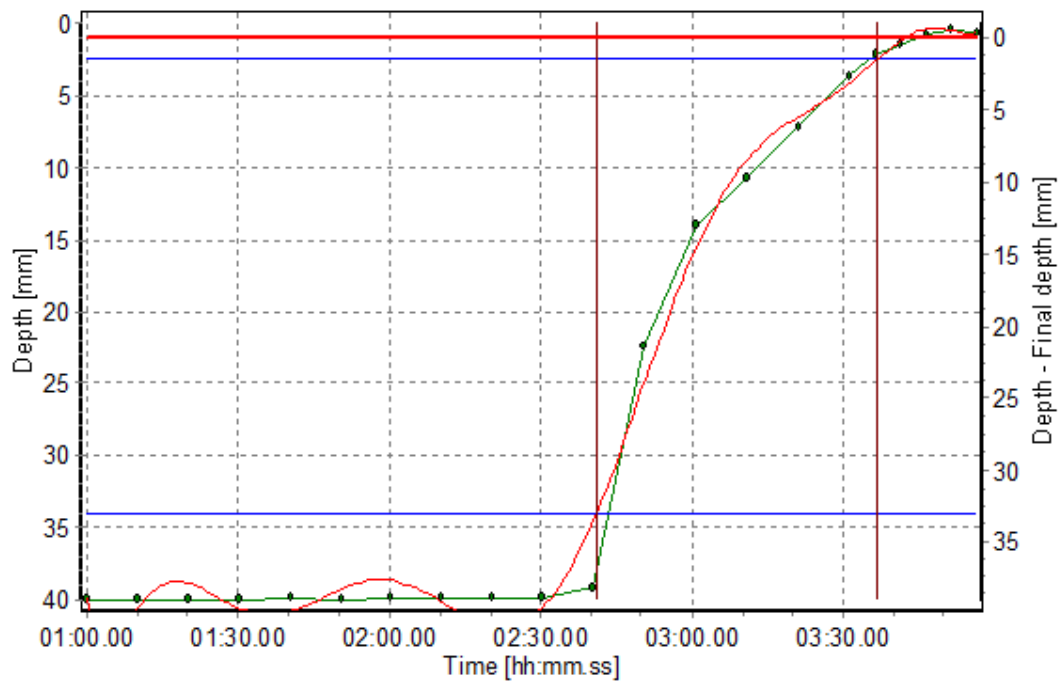Figure 107: Setting time curve of RB13.
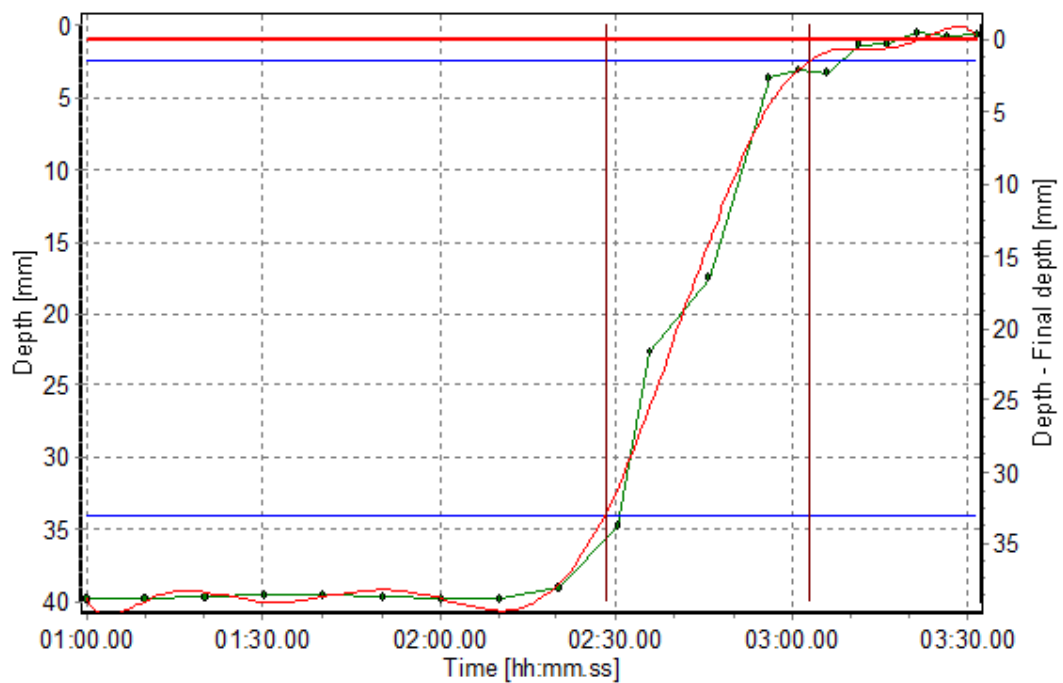
Figure 108: Setting time curve of RB14.

Figure 109: Setting time curve of RB15.

8.6 Standard Consistensy

The water percent from the standard consistency test are showed in Table 35.

Table 35: Water demand for the RB01, RB09 - RB10, and the reference sample.

Test material	Water percent [%]
Ref. Ind.	33.4
RB01	38.6
RB09	40.9
RB10	41
RB11	33.7
RB12	34.5
RB13	44
RB14	45.8
RB15	31.4